Nonconvex Robust Optimization

by

Kwong Meng Teo

B.Eng., Electrical & Electronics Engineering, University of
Manchester Institute of Science and Technology (1993)
M.Sc., Electrical Engineering, National University of Singapore (1999)
S.M., High Performance Computing, Singapore-MIT Alliance (2000)

Submitted to the Sloan School of Management
in partial fulfillment of the requirements for the degree of

Doctor of Philosophy in Operations Research

at the

MASSACHUSETTS INSTITUTE OF TECHNOLOGY

June 2007

© Massachusetts Institute of Technology 2007. All rights reserved.

Author . . . .
Sloan School of Management
May 4, 2007

Certified by . . . .
Dimitris J. Bertsimas
Boeing Professor of Operations Research
Sloan School of Management
Thesis Supervisor

Accepted by . . . .
Cynthia Barnhart
Professor, Civil and Environmental Engineering
Operations Research Center

Nonconvex Robust Optimization

by

Kwong Meng Teo

Abstract

We propose a novel robust optimization technique, which is applicable to nonconvex and simulation-based problems. Robust optimization finds decisions with the best worst-case performance under uncertainty. If constraints are present, decisions should also be feasible under perturbations. In the real-world, many problems are nonconvex and involve computer-based simulations. In these applications, the relationship between decision and outcome is not defined through algebraic functions. Instead, that relationship is embedded within complex numerical models. Since current robust optimization methods are limited to explicitly given convex problems, they cannot be applied to many practical problems. Our proposed method, however, operates on arbitrary objective functions. Thus, it is generic and applicable to most real-world problems. It iteratively moves along descent directions for the robust problem, and terminates at a robust local minimum. Because the concepts of descent directions and local minima form the building blocks of powerful optimization techniques, our proposed framework shares the same potential, but for the richer, and more realistic, robust problem. To admit additional considerations including parameter uncertainties and nonconvex constraints, we generalized the basic robust local search. In each case, only minor modifications are required - a testimony to the generic nature of the method, and its potential to be a component of future robust optimization techniques. We demonstrated the practicability of the robust local search technique in two real-world applications: nanophotonic design and Intensity Modulated Radiation Therapy (IMRT) for cancer treatment. In both cases, the numerical models are verified by actual experiments. The method significantly improved the robustness for both designs, showcasing the relevance of robust optimization to real-world problems.

Acknowledgments

I would like to thank my thesis committee members, Dimitris Bertsimas, John Tsitsiklis and Pablo Parrilo for their valuable time, suggestions and comments.

This thesis is a culmination of five years of interesting research with Dimitris. His taste and emphasis on general practical OR techniques has left a mark on me; I have also benefited from his perspective, experiences and access to applications from diverse fields. His energy and drive is certainly inspirational; his encouragement and motivation memorable.

The approach of employing scientific-mathematical analysis to make better decisions is in my blood. In my opinion, it is something everyone should do - a riskless arbitrage. My interest in computation and modeling led to a Masters degree with the Singapore-MIT Alliance. During which, I met Dimitris, and made a good friend in Melvyn Sim. However, pursuing a Ph.D. has never crossed my mind until a fortuitous five minute conversation with Melvyn in 2001. By then, he had forged a close working relationship with Dimitris. Their enthusiasm in research infected me; their encouragement was instrumental to my arrival in MIT. Furthermore, their world-class research in Robust Optimization gave me both a front row seat and a first-rate training in this exciting and highly relevant field. Thus, I would like to extend my sincere gratefulness to both of them.

Omid Nohadani is another person who had assisted me greatly. His skills in porting the nanophotonic numerical model from Matlab to Fortran enabled a quantum leap in the results obtained. I am also thankful for his patience in reviewing both my thesis and my defense presentation slides.

With reference to the nanophotonic design application, I would also like to thank D. Healy, A. Levi, P. Seliger and the research team from the University of Southern California for their encouragement and fruitful discussions on the subject matter. That part of the work is partially supported by DARPA - N666001-05-1-6030. I am also grateful to Thomas Bortfeld, David Craft and Valentina Cacchiani for their assistance in the IMRT application.

The ORC has a unique environment. We are techies bunking in with the Sloanies; the result is a cozy habitat. I enjoyed diverse discussions with friends including Margret Bjarnadottir, Timothy Chan, Lincoln Chandler, David Czerwinski, Xuan Vinh Doan, Shobhit Gupta, Pranava Goundan, Pavithra Harsha, Kathryn Kaminski, Carol Meyers, Dung Tri Nguyen, Carine Simon, Christopher Siow, Raghavendran Sivaraman, Dan Stratila, Andy Sun and Ping Xu.

I am greatly indebted to my parents and my siblings for their nurture, upbringing and unconditional love. I am also immensely grateful to my in-laws for their emotional support and frequent visits across the oceans. The distance between Boston and Singapore is certainly reduced by the care, concern and love showered by them.

To my little daughter Jay: you have brought immeasurable joy and love to this world. I want you to always be so energetic and enthusiastic about life. We will talk about this thesis and reflect on the times in Boston one day.

Finally, I want to dedicate this thesis to my loving wife, Charlotte. Through her unwavering dedication and support, she has played a significant supporting role in bringing this thesis to its fruition. She has given up a comfortable job in Nokia and an easy life in Singapore when moving to Boston. Without her securing a good job in US, her tending to domestic matters and her constant encouragements, I would not have made it through the program so smoothly. For behind every good thesis by a married man, there is a great woman.

<div align="right">

Kwong Meng Teo

kwongmeng@alum.mit.edu

May, 2007

</div>

Contents

List of Figures

11

13

14

16

List of Tables

Chapter 1

Introduction

In retrospect, it is interesting to note that the original problem that started my research is still outstanding - namely the problem of planning or scheduling dynamically over time, particularly planning dynamically under uncertainty. If such a problem could be successfully solved, it could (eventually through better planning) contribute to the well-being and stability of the world.

We have come a long way to achieving this ... ability to state general objectives and then be able to find optimal policy solutions to practical decision problems of great complexity ... but much work remains to be done, particularly in the area of uncertainties.

— George B. Dantzig, *Linear Programming:*
The Story About How It Began, 2002 [18]

The late George Dantzig, who introduced the simplex algorithm, is widely regarded as the father of linear programming. In 2002, when asked about the historical significance of linear programming and about where its many mathematical extensions may be headed, he emphasized repeatedly the importance of taking uncertainties into consideration during an optimization process. He had previously published a paper entitled *Linear Programming Under Uncertainty* in Management Science in 1955 [17]. In testimony of the importance of planning under uncertainty and how it remains an

open research problem after all these years, the same paper was *republished* by the same magazine in 2004 [19].

When specifically asked about this subject in an interview, he pulled no punches:

> Planning under uncertainty. This, I feel, is the real field that we should all be working in. The real problem is to be able to do planning under uncertainty. The mathematical models that we put together act like we have a precise knowledge about the various things that are happening and we don't. So we need to have plans that actually hedge against these various uncertainties.

> — George B. Dantzig, *In His Own Voice*, 2000 [38]

1.1 Motivation

Uncertainty is, and always will be, present in real-world applications. Information used to model a problem is often noisy, incomplete or even erroneous. In science and engineering, measurement errors are inevitable. In business applications, the cost and selling price as well as the demand of a product are, at best, expert opinions. Moreover, even if uncertainties in the model data can be ignored, solutions cannot be implemented to infinite precision, as assumed in continuous optimization. In nanophotonic device designs, prototyping and manufacturing errors are common. In antenna synthesis, amplifiers cannot be tuned to the optimal characteristics [3]. In management problems, human errors often cause deviations from the original plan. Under these uncertainties, an "optimal" solution can easily be sub-optimal or, even worse, un-implementable.

The importance of optimization under uncertainty has led to many exciting research and robust optimization is a prominent branch of it. Adopting a mini-max approach, a robust optimal design is one with the best worst-case performance. If constraints are present, a robust design shall always remain feasible. Despite significant developments in the theory of robust optimization, particularly over the past

decade, a gap remains between the robust techniques developed to date, and problems in the real-world. Robust models found in the current literature are restricted to convex problems such as linear, convex quadratic, conic-quadratic and linear discrete problems [1, 4, 6, 8]. However, an increasing number of design problems in the real-world, besides being nonconvex, involve the use of computer-based simulations. In simulation-based applications, the relationship between the design and the outcome is not defined as functions used in mathematical programming models. Instead, that relationship is embedded within complex numerical models such as partial differential equation (PDE) solvers [13, 14], response surface, radial basis functions [31] and kriging metamodels [53]. Consequently, robust techniques found in the literature cannot be applied to these important practical problems.

In this thesis, we take a new approach to robust optimization. Instead of assuming a problem structure and exploiting it, the technique operates directly on the surface of the objective function. The only assumption made by the proposed technique is a generic one: the availability of a subroutine which provides the cost as well as the gradient, given a design. Because of its generality, the proposed method is applicable to a wide range of practical problems, convex or not. To show the practicability of our robust optimization technique, we applied it to two actual nonconvex applications: nanophotonic design and Intensity Modulated Radiation Therapy (IMRT) for cancer treatment.

The proposed robust local search is analogous to local search techniques, such as gradient descent, which entails finding descent directions and iteratively taking steps along these directions to optimize the nominal cost. The proposed robust local search iteratively takes appropriate steps along descent directions for the robust problem, in order to find robust designs. This analogy continues to hold through the iterations; the robust local search is designed to terminate at a robust local minimum, a point where no improving direction exists. We introduce descent directions and the local minimum of the robust problem; the analogies of these concepts in the optimization theory are important, well studied, and form the building blocks of powerful optimization techniques, such as steepest descent and subgradient techniques. Our proposed

framework has the same potential, but for the richer robust problem or, as Dantzig puts it, for the "real" problem.

1.2   Literature Review

Traditionally, a sensitivity or post-optimality analysis [49] is performed to study the impact of perturbations on specific designs. While such an approach can be used to compare designs, it does not intrinsically generate designs that perform better under uncertainty.

Stochastic optimization [9, 45] takes a probabilistic approach. The probability distribution of the uncertainties is estimated and incorporated into the model using

(i)   chance constraints (i.e. a constraint which is violated less than $p\%$ of the time) [11],

(ii) risk measures (i.e. standard deviations, value-at-risk and conditional value-at-risk) [39, 44, 46, 48, 59], or

(iii) a large number of scenarios emulating the distribution [40, 47].

However, the actual distribution of the uncertainties is seldom available. Take the demand of a product over the coming week. Any specified probability distribution is, at best, an expert's opinion. Furthermore, even if the distribution is known, solving the resulting problem remains a challenge [22]. For instance, a chance constraint is usually "computationally intractable" [42].

Robust optimization is a name shared by a number of approaches developed to address uncertainties. In one approach, Mulvey et. al. [41] integrated goal programming formulations with a scenario-based description of the problem data, and incorporated a penalty for constraint violations within the objective. In another approach, a robust optimal solution is interpreted as one which optimizes the cost, while remaining feasible for all uncertainties belonging to a set. In 1973, Soyster [54] first proposed a linear optimization model to find a design that is robust to parameter variations within a convex set. However, in ensuring feasibility, this approach can be too conservative, i.e., it finds designs with much higher costs than what is necessary [2]. The next significant development came two decades later, when Ben-tal and Nemirovski [1, 2, 4]

and El-Ghaoui et.al. [24, 25] independently developed a theory for robust convex optimization. Their results show that a convex problem with uncertainties can be transformed to another convex problem, if certain conditions hold. Their work inspired many exciting research in both theory and applications, many of which are still on-going. In particular, Bertsimas and Sim extended robust optimization to linear discrete optimization problems [6], and proposed new methodologies to improve the tractability of robust models [7, 8].

However, there remains a gap between the robust optimization techniques developed to date, and problems in the real-world. The robust models found in the literature today are limited to explicitly given convex problems, and cannot be applied to many practical problems. In this thesis, we propose a new approach to robust optimization, which is applicable to nonconvex and simulation-based problems. To present the method, the thesis is structured as follows:

1.3   Structure of the Thesis

- **Chapter 2: Nonconvex Robust Optimization for Unconstrained Problems**   We start by developing the robust local search in the context of a nonconvex problem without constraints. Both implementation and parameter uncertainties are addressed. The technique makes no assumption on the problem structure, and operates directly on the surface of the objective function in the design space. The application of the robust local search in a robust problem is analogous to the application of a local search algorithm in an optimization problem without uncertainties. When developing the technique, we introduce the descent direction, a local minimum, and a graphical perspective, of the robust problem. The analogies of these concepts in the optimization theory are important and well studied. A convergence result is also developed in this chapter.

- **Chapter 3: Nonconvex Robust Optimization in Nano-Photonics**   We demonstrate the practicality of the robust local search in a complex real-world

problem, by applying it to an actual engineering problem in electromagnetic scattering. The problem involves the design of aperiodic dielectric structures and is relevant to nano-photonics. The spatial configuration of 50 dielectric scattering cylinders is optimized to match a desired target function, while protected against placement and prototype errors. Our optimization method inherently improves the robustness of the optimized solution with respect to relevant errors, and is suitable for real-world design of materials with novel electromagnetic functionalities.

- **Chapter 4: Nonconvex Robust Optimization for Problems with Constraints** We generalize the robust local search to problems with constraints, where the objective and the constraints can be nonconvex. Furthermore, we show how the efficiency of the algorithm can be improved, if some constraints are simple, e.g. linear constraints. To demonstrate the practicality of the robust local search, we applied it to an actual healthcare problem in Intensity Modulated Radiation Therapy (IMRT) for cancer treatment. Using the method, we find the pareto frontier, which shows the trade-off between undesirable radiation introduced into the body, and the probability of applying insufficient dosage to the tumor.

- **Chapter 5: Conclusions.** This chapter contains the concluding remarks, and suggests areas of future research in optimization under uncertainties.

Chapter 2

Nonconvex Robust Optimization for Unconstrained Problems

In this chapter, we develop the robust local search algorithm for an unconstrained optimization problem. It has the following features:

- applicable to nonconvex and simulation-based problems

- operates directly on surface of objective function

- generic assumption applicable to most real-world problems

To illustrate the technique more clearly, we start by considering a problem with implementation errors only, before generalizing it to admit both implementation and parameter uncertainties. The chapter is structured as follows.

Structure of the chapter: In Section 2.1, we define the robust optimization problem under implementation errors, and introduce the concept of (i) a descent direction for the robust problem, and (ii) a robust local minimum. We study the conditions under which a descent direction can be found, and present a convergence result. Because it is difficult to find the descent direction exactly in general, we adopt a heuristic strategy and develop it into a practical robust local search algorithm. In Section 2.2, we discuss the implementation of the algorithm in detail. The

performance of the algorithm is then demonstrated in a problem with a nonconvex polynomial objective function in Section 2.3. It is a simple application, designed to illustrate the algorithm at work and to develop intuition into the robust nonconvex optimization problem. In Section 2.4, we generalize the algorithm to admit both implementation and parameter uncertainties. The inclusion of parameter uncertainties, surprisingly, introduce only minor modifications to the algorithm. In Section 2.5, we apply the algorithm in first application, but with parameter uncertainties as well. Improving the efficiency is a common consideration in the real world. This is discussed in Section 2.6. In Section 2.7, we consider problems without gradient information, and finally, in Section 2.8 we present our conclusions.

2.1 The Robust Optimization Problem Under Implementation Errors

2.1.1 Problem Definition

The problem of interest, without considerations for uncertainty, is

$$\min_{\mathbf{x}} \quad f(\mathbf{x}). \tag{2.1}$$

It is referred to as the *nominal problem*, and $f(\mathbf{x})$ is the *nominal cost* of design vector $\mathbf{x} \in \mathbb{R}^n$. This objective function can be nonconvex. It can even be the output of a numerical solver, such as a PDE solver.

Suppose that errors $\Delta\mathbf{x} \in \mathbb{R}^n$ are introduced when $\mathbf{x}$ is implemented, due to, perhaps, an imperfect manufacturing process. The eventual implementation is then $\mathbf{x} + \Delta\mathbf{x}$. We consider all errors that reside within an ellipsoidal uncertainty set

$$\mathcal{U} \quad := \quad \left\{ \Delta\mathbf{x} \in \mathbb{R}^n \mid \|\Delta\mathbf{x}\|_2 \leq \Gamma \right\}, \tag{2.2}$$

where Γ is a positive scalar describing the size of errors against which the design should be protected.

Instead of the nominal cost, the robust problem optimizes against the *worst case cost*, i.e., the maximum implementation cost under an error from the uncertainty set. The worst case cost is, equivalently,

$$g(\mathbf{x}) \quad := \quad \max_{\Delta\mathbf{x}\in\mathcal{U}} \ f(\mathbf{x}+\Delta\mathbf{x}). \qquad (2.3)$$

Therefore, the *robust optimization problem* is

$$\min_{\mathbf{x}} \ g(\mathbf{x}) \quad \equiv \quad \min_{\mathbf{x}} \ \max_{\Delta\mathbf{x}\in\mathcal{U}} \ f(\mathbf{x}+\Delta\mathbf{x}). \qquad (2.4)$$

2.1.2 A Graphical Perspective of the Robust Problem

When implementing a certain design $\mathbf{x} = \hat{\mathbf{x}}$, the possible realization due to implementation errors $\Delta\mathbf{x} \in \mathcal{U}$ lies in the set

$$\mathcal{N} \quad := \quad \left\{ \mathbf{x} \mid \|\mathbf{x}-\hat{\mathbf{x}}\|_2 \le \Gamma \right\}. \qquad (2.5)$$

We call $\mathcal{N}$ the *neighborhood* of $\hat{\mathbf{x}}$; such a neighborhood is illustrated in Figure 2-1. A design $\mathbf{x}$ is a *neighbor* of $\hat{\mathbf{x}}$, if it is in $\mathcal{N}$. Therefore, the worst case cost of $\hat{\mathbf{x}}$, $g(\hat{\mathbf{x}})$, is the maximum cost attained within $\mathcal{N}$. Let $\Delta\mathbf{x}^*$ be one of the worst implementation error at $\hat{\mathbf{x}}$, $\Delta\mathbf{x}^* = \arg\max_{\Delta\mathbf{x}\in\mathcal{U}} \ f(\hat{\mathbf{x}}+\Delta\mathbf{x})$. Then, $g(\hat{\mathbf{x}})$ is given by $f(\hat{\mathbf{x}}+\Delta\mathbf{x}^*)$. Because the worst neighbors hold the information to improving a design's robustness, the *set of worst implementation errors* is important. Thus, we define this set at $\hat{\mathbf{x}}$,

$$\mathcal{U}^*(\hat{\mathbf{x}}) \quad := \quad \left\{ \Delta\mathbf{x}^* \mid \Delta\mathbf{x}^* = \arg\max_{\Delta\mathbf{x}\in\mathcal{U}} \ f(\hat{\mathbf{x}}+\Delta\mathbf{x}) \right\}. \qquad (2.6)$$

2.1.3 Descent Directions

Clearly, it would be interesting and beneficial if we can find *descent directions* which reduce the worst case cost. Such a direction is defined as:

Definition 1
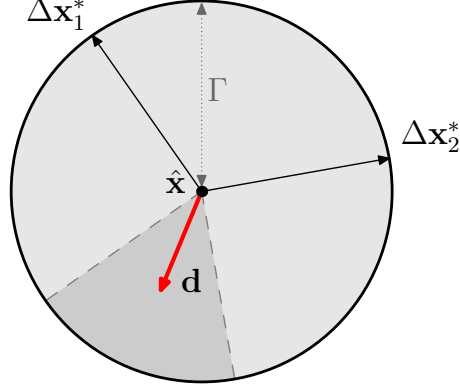
Figure 2-1: A 2-D illustration of the neighborhood $\mathcal{N} = \{\mathbf{x} \mid \|\mathbf{x} - \hat{\mathbf{x}}\|_2 \leq \Gamma\}$. The shaded circle contains all possible realizations when implementing $\hat{\mathbf{x}}$, when we have errors $\Delta\mathbf{x} \in \mathcal{U}$. The bold arrow $\mathbf{d}$ shows a possible descent direction pointing away from all the worst implementation errors $\Delta\mathbf{x}_i^*$, represented by thin arrows. All the descent directions lie within the cone, which is of a darker shade and demarcated by broken lines.

$\mathbf{d}$ *is a descent direction for the robust optimization problem (2.4) at* $\mathbf{x}$*, if the directional derivative in direction* $\mathbf{d}$ *satisfies the following condition:*

$$g'(\mathbf{x}; \mathbf{d}) \quad < \quad 0. \tag{2.7}$$

The directional derivative at $\mathbf{x}$ in the direction $\mathbf{d}$ is defined as:

$$g'(\mathbf{x}; \mathbf{d}) \quad = \quad \lim_{t \downarrow 0} \frac{g(\mathbf{x} + t\mathbf{d}) - g(\mathbf{x})}{t}. \tag{2.8}$$

Note, that in the robust problem (2.4), a directional derivative exists for all $\mathbf{x}$ and for all $\mathbf{d}$. This is a result of Danskin's Min-Max Theorem, which will be discussed in greater detail in a later section.

A descent direction $\mathbf{d}$ is a direction which will reduce the worst case cost if it is used to update the design $\mathbf{x}$. We seek an efficient way to find such a direction. The following Theorem shows that a descent direction is equivalent to a vector pointing away from all the worst implementation errors in $\mathcal{U}$:

Theorem 1

Suppose that $f(\mathbf{x})$ is continuously differentiable, $\mathcal{U} = \{\Delta\mathbf{x} \mid \|\Delta\mathbf{x}\|_2 \leq \Gamma\}$ with $\Gamma > 0$, $g(\mathbf{x}) := \max\limits_{\Delta\mathbf{x} \in \mathcal{U}} f(\mathbf{x} + \Delta\mathbf{x})$ and $\mathcal{U}^*(\mathbf{x}) := \left\{\Delta\mathbf{x}^* \mid \Delta\mathbf{x}^* = \arg\max\limits_{\Delta\mathbf{x} \in \mathcal{U}} f(\mathbf{x} + \Delta\mathbf{x})\right\}$. Then, $\mathbf{d} \in \mathbb{R}^n$ is a descent direction for the worst case cost function $g(\mathbf{x})$ at $\mathbf{x} = \hat{\mathbf{x}}$ if and only if

$$\mathbf{d}'\Delta\mathbf{x}^* \; < \; 0,$$

$$\nabla_{\mathbf{x}} f(\mathbf{x})|_{\mathbf{x} = \hat{\mathbf{x}} + \Delta\mathbf{x}^*} \; \neq \; \mathbf{0},$$

for all $\Delta\mathbf{x}^* \in \mathcal{U}^*(\hat{\mathbf{x}})$.

Note, that the condition $\nabla_{\mathbf{x}} f(\mathbf{x})|_{\mathbf{x} = \hat{\mathbf{x}} + \Delta\mathbf{x}^*} \neq \mathbf{0}$, or $\hat{\mathbf{x}} + \Delta\mathbf{x}^*$ not being a uncon-strained local maximum of $f(\mathbf{x})$ is equivalent to the condition $\|\Delta\mathbf{x}^*\|_2 = \Gamma$. Fig-ure 2-1 illustrates a possible scenario under Theorem 1. All the descent directions $\mathbf{d}$ lie in the strict interior of a cone, the normal of the cone spanned by all the vectors $\Delta\mathbf{x}^* \in \mathcal{U}^*(\hat{\mathbf{x}})$. Consequently, all descent directions point away from all the worst implementation errors. From $\hat{\mathbf{x}}$, the worst case cost can be strictly decreased if we take a sufficiently small step along any directions within this cone, leading to solu-tions that are more robust. All the worst designs, $\hat{\mathbf{x}} + \Delta\mathbf{x}^*$, would also lie outside the neighborhood of the new design.

Because the proof involves lengthy arguments, we present it separately in Sec-tion 2.1.4. The main ideas behind the proof are

(i) the directional derivative of the worst case cost function, $g'(\mathbf{x}; \mathbf{d})$, equals the maximum value of $\mathbf{d}' \nabla_{\mathbf{x}} f(\mathbf{x} + \Delta\mathbf{x}^*)$, for all $\Delta\mathbf{x}^*$ (See Corollary 1(a)), and

(ii) the gradient at $\mathbf{x} + \Delta\mathbf{x}^*$ is parallel to $\Delta\mathbf{x}^*$, due to the Karush-Kuhn-Tucker conditions (See Proposition 1).

Therefore, in order for $g'(\mathbf{x}; \mathbf{d}) < 0$, we require $\mathbf{d}' \Delta\mathbf{x}^* < 0$ and $\nabla_{\mathbf{x}} f(\mathbf{x} + \Delta\mathbf{x}^*) \neq \mathbf{0}$, for all $\Delta\mathbf{x}^*$. The intuition behind Theorem 1 is: we have to move sufficiently far away from all the designs $\hat{\mathbf{x}} + \Delta\mathbf{x}^*$ for there to be a chance to decrease the worst case cost.

2.1.4 Proof of Theorem 1

Before proving Theorem 1, we first observe the following result:

Proposition 1

Suppose that $f(\mathbf{x})$ is continuously differentiable in $\mathbf{x}$, $\mathcal{U} = \{\Delta\mathbf{x} \mid \|\Delta\mathbf{x}\|_2 \leq \Gamma\}$ where $\Gamma > 0$ and $\mathcal{U}^*(\mathbf{x}) := \left\{\Delta\mathbf{x}^* \mid \Delta\mathbf{x}^* = \arg\max\limits_{\Delta\mathbf{x}\in\mathcal{U}} f(\mathbf{x}+\Delta\mathbf{x})\right\}$. Then, for any $\hat{\mathbf{x}}$ and $\Delta\mathbf{x}^* \in \mathcal{U}^*(\mathbf{x}=\hat{\mathbf{x}})$,

$$\nabla_{\mathbf{x}} f(\mathbf{x})\big|_{\mathbf{x}=\hat{\mathbf{x}}+\Delta\mathbf{x}^*} = k\Delta\mathbf{x}^*$$

where $k \geq 0$.

In words, the gradient at a worst neighbor, $\mathbf{x} = \hat{\mathbf{x}} + \Delta\mathbf{x}^*$, is parallel to its corresponding (worst) implementation error, vector $\Delta\mathbf{x}^*$.

Proof of Proposition 1:

Since $\Delta\mathbf{x}^*$ is a maximizer of the problem $\max\limits_{\Delta\mathbf{x}\in\mathcal{U}} f(\hat{\mathbf{x}} + \Delta\mathbf{x})$ and a regular point[1], because of the Karush-Kuhn-Tucker necessary conditions, there exists a scalar $\mu \geq 0$ such that

$$-\nabla_{\mathbf{x}} f(\mathbf{x})\big|_{\mathbf{x}=\hat{\mathbf{x}}+\Delta\mathbf{x}^*} + \mu\nabla_{\Delta\mathbf{x}}(\Delta\mathbf{x}'\Delta\mathbf{x} - \Gamma)\big|_{\Delta\mathbf{x}=\Delta\mathbf{x}^*} = 0.$$

This is equivalent to the condition

$$\nabla_{\mathbf{x}} f(\mathbf{x})\big|_{\mathbf{x}=\hat{\mathbf{x}}+\Delta\mathbf{x}^*} = 2\mu\Delta\mathbf{x}^*.$$

The result follows by choosing $k = 2\mu$. □

Then, observe that the robust problem (2.4) is a special instance of the Min-Max problem considered by Danskin in the following theorem.

---

[1]In this context, a feasible vector is said to be a regular point if all the active inequality constraints are linearly independent, or if all the inequality constraints are inactive. Since there is only one constraint in the problem $\max\limits_{\Delta\mathbf{x}\in\mathcal{U}} f(\hat{\mathbf{x}} + \Delta\mathbf{x})$ which is either active or not, $\Delta\mathbf{x}^*$ is always a regular point. Furthermore, note that where $\|\Delta\mathbf{x}^*\|_2 < \Gamma$, $\hat{\mathbf{x}} + \Delta\mathbf{x}^*$ is an unconstrained local maximum of f and it follows that $\nabla_{\mathbf{x}} f(\mathbf{x})\big|_{\mathbf{x}=\hat{\mathbf{x}}+\Delta\mathbf{x}^*} = \mathbf{0}$ and $k = 0$.

Theorem 2 (Danskin's Min-Max Theorem)

Let $\mathcal{C} \subset \mathbb{R}^m$ be a compact set, $\phi : \mathbb{R}^n \times \mathcal{C} \mapsto \mathbb{R}$ be continuously differentiable in $\mathbf{x}$, and $\psi : \mathbb{R}^n \mapsto \mathbb{R}$ be the max-function $\psi(\mathbf{x}) := \max_{\mathbf{y} \in \mathcal{C}} \phi(\mathbf{x}, \mathbf{y})$.

(a) Then, $\psi(\mathbf{x})$ is directionally differentiable with directional derivatives

$$\psi'(\mathbf{x}; \mathbf{d}) = \max_{\mathbf{y} \in \mathcal{C}^*(x)} \mathbf{d}' \nabla_x \phi(\mathbf{x}, \mathbf{y}),$$

where $\mathcal{C}^*(\mathbf{x})$ is the set of maximizing points

$$\mathcal{C}^*(\mathbf{x}) = \left\{ \mathbf{y}^* \mid \phi(\mathbf{x}, \mathbf{y}^*) = \max_{\mathbf{y} \in \mathcal{C}} \phi(\mathbf{x}, \mathbf{y}) \right\}.$$

(b) If $\phi(\mathbf{x}, \mathbf{y})$ is convex in $\mathbf{x}$, $\phi(\cdot, \mathbf{y})$ is differentiable for all $\mathbf{y} \in \mathcal{C}$ and $\nabla_{\mathbf{x}} \phi(\mathbf{x}, \cdot)$ is continuous on $\mathcal{C}$ for each $\mathbf{x}$, then $\psi(\mathbf{x})$ is convex in $\mathbf{x}$ and $\forall \mathbf{x}$,

$$\partial \psi(\mathbf{x}) = conv \left\{ \nabla_{\mathbf{x}} \phi(\mathbf{x}, \mathbf{y}) \mid \mathbf{y} \in \mathcal{C}^*(x) \right\} \tag{2.9}$$

where $\partial \psi(\mathbf{x})$ is the subdifferential of the convex function $\psi(\mathbf{x})$ at $\mathbf{x}$

$$\partial \psi(\mathbf{x}) = \{ \mathbf{z} \mid \psi(\bar{\mathbf{x}}) \geq \psi(\mathbf{x}) + \mathbf{z}'(\bar{\mathbf{x}} - \mathbf{x}), \forall \bar{\mathbf{x}} \}$$

and conv denotes the convex hull.

For a proof of Theorem 2, see Reference [15, 16]. Using Proposition 1, we obtain the following corollary from Danskin's Theorem 2:

Corollary 1

Suppose that $f(\mathbf{x})$ is continuously differentiable, $\mathcal{U} = \{ \Delta \mathbf{x} \mid \|\Delta \mathbf{x}\|_2 \leq \Gamma \}$ where $\Gamma > 0$, $g(\mathbf{x}) := \max_{\Delta \mathbf{x} \in \mathcal{U}} f(\mathbf{x} + \Delta \mathbf{x})$ and $\mathcal{U}^*(\mathbf{x}) := \left\{ \Delta \mathbf{x}^* \mid \Delta \mathbf{x}^* = \arg \max_{\Delta \mathbf{x} \in \mathcal{U}} f(\mathbf{x} + \Delta \mathbf{x}) \right\}$.

(a) Then, $g(\mathbf{x})$ is directionally differentiable and its directional derivatives $g'(\mathbf{x}; \mathbf{d})$ are given by

$$g'(\mathbf{x}; \mathbf{d}) = \max_{\Delta \mathbf{x} \in \mathcal{U}^*(x)} f'(\mathbf{x} + \Delta \mathbf{x}; \mathbf{d}).$$

(b) If $f(\mathbf{x})$ is convex in $\mathbf{x}$, then $g(\mathbf{x})$ is convex in $\mathbf{x}$ and $\forall \mathbf{x}$,

$$\partial g(\mathbf{x}) = conv\left\{\Delta\mathbf{x} \mid \Delta\mathbf{x} \in \mathcal{U}^*(x)\right\}.$$

Proof of Corollary 1:

Referring to the notation in Theorem 2, if we let $\mathbf{y} = \Delta\mathbf{x}$, $\mathcal{C} = \mathcal{U}$, $\mathcal{C}^* = \mathcal{U}^*$, $\phi(\mathbf{x}, \mathbf{y}) = f(\mathbf{x}, \Delta\mathbf{x}) = f(\mathbf{x} + \Delta\mathbf{x})$, then $\psi(\mathbf{x}) = g(\mathbf{x})$. Because all the conditions in Theorem 2 are satisfied, it follows that

(a) $g(\mathbf{x})$ is directionally differentiable with

$$\begin{aligned} g'(\mathbf{x}; \mathbf{d}) &= \max_{\Delta\mathbf{x} \in \mathcal{U}^*(x)} \mathbf{d}' \nabla_{\mathbf{x}} f(\mathbf{x} + \Delta\mathbf{x}) \\ &= \max_{\Delta\mathbf{x} \in \mathcal{U}^*(x)} f'(\mathbf{x} + \Delta\mathbf{x}; \mathbf{d}). \end{aligned}$$

(b) $g(\mathbf{x})$ is convex in $\mathbf{x}$ and $\forall \mathbf{x}$,

$$\begin{aligned} \partial g(\mathbf{x}) &= conv\left\{\nabla_{\mathbf{x}} f(\mathbf{x}, \Delta\mathbf{x}) \mid \Delta\mathbf{x} \in \mathcal{U}^*(x)\right\} \\ &= conv\left\{\Delta\mathbf{x} \mid \Delta\mathbf{x} \in \mathcal{U}^*(x)\right\}. \end{aligned}$$

The last equality is due to Proposition 1. $\square$

With these results, we shall now prove Theorem 1:

Proof of Theorem 1:

From Corollary 1, for a given $\hat{\mathbf{x}}$

$$\begin{aligned} g'(\hat{\mathbf{x}}; \mathbf{d}) &= \max_{\Delta\mathbf{x}^* \in \mathcal{U}^*(\hat{\mathbf{x}})} f'(\hat{\mathbf{x}} + \Delta\mathbf{x}; \mathbf{d}) \\ &= \max_{\Delta\mathbf{x}^* \in \mathcal{U}^*(\hat{\mathbf{x}})} \mathbf{d}' \nabla_{\mathbf{x}} f(\mathbf{x})|_{\mathbf{x} = \hat{\mathbf{x}} + \Delta\mathbf{x}^*} \\ &= \max_{\Delta\mathbf{x}^* \in \mathcal{U}^*(\hat{\mathbf{x}})} k\mathbf{d}' \Delta\mathbf{x}^*. \end{aligned}$$
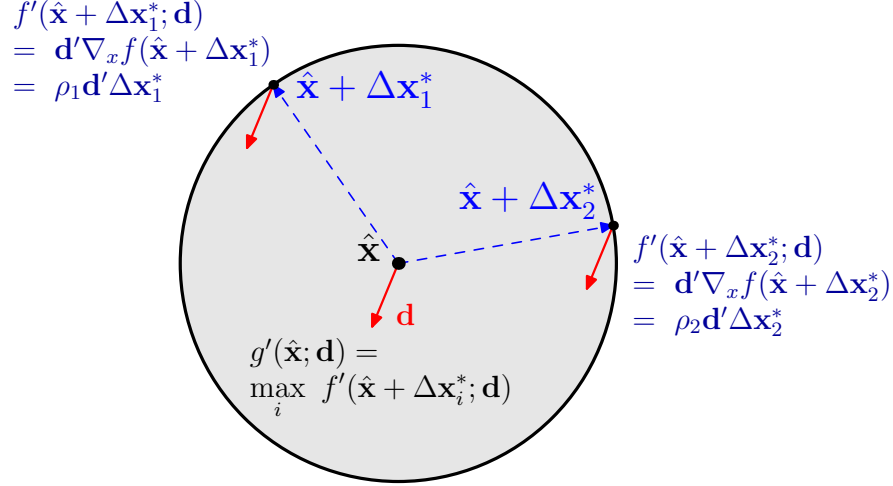
Figure 2-2: A 2-D illustration of proof to Theorem 1. The directional derivative of the worst case cost function, $g'(\mathbf{x}; \mathbf{d})$, equals the maximum value of $\mathbf{d}'\nabla_{\mathbf{x}}f(\mathbf{x} + \Delta\mathbf{x}^*)$, for all $\Delta\mathbf{x}^*$. The gradient at $\mathbf{x} + \Delta\mathbf{x}^*$ is parallel to $\Delta\mathbf{x}^*$, due to the Karush-Kuhn-Tucker conditions.

The last equality follows from Proposition 1. $k \geq 0$ but may be different for each $\Delta\mathbf{x}^*$. Therefore, for $\mathbf{d}$ to be a descent direction,

$$\max_{\Delta\mathbf{x}^* \in \mathcal{U}^*(\hat{\mathbf{x}})} k\mathbf{d}'\Delta\mathbf{x}^* \;<\; 0. \tag{2.10}$$

Eqn. 2.10 is satisfied if and only if for all $\Delta\mathbf{x}^* \in \mathcal{U}^*(\hat{\mathbf{x}})$,

$$\mathbf{d}'\Delta\mathbf{x}^* \;<\; 0,$$
$$\nabla_{\mathbf{x}}f(\mathbf{x})|_{\mathbf{x}=\hat{\mathbf{x}}+\Delta\mathbf{x}^*} \;\neq\; 0, \quad \text{for } k \neq 0.$$

The proof is now complete. □

This proof to Theorem 1 is also illustrated in Fig. 2-2.

2.1.5 Robust Local Minima

Definition 1 for a descent direction leads naturally to the following concept of a robust local minimum:

Definition 2

$\mathbf{x}^*$ *is a robust local minimum, if there exists no descent directions for the robust problem at* $\mathbf{x} = \mathbf{x}^*$.

Similarly, Theorem 1 leads the following characterization of a robust local minimum:

Corollary 2 (Robust Local Minimum)

Suppose that $f(\mathbf{x})$ *is continuously differentiable. Then,* $\mathbf{x}^*$ *is a robust local minimum, if and only if, either one of the following two conditions are satisfied:*

i. there does not exist a $\mathbf{d} \in \mathbb{R}^n$ *such that for all* $\Delta\mathbf{x}^* \in \mathcal{U}^*(\mathbf{x}^*)$,

$$\mathbf{d}'\Delta\mathbf{x}^* \quad < \quad 0,$$

ii. there exists a $\Delta\mathbf{x}^* \in \mathcal{U}^*(\mathbf{x}^*)$ *such that* $\nabla_{\mathbf{x}}f(\mathbf{x} + \Delta\mathbf{x}^*) = \mathbf{0}$.

Given Corollary 2, we illustrate common types of robust local minima, where either one of the two conditions are satisfied.

Convex case. If f is convex, there are no local maxima in f and therefore, the condition $\nabla_{\mathbf{x}}f(\mathbf{x} + \Delta\mathbf{x}^*) = \mathbf{0}$ is never satisfied. The only condition for the lack of descent direction is (i) where there are no $\mathbf{d}$ satisfying the condition $\mathbf{d}'\Delta\mathbf{x}_i^* < 0$, as shown in Fig. 2-3(a). Furthermore, if f is convex, g is convex (see Corollary 1(b)). Thus, a robust local minimum of g is a robust global minimum of g.

General case. Three common types of robust local minimum can be present when f is nonconvex, as shown in Figure 2-3. Condition (i) in Corollary 2, that there are no direction pointing away from all the worst implementation errors $\Delta\mathbf{x}_i^*$, is satisfied by both the robust local minimum in Fig. 2-3(a) and Fig. 2-3(b). Condition (ii), that one of the worst implementation errors $\Delta\mathbf{x}_i^*$ lies in the strict interior of the neighborhood, is satisfied by Fig. 2-3(b) and Fig. 2-3(c).

36
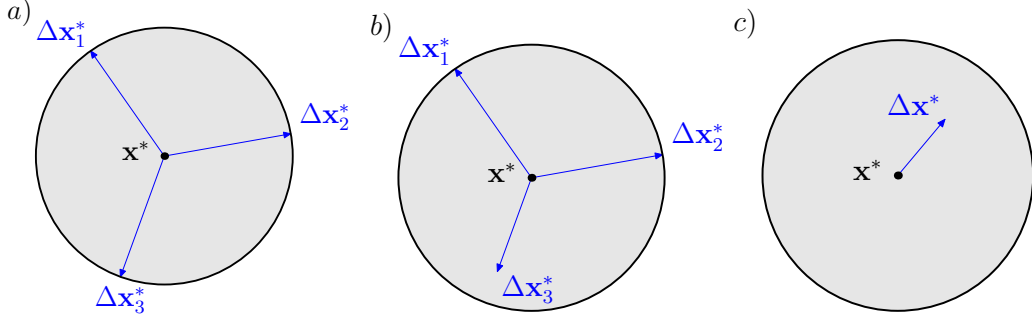
Figure 2-3: A 2-D illustration of common types of robust local minima. In (a) and (b), there are no direction pointing away from all the worst implementation errors $\Delta \mathbf{x}_i^*$, which are denoted by arrows. In (b) and (c), one of the worst implementation errors $\Delta \mathbf{x}_i^*$ lie in the strict interior of the neighborhood. Note, for convex problems, the robust local (global) minimum is of the type shown in (a).

Compared to the others, the "robust local minimum" of the type in Fig. 2-3(c) may not be as good a robust design, and can actually be a bad robust solution. For instance, we can find many such "robust local minima" near the global maximum of the nominal cost function $f(\mathbf{x})$, i.e. when $\mathbf{x}^* + \Delta \mathbf{x}^*$ is the global maximum of the nominal problem. Therefore, we seek a robust local minimum satisfying Condition (i), that there does not exist a direction pointing away from all the worst implementation errors.

The following algorithm seeks such a desired robust local minimum. We further show the convergence result in the case where f is convex.

37

2.1.6 A Local Search Algorithm for the Robust Optimization Problem

Given the set of worst implementation errors at $\hat{\mathbf{x}}$, $\mathcal{U}^*(\hat{\mathbf{x}})$, a descent direction can be found efficiently by solving the following second-order cone program (SOCP):

$$
\begin{aligned}
\min_{\mathbf{d},\beta} \quad & \beta \\
s.t. \quad & \|\mathbf{d}\|_2 \leq 1 \\
& \mathbf{d}'\Delta\mathbf{x}^* \leq \beta \quad \forall \Delta\mathbf{x}^* \in \mathcal{U}^*(\hat{\mathbf{x}}) \\
& \beta \leq -\epsilon,
\end{aligned}
\tag{2.11}
$$

where ϵ is a small positive scalar. When Problem (2.11) has a feasible solution, its optimal solution, $\mathbf{d}^*$, forms the maximum possible angle $\theta_{\max}$ with all $\Delta\mathbf{x}^*$. An example is illustrated in Fig. 2-4. This angle is always greater than $90°$ due to the constraint $\beta \leq -\epsilon < 0$. $\beta \leq 0$ is not used in place of $\beta \leq -\epsilon$, because we want to exclude the trivial solution $(\mathbf{d}^*, \beta^*) = (\mathbf{0}, 0)$. When ϵ is sufficiently small, and Problem (2.11) is infeasible, $\hat{\mathbf{x}}$ is a good estimate of a robust local minimum satisfying Condition (i) in Corollary 2. Note, that the constraint $\|\mathbf{d}^*\|_2 = 1$ is automatically satisfied if the problem is feasible. Such an SOCP can be solved efficiently using both commercial and noncommercial solvers.

Consequently, if we have an oracle returning $\mathcal{U}^*(\mathbf{x})$ for all $\mathbf{x}$, we can iteratively find descent directions and use them to update the current iterates, resulting in the following local search algorithm. The term $\mathbf{x}^k$ is the term being evaluated in iteration k.

If $f(\mathbf{x})$ is continuously differentiable and convex, Algorithm 2.1.6 converges to the robust global minimum when appropriate step size t^k are chosen. This is reflected by the following theorem:

Theorem 3 *Suppose that $f(\mathbf{x})$ is continuously differentiable and convex with a bounded set of minimum points. Then, Algorithm 2.1.6 converges to the global optimum of the robust optimization problem (2.4), when $t^k > 0$, $t^k \to 0$ as $k \to \infty$ and $\sum_{k=1}^{\infty} t^k = \infty$.*
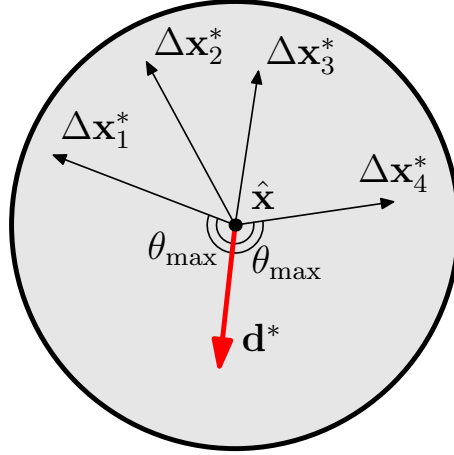
Figure 2-4: A 2-D illustration of the optimal solution of SOCP, Prob. (2.11), in the neighborhood of $\hat{\mathbf{x}}$. The solid arrow indicates the optimal direction $\mathbf{d}^*$ which makes the largest possible angle θ_{max} with all the vectors $\Delta\mathbf{x}^*$, $\Delta\mathbf{x}^*$ being the worst case implementation errors at $\hat{\mathbf{x}}$. The angle $\theta_{\max} = \cos^{-1}\beta^*$ and is at least 90° due to the constraint $\beta \leq -\epsilon$, ϵ being a small positive scalar.

Algorithm 1 Robust Local Search Algorithm

Step 0. Initialization: Let $\mathbf{x}^1$ be the initial decision vector arbitrarily chosen. Set $k := 1$.

Step 1. Neighborhood Search:
  Find $\mathcal{U}^*(\mathbf{x}^k)$, set of worst implementation errors at the current iterate $\mathbf{x}^k$.

Step 2. Robust Local Move:
  i. Solve the SOCP (Problem 2.11), terminating if the problem is infeasible.
  ii. Set $\mathbf{x}^{k+1} := \mathbf{x}^k + t^k\mathbf{d}^*$, where $\mathbf{d}^*$ is the optimal solution to the SOCP.
  iii. Set $k := k + 1$. Go to Step 1.

This Theorem follows from the fact that at every iteration, $-\mathbf{d}^*$ is a subgradient of the worst cost function $g(\mathbf{x})$ at the iterate $\mathbf{x}^k$. Therefore, Algorithm 2.1.6 is a subgradient projection algorithm, and under the stated step size rule, convergence to the global minimum is assured.

Before proving Theorem 3, we prove the following proposition:

Proposition 2 *Let $\mathcal{G} := \{\Delta\mathbf{x}_1, \ldots, \Delta\mathbf{x}_m\}$ and let $(\mathbf{d}^*, \beta^*)$ be the optimal solution to a feasible SOCP*

$$\min_{\mathbf{d}, \beta} \quad \beta$$
$$s.t. \quad \|\mathbf{d}\|_2 \leq 1,$$
$$\mathbf{d}'\Delta\mathbf{x}_i \leq \beta, \quad \forall \Delta\mathbf{x}_i \in \mathcal{G},$$
$$\beta \leq -\epsilon,$$

where ϵ is a small positive scalar. Then, $-\mathbf{d}^*$ lies in conv $\mathcal{G}$.

Proof of Proposition 2:

We show that if $-\mathbf{d}^* \notin conv\ \mathcal{G}$, $\mathbf{d}^*$ is not the optimal solution to the SOCP because a better solution can be found. Note, that for $(\mathbf{d}^*, \beta^*)$ to be an optimal solution, $\|\mathbf{d}^*\|_2 = 1$, $\beta^* < 0$ and $\mathbf{d}^{*'}\Delta\mathbf{x}_i < 0$, $\forall \Delta\mathbf{x}_i \in \mathcal{G}$.

Assume, for contradiction, that $-\mathbf{d}^* \notin conv\ \mathcal{G}$. By the separating hyperplane theorem, there exists a $\mathbf{c}$ such that $\mathbf{c}'\Delta\mathbf{x}_i \geq 0$, $\forall \Delta\mathbf{x}_i \in \mathcal{G}$ and $\mathbf{c}'(-\mathbf{d}^*) < 0$. Without any loss of generality, let $\|\mathbf{c}\|_2 = 1$, and let $\mathbf{c}'\mathbf{d}^* = \mu$. Note, that $0 < \mu < 1$, strictly less than 1 because $|\mathbf{c}| = |\mathbf{d}^*| = 1$ and $\mathbf{c} \neq \mathbf{d}^*$. The two vectors cannot be the same since $\mathbf{c}'\Delta\mathbf{x}_i \geq 0$ while $\mathbf{d}^{*'}\Delta\mathbf{x}_i < 0$.

Given such a vector $\mathbf{c}$, we can find a solution better than $\mathbf{d}^*$ for the SOCP, which is a contradiction. Consider the vector $\mathbf{q} = \frac{\lambda\mathbf{d}^* - \mathbf{c}}{\|\lambda\mathbf{d}^* - \mathbf{c}\|_2}$. $\|\mathbf{q}\|_2 = 1$, and for every $\Delta\mathbf{x}_i \in \mathcal{G}$, we have

$$
\begin{aligned}
\mathbf{q}'\Delta\mathbf{x}_i \quad &= \quad \frac{\lambda\mathbf{d}^{*'}\Delta\mathbf{x}_i - \mathbf{c}'\Delta\mathbf{x}_i}{\|\lambda\mathbf{d}^* - \mathbf{c}\|_2} \\
&= \quad \frac{\lambda\mathbf{d}^{*'}\Delta\mathbf{x}_i - \mathbf{c}'\Delta\mathbf{x}_i}{\lambda + 1 - 2\lambda\mu} \\
&\leq \quad \frac{\lambda\beta^* - \mathbf{c}'\Delta\mathbf{x}_i}{\lambda + 1 - 2\lambda\mu} \qquad \text{since } \mathbf{d}^{*'}\Delta\mathbf{x}_i \leq \beta^* \\
&\leq \quad \frac{\lambda\beta^*}{\lambda + 1 - 2\lambda\mu} \qquad \text{since } \mathbf{c}'\Delta\mathbf{x}_i \geq 0.
\end{aligned}
$$

We can ensure $\frac{\lambda}{\lambda+1-2\lambda\mu} < 1$ by choosing λ such that $\begin{cases} \frac{1}{2\mu} < \lambda, & \text{if } 0 < \mu \leq \frac{1}{2} \\ \frac{1}{2\mu} < \lambda < \frac{1}{2\mu-1}, & \text{if } \frac{1}{2} < \mu < 1 \end{cases}$.

Therefore, $\mathbf{q}'\Delta\mathbf{x}_i < \beta^*$. Let $\bar{\beta} = \max_i \mathbf{q}'\Delta\mathbf{x}_i$, so $\bar{\beta} < \beta^*$. We have arrived at a contradiction since $(\mathbf{q}, \bar{\beta})$ is a feasible solution in the SOCP and it is strictly better than $(\mathbf{d}^*, \beta^*)$ since $\bar{\beta} < \beta^*$. $\quad\square$

With Proposition 2, Theorem 3 is proved as follows:

Proof of Theorem 3:

We show that applying the algorithm on the robust optimization problem (2.4) is equivalent to applying a subgradient optimization algorithm on a convex problem. From Corollary 1(b), Problem (2.4) is a convex problem with subgradients if $f(\mathbf{x})$ is convex. Next, $-\mathbf{d}^*$ is a subgradient at every iteration because:

(i) $-\mathbf{d}^*$ lies in the convex hull spanned by the vectors $\Delta\mathbf{x}^* \in \mathcal{U}^*(\mathbf{x}^k)$ (see Proposition 2), and

(ii) this convex hull is the subdifferential of $g(\mathbf{x})$ at $\mathbf{x}^k$ (see Corollary 1(b)).

This is illustrated in Fig. 2-5.

Since a subgradient step is taken at every iteration, the algorithm is equivalent to the following subgradient optimization algorithm:

Step 0. Initialization: Let $\mathbf{x}^k$ be an arbitrary decision vector, set $k = 1$.

Step 1. Find subgradient $\mathbf{s}^k$ of $\mathbf{x}^k$. Terminate if no such subgradient exist.

Step 2. Set $\mathbf{x}^{k+1} := \mathbf{x}^k - t^k\mathbf{s}^k$.

Step 3. Set $k := k + 1$. Go to Step 1.

It is commonly known that such a subgradient optimization algorithm converges under the right step-size rule. For example, given Theorem 31 in Reference [52], this subgradient algorithm converges to the global minimum of the convex problem under the stepsize rules: $t^k > 0$, $t^k \to 0$ as $k \to 0$ and $\sum_{k=1}^{\infty} t^k = \infty$. The proof is now complete. $\quad\square$
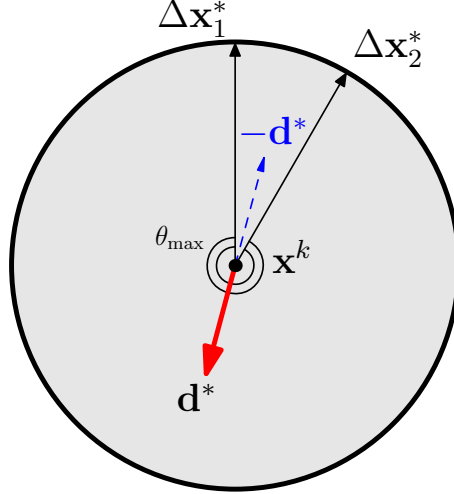
Figure 2-5: $-d^*$ is a subgradient for $g(\mathbf{x})$ because it lies within the cone spanned by $\Delta \mathbf{x}^*$.

2.1.7 Practical Implementation

Finding the set of worst implementation errors $\mathcal{U}^*(\hat{\mathbf{x}})$ equates to finding all the global maxima of the inner maximization problem

$$\max_{\|\Delta \mathbf{x}\|_2 \leq \Gamma} \quad f(\hat{\mathbf{x}} + \Delta \mathbf{x}). \tag{2.12}$$

Even though there is no closed-form solution in general, it is possible to find $\Delta \mathbf{x}^*$ in instances where the problem has a small dimension and $f(\mathbf{x})$ satisfies the Lipschtiz condition [30]. Furthermore, when $f(\mathbf{x})$ is a polynomial function, numerical experiments suggest that $\Delta \mathbf{x}^*$ can be found for many problems in the literature on global optimization [29]. If $\Delta \mathbf{x}^*$ can be found efficiently, the descent directions can be determined. Consequently, the robust optimization problem can be solved readily using Algorithm 2.1.6.

In most real-world instances, however, we cannot expect to find $\Delta \mathbf{x}^*$. Therefore, an alternative approach is required. Fortunately, the following proposition shows that we do not need to know $\Delta \mathbf{x}^*$ exactly in order to find a descent direction.

Proposition 3

Suppose that $f(\mathbf{x})$ is continuously differentiable and $\|\Delta \mathbf{x}^*\|_2 = \Gamma$, for all $\Delta \mathbf{x}^* \in \mathcal{U}^*(\hat{\mathbf{x}})$.
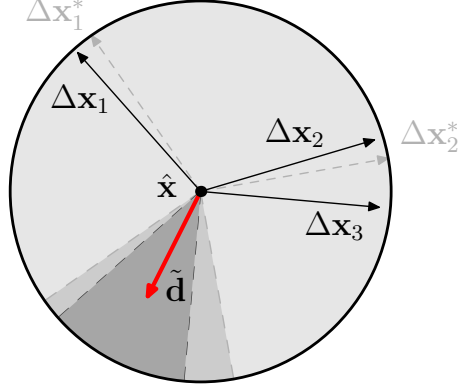
Figure 2-6: The solid bold arrow indicates a direction $\tilde{\mathbf{d}}$ pointing away from all the implementation errors $\Delta\mathbf{x}_j \in \mathcal{M}$, for $\mathcal{M}$ defined in Proposition 3. $\tilde{\mathbf{d}}$ is a descent direction if all the worst errors $\Delta\mathbf{x}_i^*$ lie within the cone spanned by $\Delta\mathbf{x}_j$. All the descent directions pointing away from $\Delta\mathbf{x}_j$ lie within the cone with the darkest shade, which is a subset of the cone illustrated in Fig. 2-1.

Let $\mathcal{M} := \{\Delta\mathbf{x}_1, \ldots, \Delta\mathbf{x}_m\}$ be a collection of $\Delta\mathbf{x}_i \in \mathcal{U}$, where there exists scalars $\alpha_i \geq 0$, $i = 1, \ldots, m$ such that

$$\Delta\mathbf{x}^* = \sum_{i|\Delta\mathbf{x}_i \in \mathcal{M}} \alpha_i \Delta\mathbf{x}_i \tag{2.13}$$

for all $\Delta\mathbf{x}^* \in \mathcal{U}^*(\hat{\mathbf{x}})$. Then, $\mathbf{d}$ is a descent direction for the worst case cost function $g(\mathbf{x} = \hat{\mathbf{x}})$, if

$$\mathbf{d}'\Delta\mathbf{x}_i < 0, \quad \forall\Delta\mathbf{x}_i \in \mathcal{M} . \tag{2.14}$$

Proof of Proposition 3:

Given conditions (2.13) and (2.14),

$$\mathbf{d}'\Delta\mathbf{x}^* = \sum_{i|\Delta\mathbf{x}_i \in \mathcal{M}} \alpha_i \mathbf{d}'\Delta\mathbf{x}_i < 0,$$

we have $\Delta\mathbf{x}^{*'}\mathbf{d} < 0$, for all $\Delta\mathbf{x}^*$ in set $\mathcal{U}^*(\hat{\mathbf{x}})$. Since the "sufficient" conditions in Theorem 1 are satisfied, the result follows. $\square$

Proposition 3 shows that descent directions can be found without knowing the

worst implementation errors $\Delta \mathbf{x}^*$ exactly. As illustrated in Fig. 2-6, finding a set $\mathcal{M}$ such that all the worst errors $\Delta \mathbf{x}^*$ are confined to the sector demarcated by $\Delta \mathbf{x}_i \in \mathcal{M}$ would suffice. The set $\mathcal{M}$ does not have to be unique and if it satisfies Condition (2.13), the cone of descent directions pointing away from $\Delta \mathbf{x}_i \in \mathcal{M}$ is a subset of the cone of directions pointing away from $\Delta \mathbf{x}^*$.

Because $\Delta \mathbf{x}^*$ usually reside among designs with nominal costs higher than the rest of the neighborhood, the following algorithm is a good heuristic strategy to finding a more robust neighbor:

Algorithm 2 Practical Robust Local Search Algorithm

Step 0. Initialization: Let $\mathbf{x}^1$ be an arbitrarily chosen initial decision vector. Set $k := 1$.

Step 1. Neighborhood Search:
Find $\mathcal{M}^k$, a set containing implementation errors $\Delta \mathbf{x}_i$ which gives rise to costs that are among the highest in the neighborhood of $\mathbf{x}^k$.

Step 2. Robust Local Move:
    i. Solve a SOCP (similar to Problem 2.11, but with the set $\mathcal{U}^*(\mathbf{x}^k)$ replaced by set $\mathcal{M}^k$), terminating if the problem is infeasible.
    ii. Set $\mathbf{x}^{k+1} := \mathbf{x}^k + t^k \mathbf{d}^*$, where $\mathbf{d}^*$ is the optimal solution to the SOCP.
    iii. Set $k := k + 1$. Go to Step 1.

This algorithm is the robust local search, to be elaborated upon in the next section.

2.2 Local Search Algorithm when Implementation Errors are present

The robust local search method is an iterative algorithm with two parts in every iteration. In the first part, we explore the neighborhood of the current iterate both to estimate its worst case cost and to collect neighbors with high cost. Next, this knowledge of the neighborhood is used to make a robust local move, a step in the descent direction of the robust problem. These two parts are repeated iteratively until termination conditions are met, which is when a suitable descent direction cannot be found anymore. We now discuss these two parts in more detail.

2.2.1 Neighborhood Search

In this subsection, we describe a generic neighborhood search algorithm employing $n + 1$ gradient ascents from different starting points within the neighborhood. When exploring the neighborhood of $\hat{\mathbf{x}}$, we are essentially trying to solve the inner maximization problem (2.12).

We first apply a gradient ascent with a diminishing step size. The initial step size used is $\frac{\Gamma}{5}$, decreasing with a factor of 0.99 after every step. The gradient ascent is terminated after either the neighborhood is breached or a time-limit is exceeding. Then, we use the last point that is inside the neighborhood as an initial solution to solve the following sequence of unconstrained problems using gradient ascents:

$$\max_{\Delta \mathbf{x}} \quad f(\hat{\mathbf{x}} + \Delta \mathbf{x}) + \epsilon_r \ln\{\Gamma - \|\Delta \mathbf{x}\|_2\}. \tag{2.15}$$

The positive scalar ϵ_r is chosen so that the additional term $\epsilon_r \ln\{\Gamma - \|\Delta \mathbf{x}\|_2\}$ projects the gradient step back into the strict interior of the neighborhood, so as to ensure that the ascent stays strictly within it. A good estimate of a local maximum is found quickly this way.

Such an approach is modified from a barrier method on the inner maximization problem (2.12). Under the standard barrier method, one would solve a sequence of Problem (2.15) using gradient ascents, where ϵ_r are small positive diminishing scalars, $\epsilon_r \to 0$ as $r \to \infty$. However, empirical experiments indicate that using the standard method, the solution time required to find a local maximum is unpredictable and can be very long. Since (i) we want the time spent solving the neighborhood search subproblem to be predictable, and (ii) we do not have to find the local maximum exactly, as indicated by Proposition 3, the standard barrier method was not used. Our approach gives a high quality estimate of a local maximum efficiently.

The local maximum obtained using a single gradient ascent can be an inferior estimate of the global maximum when the cost function is nonconcave. Therefore, in every neighborhood search, we solve the inner maximization problem (2.12) using multiple gradient ascents, each with a different starting point. A generic neighborhood

search algorithm is: for a n-dimensional problem, use $n + 1$ gradient ascents starting from $\Delta \mathbf{x} = \mathbf{0}$ and $\Delta \mathbf{x} = sign(\frac{\partial f(\mathbf{x} = \hat{\mathbf{x}})}{\partial x_i}) \frac{\Gamma}{3} \mathbf{e}_i$ for $i = 1, \ldots, n$, where $\mathbf{e}_i$ is the unit vector along the i-th coordinate.

During the neighborhood search in iteration k, the results of all function evaluations $(\mathbf{x}, f(\mathbf{x}))$ made during the multiple gradient ascents are recorded in a history set $\mathcal{H}^k$, together with all past histories. This history set is then used to estimate the worst case cost of $\mathbf{x}^k$, $\tilde{g}(\mathbf{x}^k)$.

2.2.2 Robust Local Move

In the second part of the robust local search algorithm, we update the current iterate with a local design that is more robust, based on our knowledge of the neighborhood $\mathcal{N}^k$. The new iterate is found by finding a direction and a distance to take, so that all the neighbors with high cost will be excluded from the new neighborhood. In the following, we discuss in detail how the direction and the distance can be found efficiently.

Finding the Direction

To find the direction at $\mathbf{x}^k$ which improves $\tilde{g}(\mathbf{x}^k)$, we include all known neighbors with high cost from $\mathcal{H}^k$ in the set

$$\mathcal{M}^k \quad := \quad \left\{ \ \mathbf{x} \mid \mathbf{x} \in \mathcal{H}^k, \mathbf{x} \in \mathcal{N}^k, f(\mathbf{x}) \geq \tilde{g}(\mathbf{x}^k) - \sigma^k \right\}. \tag{2.16}$$

The cost factor σ^k governs the size of the set and may be changed within an iteration to ensure a feasible move. In the first iteration, σ^1 is first set to $0.2 \times \left(\tilde{g}(\mathbf{x}^1) - f(\mathbf{x}^1) \right)$. In subsequent iterations, σ^k is set using the final value of σ^{k-1}.

The problem of finding a good direction $\mathbf{d}$, which points away from bad neighbors
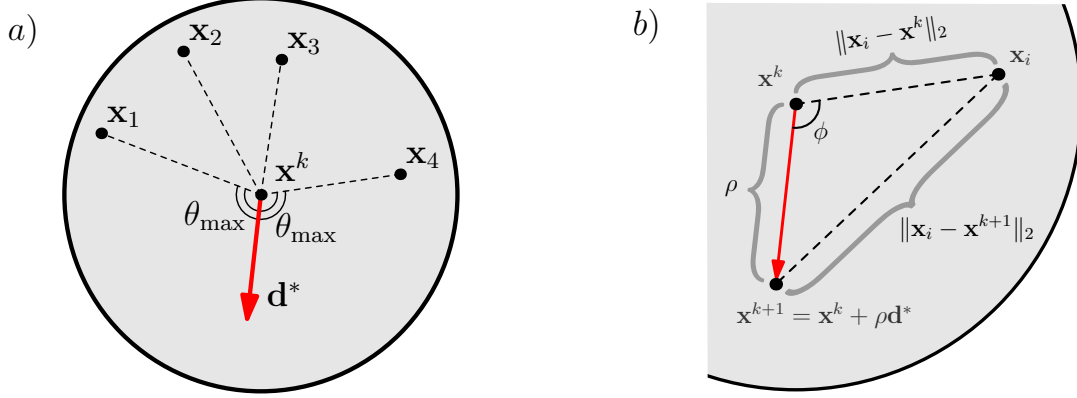
Figure 2-7: a) A 2-D illustration of the optimal solution of the SOCP, Prob. (2.17). Compare with Fig. 2-4. b) Illustration showing how the distance $\|\mathbf{x}_i - \mathbf{x}^{k+1}\|_2$ can be found by cosine rule using ρ, $\mathbf{d}^*$ and $\|\mathbf{x}_i - \mathbf{x}^k\|_2$ when $\mathbf{x}^{k+1} = \mathbf{x}^k + \rho\mathbf{d}^*$. $\cos\phi = \rho(\mathbf{x}_i - \mathbf{x}^k)'\mathbf{d}^*$.

as collected in $\mathcal{M}^k$, can be formulated as a SOCP

$$
\begin{aligned}
\min_{\mathbf{d},\beta} \quad & \beta \\
s.t. \quad & \|\mathbf{d}\|_2 \leq 1 \\
& \mathbf{d}' \left(\frac{\mathbf{x}_i - \mathbf{x}^k}{\|\mathbf{x}_i - \mathbf{x}^k\|_2} \right) \leq \beta \quad \forall \mathbf{x}_i \in \mathcal{M}^k \\
& \beta \leq -\epsilon,
\end{aligned}
\tag{2.17}
$$

where ϵ is a small positive scalar. The discussion for the earlier SOCP (2.11) applies to this SOCP as well.

We want to relate Problem (2.17) with the result in Proposition 3. Note, that $\mathbf{x}_i - \mathbf{x}^k = \Delta\mathbf{x}_i \in \mathcal{U}$ and $\|\mathbf{x}_i - \mathbf{x}^k\|$ is a positive scalar, assuming $\mathbf{x}_i \neq \mathbf{x}^k$. Therefore, the constraint $\mathbf{d}' \left(\frac{\mathbf{x}_i - \mathbf{x}^k}{\|\mathbf{x}_i - \mathbf{x}^k\|} \right) \leq \beta < 0$ maps to the condition $\mathbf{d}'\Delta\mathbf{x}_i < 0$ in Proposition 3, while the set $\mathcal{M}^k$ maps to the set $\mathcal{M}$. Comparison between Fig. 2-4 and Fig. 2-7(a) shows that we can find a descent direction pointing away from all the implementation errors with high costs. Therefore, if we have a sufficiently detailed knowledge of the neighborhood, $\mathbf{d}^*$ is a descent direction for the robust problem.

When Problem (2.17) is infeasible, $\mathbf{x}^k$ is surrounded by "bad" neighbors. However, since we may have been too stringent in classifying the bad neighbors, we reduce σ^k, reassemble $\mathcal{M}^k$, and solve the updated SOCP. When reducing σ^k, we divide it by a

factor of 1.05. The terminating condition is attained, when the SOCP is infeasible and σ^k is below a threshold. If $\mathbf{x}^k$ is surrounded by "bad" neighbors and σ^k is small, we presume that we have attained a robust local minimum, of the type as illustrated in Fig. 2-3(a). and Fig. 2-3(b).

Finding the Distance

After finding the direction $\mathbf{d}^*$, we want to choose the smallest stepsize ρ^* such that every element in the set of bad neighbors $\mathcal{M}^k$ would lie at least on the boundary of the neighborhood of the new iterate, $\mathbf{x}^{k+1} = \mathbf{x}^k + \rho^* \mathbf{d}^*$. To make sure that we make meaningful progress at every iteration, we set a minimum stepsize of $\frac{\Gamma}{100}$ in the first iteration, and decreases it successively by a factor of 0.99.

Figure 2-7(b) illustrates how $\|\mathbf{x}_i - \mathbf{x}^{k+1}\|_2$ can be evaluated when $\mathbf{x}^{k+1} = \mathbf{x}^k + \rho \mathbf{d}^*$ since

$$\|\mathbf{x}_i - \mathbf{x}^{k+1}\|_2^2 = \rho^2 + \|\mathbf{x}_i - \mathbf{x}^k\|_2^2 - 2\rho(\mathbf{x}_i - \mathbf{x}^k)'\mathbf{d}^*.$$

Consequently,

$$
\begin{aligned}
\rho^* &= \arg\min_{\rho} \quad \rho \\
&\quad s.t. \quad \rho \geq \mathbf{d}^{*'}(\mathbf{x}_i - \mathbf{x}^k) + \sqrt{(\mathbf{d}^{*'}(\mathbf{x}_i - \mathbf{x}^k))^2 - \|\mathbf{x}_i - \mathbf{x}^k\|_2^2 + \Gamma^2}, \quad \forall \mathbf{x}_i \in \mathcal{M}^k.
\end{aligned}
$$

$$(2.18)$$

Note, that this problem can be solved with $|\mathcal{M}^k|$ function evaluations without resorting to a formal optimization procedure.

Checking the Direction

Knowing that we aim to take the update direction $\mathbf{d}^*$ and a stepsize ρ^*, we update the set of bad neighbors with the set

$$\mathcal{M}^k_{updated} := \left\{ \mathbf{x} \mid \mathbf{x} \in \mathcal{H}^k, \|\mathbf{x} - \mathbf{x}^k\|_2 \leq \Gamma + \rho^*, f(\mathbf{x}) \geq \tilde{g}(\mathbf{x}^k) - \sigma^k \right\}. \quad (2.19)$$

This set will include all the known neighbors lying slightly beyond the neighborhood, and with a cost higher than $\tilde{g}(\mathbf{x}^k) - \sigma^k$.

We check whether the desired direction $\mathbf{d}^*$ is still a descent direction pointing away from all the members in set $\mathcal{M}^k_{updated}$. If it is, we accept the update step $(\mathbf{d}^*, \rho^*)$ and proceed with the next iteration. If $\mathbf{d}^*$ is not a descent direction for the new set, we repeat the robust local move by solving the SOCP (2.17) but with $\mathcal{M}^k_{updated}$ in place of $\mathcal{M}^k$. Again, the value σ^k might be decreased in order to find a feasible direction. Consequently, within an iteration, the robust local move might be attempted several times. From computational experience, this additional check becomes more important as we get closer to a robust local minimum.

2.3 Application I - A Problem with a Nonconvex Polynomial Objective Function

2.3.1 Problem Description

For the first problem, we chose a polynomial problem. Having only two dimensions, we can illustrate the cost surface over the domain of interest to develop intuition into the algorithm. Consider the nonconvex polynomial function

$$
\begin{aligned}
f_{poly}(x, y) \;=\; & 2x^6 - 12.2x^5 + 21.2x^4 + 6.2x - 6.4x^3 - 4.7x^2 + y^6 - 11y^5 + 43.3y^4 \\
& -10y - 74.8y^3 + 56.9y^2 - 4.1xy - 0.1y^2x^2 + 0.4y^2x + 0.4x^2y.
\end{aligned}
$$

Given implementation errors $\Delta = (\Delta x, \Delta y)$ where $\|\Delta\|_2 \leq 0.5$, the robust optimization problem is

$$
\min_{x,y} \; g_{poly}(x, y) \;\equiv\; \min_{x,y} \max_{\|\Delta\|_2 \leq 0.5} \; f_{poly}(x + \Delta x, y + \Delta y). \tag{2.20}
$$

Note that even though this problem has only two dimensions, it is already a difficult problem [34]. Recently, relaxation methods have been applied successfully
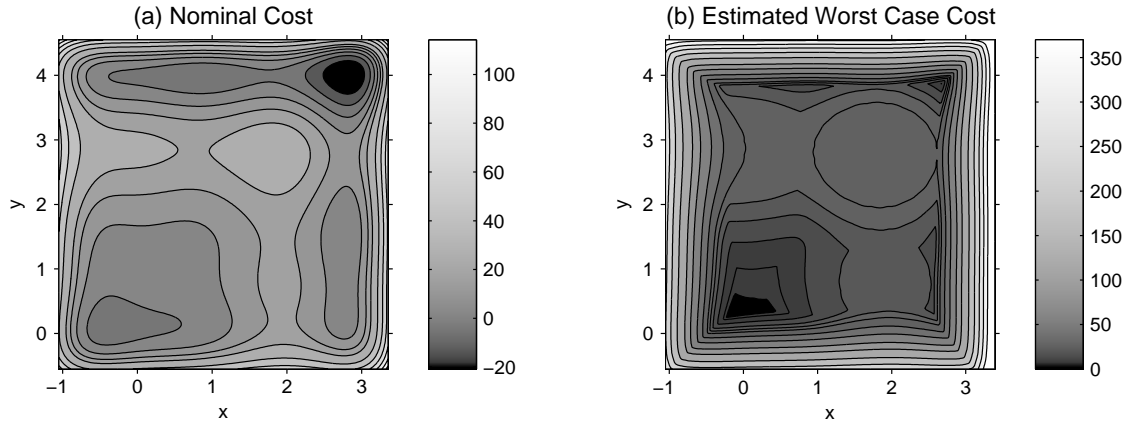
Figure 2-8: Contour plot of nominal cost function $f_{poly}(x, y)$ and the estimated worst case cost function $g_{poly}(x, y)$ in Application I.

to solve polynomial optimization problems [29]. Applying the same technique to Problem (2.20), however, leads to polynomial semidefinite programs (SDP), where the entries of the semidefinite constraint are made up of multivariate polynomials. Solving a problem approximately involves converting it into a substantially larger SDP, the size of which increases very rapidly with the size of the original problem, the maximum degree of the polynomials involved, and the number of variables. In practice, polynomial SDPs from being used widely in practice [33]. Therefore, we applied the local search algorithm on Problem (2.20).

2.3.2 Computation Results

Figure 2-8(a) shows a contour plot of the nominal cost of $f_{poly}(x, y)$. It has multiple local minima and a global minimum at $(x^*, y^*) = (2.8, 4.0)$, where $f(x^*, y^*) = -20.8$. The global minimum is found using the Gloptipoly software as discussed in Reference [29] and verified using multiple gradient descents. The worst case cost function $g_{poly}(x, y)$, estimated by evaluating discrete neighbors using data in Fig. 2-8(a), is shown in Fig. 2-8(b). Fig. 2-8(b) suggests that $g_{poly}(x, y)$ has multiple local minima.

We applied the robust local search algorithm in this problem using two initial design (x, y), A and B; terminating when the SOCP (See Problem (2.17)) remains
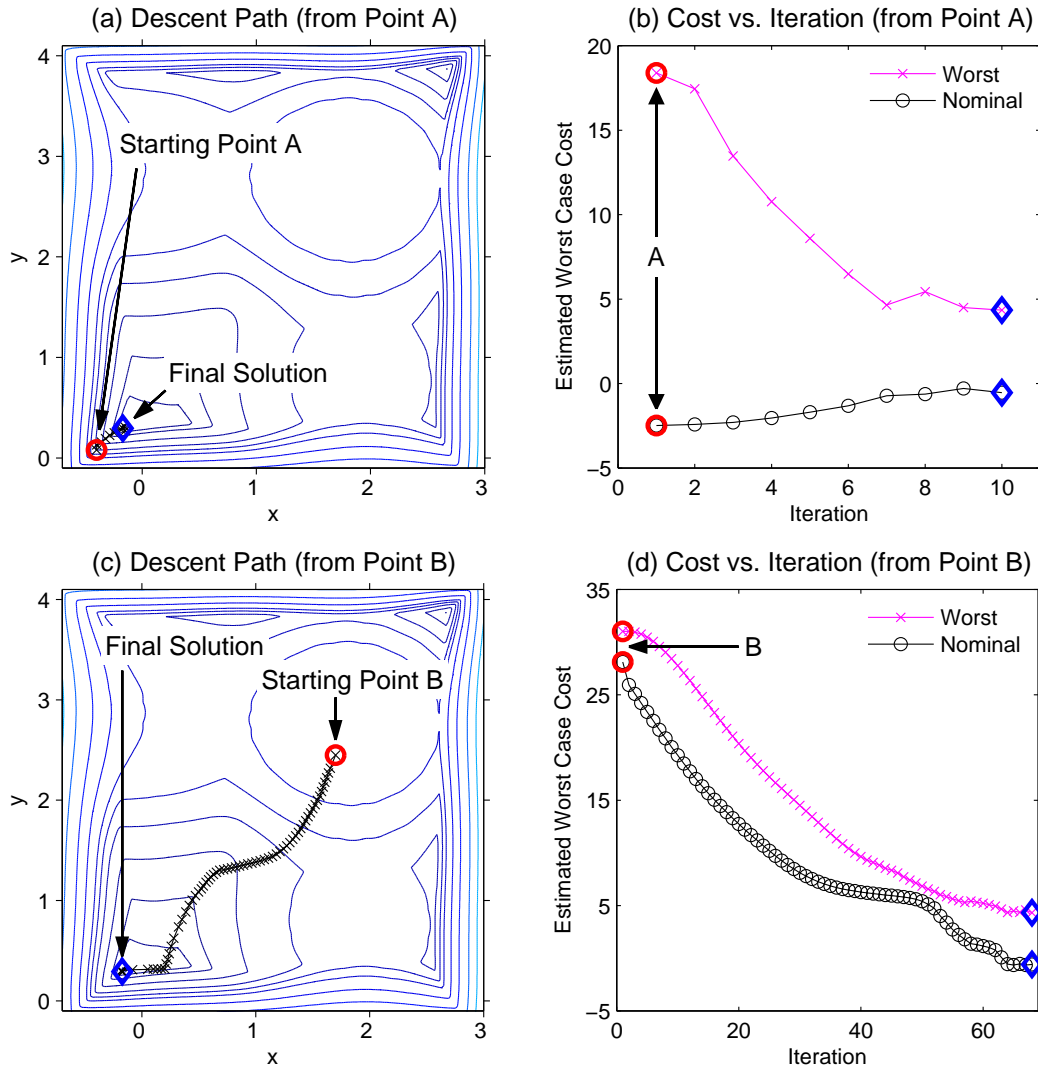
Figure 2-9: Performance of the robust local search algorithm in Application I from 2 different starting points A and B. The circle marker and the diamond marker denote the starting point and the final solution, respectively. (a) The contour plot showing the estimated surface of the worst case cost, $g_{poly}(x, y)$. The descent path taken to converge at the robust solution is shown; point A is a local minimum of the nominal function. (b) From starting point A, the algorithm reduces the worst case cost significantly while increasing the nominal cost slightly. (c) From an arbitrarily chosen starting point B, the algorithm converged at the same robust solution as starting point A. (d) Starting from point B, both the worst case cost and the nominal cost are decreased significantly under the algorithm.
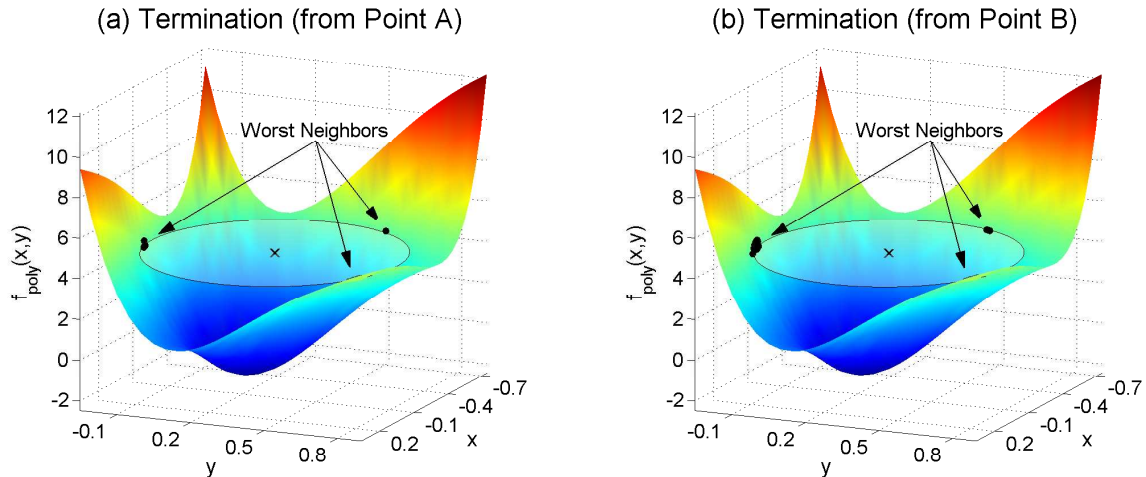
Figure 2-10: Surface plot shows the cost surface of the nominal function $f_{poly}(x, y)$. The same robust local minimum, denoted by the cross, is found from both starting points A and B. Point A is a local minimum of the nominal function, while point B is arbitrarily chosen. The worst neighbors are indicated by black dots. At termination, these neighbors lie on the boundary of the uncertainty set, which is denoted by the transparent discs. At the robust local minimum, with the worst neighbors forming the "supports", both discs cannot be lowered any further. Compare these figures with Fig. 2-3(a) where the condition of a robust local minimum is met

infeasible when σ^k is decreased below the threshold of 0.001. Referring to Fig. 2-9, Point A is a local minimum of the nominal problem, while B is arbitrarily chosen. Fig. 2-9(a) and Fig. 2-9(c) show that the algorithm converges to the same robust local minimum from both starting points. However, depending on the problem, this observation cannot be generalized. Figure 2-9(b) shows that the worst case cost of A is much higher than its nominal cost, and clearly a local minimum to the nominal problem need not be a robust local minimum. The algorithm decreases the worst case cost significantly while increasing the nominal cost slightly. A much lower number of iterations is required when starting from point A when compared to starting from point B. As seen in Fig. 2-9(d), both the nominal and the worst case costs decrease as the iteration count increases when starting from point B. While the decrease in worst case costs is not monotonic for both instances, the overall decrease in the worst case cost is significant.

Figure 2-10 shows the distribution of the bad neighbors upon termination. At

termination, these neighbors lie on the boundary of the uncertainty set. Note, that there is no good direction to move the robust design away from these bad neighbors, so as to lower the disc any further. The bad neighbors form the support of the discs. Compare these figures with Fig. 2-3(a) where Condition (i) of Corollary 2 was met, indicating the arrival at a robust local minimum. The surface plot of the nominal cost function in Fig. 2-10 further confirms that the terminating solutions are close to a true robust local minimum.

2.4 Generalized Method for Problems with Both Implementation Errors and Parameter Uncertainties

In addition to implementation errors, uncertainties can reside in problem coefficients. These coefficients often cannot be defined exactly, because of either insufficient knowledge or the presence of noise. In this section, we generalize the robust local search algorithm to include considerations for such parameter uncertainties.

2.4.1 Problem Definition

Let $f(\mathbf{x}, \bar{\mathbf{p}})$ be the *nominal cost* of design vector $\mathbf{x}$, where $\bar{\mathbf{p}}$ is an estimation of the true problem coefficient $\mathbf{p}$. For example, for the case $f(\mathbf{x}, \bar{\mathbf{p}}) = 4x_1^3 + x_2^2 + 2x_1^2 x_2$, $\mathbf{x} = \begin{pmatrix} x_1 \\ x_2 \end{pmatrix}$ and $\bar{\mathbf{p}} = \begin{pmatrix} 4 \\ 2 \end{pmatrix}$. Since $\bar{\mathbf{p}}$ is an estimation, the true coefficient $\mathbf{p}$ can instead be $\bar{\mathbf{p}} + \Delta\mathbf{p}$, $\Delta\mathbf{p}$ being the parameter uncertainties. Often, the *nominal optimization problem*

$$\min_{\mathbf{x}} \quad f(\mathbf{x}, \bar{\mathbf{p}}), \tag{2.21}$$

is solved, ignoring the presence of uncertainties.

We consider Problem (2.21), where both $\Delta\mathbf{p} \in \mathbb{R}^m$ and implementation errors $\Delta\mathbf{x} \in \mathbb{R}^n$ are present, while further assuming $\Delta\mathbf{z} = \begin{pmatrix} \Delta\mathbf{x} \\ \Delta\mathbf{p} \end{pmatrix}$ lies within the uncertainty

set

$$\mathcal{U} \;=\; \left\{\; \Delta\mathbf{z} \in \mathbb{R}^{n+m} \;\mid\; \|\Delta\mathbf{z}\|_2 \;\leq\; \Gamma \;\right\}. \tag{2.22}$$

As in Eqn. (2.2), $\Gamma > 0$ is a scalar describing the size of perturbations. We seek a robust design $\mathbf{x}$ by minimizing the worst case cost given a perturbation in $\mathcal{U}$,

$$g(\mathbf{x}) \;:=\; \max_{\Delta\mathbf{z}\in\mathcal{U}} \; f\left(\mathbf{x} + \Delta\mathbf{x}, \bar{\mathbf{p}} + \Delta\mathbf{p}\right). \tag{2.23}$$

The *generalized robust optimization problem* is consequently

$$\min_{\mathbf{x}} \; g(\mathbf{x}) \;\equiv\; \min_{\mathbf{x}} \; \max_{\Delta\mathbf{z}\in\mathcal{U}} \; f(\mathbf{x} + \Delta\mathbf{x}, \bar{\mathbf{p}} + \Delta\mathbf{p}). \tag{2.24}$$

2.4.2 Basic Idea Behind Generalization

To generalize the robust local search to consider parameter uncertainties, note that Problem (2.24) is equivalent to the problem

$$\begin{aligned} \min_{\mathbf{z}} \; \max_{\Delta\mathbf{z}} \quad & f(\mathbf{z} + \Delta\mathbf{z}) \\ s.t. \quad & \mathbf{p} = \bar{\mathbf{p}}, \end{aligned} \tag{2.25}$$

where $\mathbf{z} = \left(\begin{smallmatrix}\mathbf{x}\\\mathbf{p}\end{smallmatrix}\right)$. This formulation is similar to Problem (2.4), the robust problem with implementation errors only, but with some decision variables fixed; the feasible region is the intersection of the hyperplanes $p_i = \bar{p}_i$, $i = 1, \ldots, m$.

The graphical perspective is updated to capture these equality constraints and presented in Fig. 2-11. Thus, the necessary modifications to the local search algorithm are:

i. Neighborhood Search : Given a design $\hat{\mathbf{x}}$, or equivalently $\hat{\mathbf{z}} = \left(\begin{smallmatrix}\hat{\mathbf{x}}\\\bar{\mathbf{p}}\end{smallmatrix}\right)$, the neighborhood is

$$\mathcal{N} \;:=\; \{\mathbf{z} \mid \|\mathbf{z} - \hat{\mathbf{z}}\|_2 \leq \Gamma\} \;=\; \left\{\left(\begin{smallmatrix}\mathbf{x}\\\mathbf{p}\end{smallmatrix}\right) \mid \left\|\begin{smallmatrix}\mathbf{x}-\hat{\mathbf{x}}\\\mathbf{p}-\bar{\mathbf{p}}\end{smallmatrix}\right\|_2 \leq \Gamma\right\}. \tag{2.26}$$
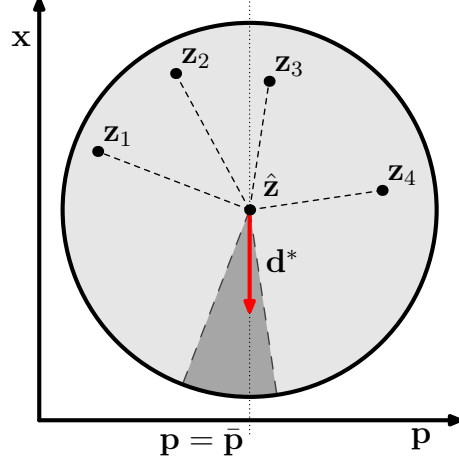
Figure 2-11: A 2-D illustration of Prob. (2.25), and equivalently Prob. (2.24). Both implementation errors and uncertain parameters are present. Given a design $\hat{\mathbf{x}}$, the possible realizations lie in the neighborhood $\mathcal{N}$, as defined in Eqn. (2.26). $\mathcal{N}$ lies in the space $\mathbf{z} = (\mathbf{x}, \mathbf{p})$. The shaded cone contains vectors pointing away from the bad neighbors, $\mathbf{z}_i = (\mathbf{x}_i, \mathbf{p}_i)$, while the vertical dotted denotes the intersection of hyperplanes $\mathbf{p} = \bar{\mathbf{p}}$. For $\mathbf{d}^* = (\mathbf{d}_x^*, \mathbf{d}_p^*)$ to be a feasible descent direction, it must lie in the intersection between the both the cone and the hyperplanes, i.e. $\mathbf{d}_p^* = \mathbf{0}$.

ii. <u>Robust Local Move</u> : Ensure that every iterate satisfies $\mathbf{p} = \bar{\mathbf{p}}$.

2.4.3 Generalized Local Search Algorithm

For ease of exposition, we shall only highlight the key differences to the local search algorithm previously discussed in Section 2.2.

Neighborhood Search

The implementation is similar to that in Section 2.2.1. However, $n + m + 1$ gradient ascents are used instead, since the neighborhood $\mathcal{N}$ now lies in the space $\mathbf{z} = \left(\begin{smallmatrix}\mathbf{x}\\\mathbf{p}\end{smallmatrix}\right)$ (see Fig. 2-11), and the inner maximization problem is now

$$\max_{\Delta \mathbf{z} \in \mathcal{U}} \; f\left(\hat{\mathbf{z}} + \Delta \mathbf{z}\right) \;\; \equiv \;\; \max_{\Delta \mathbf{z} \in \mathcal{U}} \; f\left(\hat{\mathbf{x}} + \Delta \mathbf{x}, \bar{\mathbf{p}} + \Delta \mathbf{p}\right). \tag{2.27}$$

The $n + m + 1$ sequences start from $\Delta \mathbf{z} = \mathbf{0}$, $\Delta \mathbf{z} = sign(\frac{\partial f(\mathbf{x} = \hat{\mathbf{x}})}{\partial x_i})\frac{\Gamma}{3}\mathbf{e}_i$ for $i = 1, \ldots, n$ and $\Delta \mathbf{z} = sign(\frac{\partial f(\mathbf{p} = \bar{\mathbf{p}})}{\partial p_{i-n}})\frac{\Gamma}{3}\mathbf{e}_i$ for $i = n + 1, \ldots, n + m$.

Robust Local Move

At every iterate, the condition $\mathbf{p} = \bar{\mathbf{p}}$ is satisfied by ensuring that the descent direction $\mathbf{d}^* = \begin{pmatrix} \mathbf{d}^*_x \\ \mathbf{d}^*_p \end{pmatrix}$ fulfills the condition $\mathbf{d}^*_p = \mathbf{0}$ (see Fig. 2-11). Referring to the robust local move discussed in Section 2.2.2, we solve the modified SOCP:

$$
\begin{aligned}
\min_{\mathbf{d},\beta} \quad & \beta \\
s.t. \quad & \|\mathbf{d}\|_2 \leq 1 \\
& \mathbf{d}' \begin{pmatrix} \mathbf{x}_i - \mathbf{x}^k \\ \mathbf{p}_i - \bar{\mathbf{p}} \end{pmatrix} \leq \beta \left\| \begin{pmatrix} \mathbf{x}_i - \mathbf{x}^k \\ \mathbf{p}_i - \bar{\mathbf{p}} \end{pmatrix} \right\|_2 \quad \forall \begin{pmatrix} \mathbf{x}_i \\ \mathbf{p}_i \end{pmatrix} \in \mathcal{M}^k \\
& \mathbf{d}_p = \mathbf{0} \\
& \beta \leq -\epsilon,
\end{aligned}
\tag{2.28}
$$

which reduces to

$$
\begin{aligned}
\min_{\mathbf{d}_x,\beta} \quad & \beta, \\
s.t. \quad & \|\mathbf{d}_x\|_2 \leq 1, \\
& \mathbf{d}'_x \left(\mathbf{x}_i - \mathbf{x}^k \right) \leq \beta \left\| \begin{pmatrix} \mathbf{x}_i - \mathbf{x}^k \\ \mathbf{p}_i - \bar{\mathbf{p}} \end{pmatrix} \right\|_2, \quad \forall \begin{pmatrix} \mathbf{x}_i \\ \mathbf{p}_i \end{pmatrix} \in \mathcal{M}^k, \\
& \beta \leq -\epsilon.
\end{aligned}
\tag{2.29}
$$

2.5 Application II - Problem with Implementation and Parameter Uncertainties

2.5.1 Problem Description

To illustrate the performance of the generalized robust local search algorithm, we revisit Application I from Section 2.3 where polynomial objective function is

$$
\begin{aligned}
f_{poly}(x, y) &= 2x^6 - 12.2x^5 + 21.2x^4 + 6.2x - 6.4x^3 - 4.7x^2 + y^6 - 11y^5 + 43.3y^4 \\
&\quad -10y - 74.8y^3 + 56.9y^2 - 4.1xy - 0.1y^2x^2 + 0.4y^2x + 0.4x^2y \\
&= \sum_{\substack{r>0,\ s>0 \\ r+s\leq 6}} c_{rs}x^r y^s.
\end{aligned}
$$

In addition to implementation errors as previously described, there is uncertainty in each of the 16 coefficients of the objective function. Consequently, the objective function with uncertain parameters is

$$\tilde{f}_{poly}(x, y) \;=\; \sum_{\substack{r>0,\ s>0 \\ r+s\le 6}} c_{rs}(1 + 0.05\Delta p_{rs})x^r y^s,$$

where $\Delta \mathbf{p}$ is the vector of uncertain parameters; the robust optimization problem is

$$\min_{x,y} \; g_{poly}(x, y) \;\equiv\; \min_{x,y} \max_{\|\Delta\|_2 \le 0.5} \; \tilde{f}_{poly}(x + \Delta x, y + \Delta y),$$

where $\Delta = \begin{pmatrix} \Delta x \\ \Delta y \\ \Delta \mathbf{p} \end{pmatrix}$.

2.5.2 Computation Results

Observations on the nominal cost surface has been discussed in Application I. Given both implementation errors and parameter uncertainties, the estimated cost surface of $g_{poly}(x, y)$ is shown in Fig. 2-12(a). This estimation is done computationally through simulations using 1000 joint perturbations in all the uncertainties. Fig. 2-12(a) suggests that $g_{poly}(x, y)$ has local minima, or possibly a unique local minimum, in the vicinity of $(x, y) = (0, 0.5)$.

We applied the generalized robust local search algorithm on this problem starting from the global minimum of the nominal cost function $(x, y) = (2.8, 4.0)$. Figure 2-12(b) shows the performance of the algorithm. Although the initial design has a nominal cost of -20.8, it has a large worst case cost of 450. The algorithm finds a robust design with a significantly lower worst case cost. Initially, the worst case cost decreases monotonically with increasing iteration count, but fluctuates when close to convergence. On the other hand, the nominal cost increases initially, and decreases later with increasing iteration count.

Figure 2-12(a) shows that the robust search finds the region where the robust local minimum is expected to reside. The inset in Fig. 2-12(b) shows the path of the robust search "escaping" the global minimum. Because the local search operates on
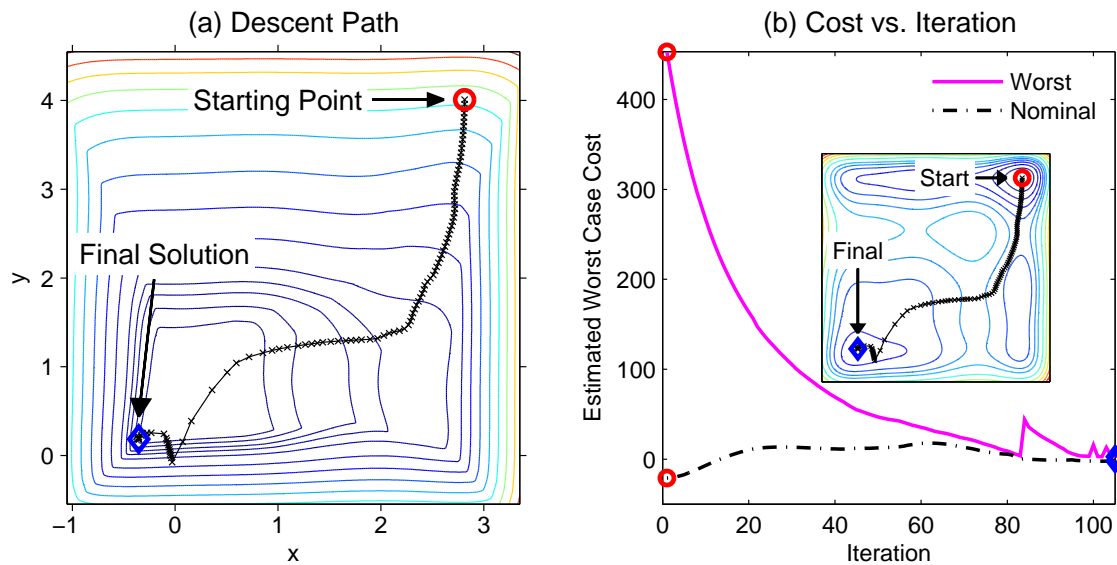
Figure 2-12: Performance of the generalized robust local search algorithm in Application II. (a) Path taken on the estimated worst case cost surface $g_{poly}(x,y)$. Algorithm converges to region with low worst case cost. (b) The worst cost is decreased significantly; while the nominal cost increased slightly. Inset shows the nominal cost surface $f_{poly}(x,y)$, indicating that the robust search moves from the global minimum of the nominal function to the vicinity of another local minimum.

the worst cost surface in Fig. 2-12(a) and not the nominal cost surface in the inset of Figure 2-12(b), such an "escape" is possible.

2.6 Improving the Efficiency of the Robust Local Search

For a large-scale problem, the computation effort of the robust local search can be significant. Moreover, multiple robust local searches can be required. Therefore, it is natural to consider ways that can improve the efficiency of the robust local search. This section discusses a number of possibilities.

Neighborhood Search From empirical observations, the most time-consuming step is the neighborhood search, because multiple gradient ascents are used to solve the nonconvex inner maximization problem (2.12). The following strategies can be considered to improve the efficiency in this aspect:

(a) Reducing number of gradient ascents: In the local search algorithm, $n + 1$ gradient ascents are carried out when the perturbations has n dimensions (See Section 2.2.1). Clearly, if the cost function is less nonlinear over the neighborhood, less gradient ascents will suffice in finding the bad neighbors. However, the converse is also true. Therefore, for a particular problem, one can investigate empirically the tradeoff between the depth of neighborhood search (i.e., number of gradient ascents) and the overall run-time required for robust optimization.

We investigate this tradeoff using Application II (see Section 2.5) with (i) the standard $n+1$ gradient ascents, (ii) $10+1$, and (iii) $3+1$ gradient ascents, in every iteration. The dimension of the perturbation, n is 18: 2 for implementation errors and 16 for parameter uncertainties. Case (i) has been discussed in Section 2.2.1 and serves as the benchmark. In case (ii), 1 ascent starts from $\mathbf{z}^k$, while the remaining 10 start from $\mathbf{z}^k + sign\left(\frac{\partial f(\mathbf{z}^k)}{\partial z_i}\right)\frac{\Gamma}{3}\mathbf{e}_i$, where i denotes coordinates with the 10 largest partial derivatives $\left|\frac{\partial f(\mathbf{z}^k)}{\partial z_i}\right|$. This strategy is similarly applied in
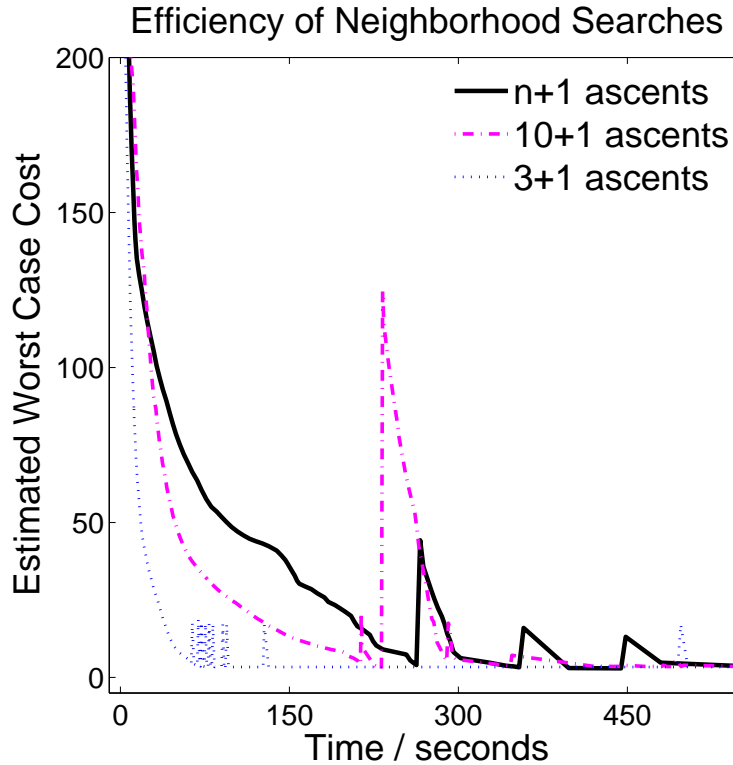
Figure 2-13: Performance under different number of gradient ascents during the neighborhood search in Application II. In all instances, the worst case cost is lowered significantly. While the decrease is fastest when only $3+1$ gradient ascents are used, the terminating conditions were not attained. The instance with $10+1$ gradient ascents took the shortest time to attain convergence.

case (iii), but on coordinates with the 3 largest partial derivatives.

As shown in Fig. 2-13, the worst case cost is lowered in all three cases. Because of the smaller number of gradient ascents per iteration, the initial decrease in worst case cost is the fastest in case (iii). However, the algorithm in case (iii) fails to converge long after terminating conditions have been attained in the other two cases. In this example, case (ii) took the shortest time, taking 550 seconds to converge compared to 600 seconds in case (i). The results seem to indicate that depending on the problem, the efficiency of the algorithm can be improved by using a smaller number of gradient ascents.

Unfortunately, we do not know the best number of gradient ascents a priori. Furthermore, if too few gradient ascents are used, terminating conditions might

not be attained because the algorithm may fail to appreciate the true features of the cost surface.

(b) Parallel processing: The multiple gradient ascents can be carried out independently on different processors. Implemented on a parallel processing platform, the neighborhood search can take a fraction of the time required otherwise.

(c) Terminating redundant gradient ascents: The gradient ascent is a deterministic algorithm. From the same point, separate gradient ascents would make identical moves under the same step size. In the neighborhood search, it is reasonable to expect that two or more gradient ascents would converge to bad neighbors that are close by, once they visit iterates that are close to each other. If a gradient ascent has explored a subset of the neighborhood, it may not be cost-effective to check it again. Therefore, during the gradient ascent, it may be worthwhile to check whether the algorithm is visiting points which has been encountered before in previous gradient ascents, and truncating early if that is the case.

Handling Large History Set $\mathcal{H}^k$ Under the robust local search, the history set $\mathcal{H}^k$ can become very large, especially after many iterations have been carried out. A large history set reduces the efficiency of both the algorithm (i.e. when retrieving neighboring designs from history) and the processor (i.e. when saving history set to the hard-disk), resulting in a longer run-time. A few practical ways to mitigate this issue include:

(a) Removing redundant designs: When the history set is large, there can be many clusters of designs in it. A cluster consists of numerous designs that are close together (measured by distance in the design space). It is reasonable to assume that little difference is made to the robust local search, if the design with the highest cost within the cluster is retained, while the rest are purged.

(b) Checking before adding designs: This strategy tries to prevent clusters of designs from forming. Before adding a design to the history set, an additional algorithm will make sure that it is sufficiently far away from all the designs within the set.

(c) Removing designs with low objective costs: Because the robust local search considers the worst case cost, only designs with high costs make a difference in the algorithm. To reduce the history set, a design with a cost lower than the nominal cost of the current iterate can be removed and stored in a separate archive set.

(d) Removing designs that are far away: After numerous iterations, the current iterate might be far away from designs evaluated earlier. Furthermore, if the worst case cost has been dropping, future iterations should not revisit the vicinities of these initial neighbors. Therefore, these redundant designs can be carefully removed from the history set, and be stored in a separate archive set.

However, it is important to understand the processing overhead introduced in these enhancement strategies. The right strategy to use depends on the problem and the computing environment. The best approach may be to use the robust local search without these strategies.

2.7 Robust Optimization for Problems Without Gradient Information

The robust local search can be applied to many practical problems because only a generic assumption is made: the cost and the gradient is available for any design. To admit even more problems, this assumption can be further relaxed, to the case where gradient is not available.

The gradient information is used only in the neighborhood search, when the inner maximization problem (2.12) is solved with multiple gradient ascents. Therefore, if Problem (2.12) can be solved adequately using nonderivative techniques, then the robust local search can be used without further modifications.

Optimization without a gradient is a rich area of research with interesting results, we will just mention two possible approaches here. When gradient is not available, Problem (2.12) can be solved using (i) gradient ascents with finite-difference gradient estimates [43], and (ii) ascents using the Simultaneous Perturbation Gradient Approx-

imation (SPSA) [55] technique, both from multiple starting points. However, using such nonderivative techniques in the robust local search would result in a longer runtime in general, compared to the case where gradient information is available cheaply.

2.8   Conclusions

We have developed a general robust optimization technique, applicable to nonconvex and simulated-based problems. It makes only one generic assumption: the availability of a subroutine which provides the objective cost as well as the gradient, given a design. Consequently, the technique is applicable to many practical problems, where current robust techniques fail.

The technique takes a new approach to robust optimization. Instead of assuming a problem structure and exploiting it, we operate directly on the surface of the objective function. We discover that, in a problem with implementation errors, a descent direction of the robust problem at any design must point away from all the design's worst neighbors. Naturally, when no such direction exists, the design is a robust local minimum. The proposed robust local search algorithm uses these conditions in a practical manner. It iteratively moves along descent directions and terminates at a robust local minimum. The quality of this algorithm is supported by a convergence result: in a convex problem, if the worst neighbors can always be found for any design, this algorithm is a subgradient optimization algorithm for the *robust* problem, and converges to the robust global minimum.

When parameter uncertainties are present, the basic idea behind the robust local search does not change. At a design, a descent direction for the robust problem is still pointing away from all the worst errors. However, because there are more uncertainties, additional effort is required to locate the worst errors.

The performance of the technique is demonstrated in two applications. Both problems have the same nonconvex polynomial objective. Implementation errors are considered in Application I, while both implementation and parameter uncertainties are considered in Application II. In both problems, the robust local search significantly

reduces the worst case cost (50-90% reduction) and finds the robust local minima.

Chapter 3

Nonconvex Robust Optimization in Nano-Photonics

Optimization is widely used in engineering design. While the need to address uncertainty in optimization is well recognized, robust optimization is, however, seldom adopted. There remains a huge gulf between the robust optimization techniques developed to date, and problems in the real-world. While the robust models, found in literature today [1, 4, 7, 8], assume the problem is convex and defined with linear, convex quadratic, conic-quadratic and semidefinite functions, an increasing number of engineering design problems in reality, besides being nonconvex, involve the use of computer-based simulations. In simulation-based applications, the relationship between the design and the outcome is not defined as functions used in mathematical programming models. Instead, that relationship is embedded within complex numerical models such as PDE solvers [13, 14], response surface, radial basis functions [31] and kriging metamodels [53]. Consequently, the robust techniques in the literature cannot be applied to important problems in engineering analysis and design today.

Our proposed robust optimization technique takes an entirely new approach to finding robust designs. Instead of assuming a simple or special problem structure, and proceeding to exploit it, the technique operates on the objective cost surface directly. Because of this generic nature, the proposed method is applicable to a wide range of practical problems, convex or not. In this chapter, we describe the application

of the robust local search in an actual real-world problem of substantial size. The engineering problem involved is an electromagnetic scattering design problem with a 100-dimensional design space. The result shows that the proposed robust optimization method improves the robustness significantly, while maintaining optimality of the nominal solution.

The search for attractive and novel materials in controlling and manipulating electromagnetic field propagation has identified a plethora of unique characteristics in photonic crystals (PCs). Their novel functionalities are based on diffraction phenomena, which require periodic structures. While three-dimensional PC structures are still far from commercial manufacturing, two-dimensionally periodic PCs have already been introduced to integrated-device applications, e.g. through PC fibers [58]. However, technical difficulties such as ability to manufacture and disorder control pose restrictions on functionality and versatility. Upon breaking the spatial symmetry, new degrees of freedom are revealed which allow for additional functionality and, possibly, for higher levels of control. Previous studies introduced the broken symmetry to PC structures of dielectric scatterers by diluting sites and optimizing the location of the missing scattering sites. Because of the underlying periodic structure, the additional degrees of freedom and, hence, their benefit have been very restricted [23, 28, 50]. More recently, unbiased optimization schemes were performed on the spatial distribution (aperiodic) of a large number of identical dielectric cylinders [26, 51]. The resulting aperiodic structure, using an effective gradient-based optimization was reported to match a desired target function up to 95% [51].

When implemented in the real-world, however, the performance of many engineering designs often deviates from the predicted performance in the lab. A key source of this deviation lies in the presence of uncontrollable implementation errors. Traditionally, a sensitivity or post-optimality analysis was performed to study the impact of perturbations on specific designs. While such an approach can be used to compare designs, it does not intrinsically find one with lower sensitivities. Another class of robust design methods explored interactions between the uncertainties and the design variables by conducting a series of designed experiments [35, 57]. This approach

can fail for highly nonlinear systems with a large number of design variables [12]. Alternatively, the original objective function was replaced with a statistical measure consisting of expected values and standard deviations [46]. This method requires the knowledge of the probability distribution governing the errors, which usually cannot be easily obtained. Another approach suggested adding the first and, possibly, the second order approximation terms to the objective function [56]. Consequently, this is not suitable for highly nonlinear systems with sizeable perturbations. At the other end of the spectrum, the mathematics programming community has made much advances in the area of robust optimization over the past decade [4, 8]. However, their results are confined to problems with more structures; for example, convex problems defined with linear, convex quadratic, conic-quadratic and semidefinite functions. Since our intention is not to review the rich literature in robust, convex optimization, we refer interested readers to References [4, 44].

The proposed robust local search is a novel robust optimization method applicable to electromagnetic scattering problems with large degrees of freedom. In this application, the technique is applied to the optimization of an aperiodic dielectric structure. Previous optimization efforts in this area [51] did not take into account implementation errors that can lead to suboptimal solutions. Applicable of robust optimization inherently improves the robustness of the optimized solution with respect to relevant errors and is suitable for real-world implementation. The objective is to mimic a desired power distribution along a target surface. Our model is based on a two-dimensional Helmholtz equation for lossless dielectric scatterers. Therefore, this approach scales with frequency and allows to model nanophotonic design. The chapter is structured as follows.

Structure of the chapter: In Section 3.1, we describe in detail how the electromagnetic scattering of an aperiodic dielectric structure is modeled. In Section 3.2, we define the robust optimization problem and carry out the robust local search. The result obtained is also reported. Because sensitivity analysis is often performed in engineering problems, we carry out such an analysis for the robust design, and report
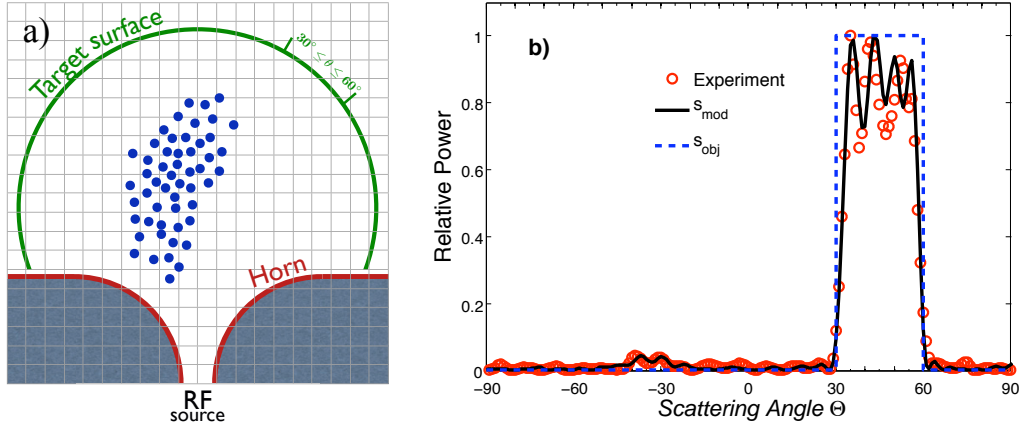
Figure 3-1: (a) the desired top-hat power distribution along the target surface.. (b) schematic setup: the RF-source couples to the wave guide. Blue circles sketch the positions of scattering cylinders for a desired top-hat power profile.

the result in Section 3.3. In Section 3.4 we present our conclusions.

3.1 Model

To study the real-world aspect of robust optimization in design of dielectric structures, we adapted our model to actual laboratory experiments such as in Reference [51]. The incoming electromagnetic field couples in its lowest mode to the perfectly conducting metallic wave-guide (Dirichlet boundary conditions, therefore only the lowest transverse electric mode $TE_{1,0}$). Figure 3-1(b) sketches the horizontal set-up. In the vertical direction, the domain is bound by two perfectly conducting plates, which are separated by less than 1/2 the wave length, in order to warrant a two-dimensional wave propagation. Identical dielectric cylinders are placed in the domain between the plates. The sides of the domain are open in the forward direction. In order to account for a finite total energy and to warrant a realistic decay of the field at infinity, the open sides are modeled by perfectly matching layers [32, 5]. The objective of the optimization is to determine the position of the cylinders such that the forward electromagnetic power matches the shape of a desired power distribution, as shown in Fig. 3-1(a).

68

For the power distribution, the electromagnetic field over the entire domain, including the scattering cylinders, is determined. As in the experimental measurements, the frequency is fixed to $f = 37.5$ GHz [51]. Furthermore, the dielectric scatterers are nonmagnetic and lossless. Therefore, stationary solutions of the Maxwell equations are given through the two-dimensional Helmholtz equations, taking the boundary conditions into account. This means, that only the z-component of the electric field E_z can propagate in the domain. The magnitude of E_z in the domain is given through the partial differential equation (PDE)

$$(\partial_x(\mu_{r_y}^{-1}\partial_x) + \partial_y(\mu_{r_x}^{-1}\partial_y))E_z - \omega_0^2\mu_0\epsilon_0\epsilon_{r_z}E_z = 0 \qquad (3.1)$$

with μ_r the relative and μ_0 the vacuum permeability. ϵ_r denotes the relative and ϵ_0 the vacuum permittivity. Equation (3.1) is numerically determined using an evenly meshed square-grid (x_i, y_i). The resulting finite-difference PDE approximates the field $E_{z,i,j}$ everywhere inside the domain including the dielectric scatterers. The imposed boundary conditions (Dirichlet condition for the metallic horn and perfectly matching layers) are satisfied. This linear equation system is solved by ordering the values of $E_{z,i,j}$ of the PDE into a column vector. Hence, the finite-difference PDE can be rewritten as

$$\mathbf{L} \cdot \mathbf{E}_z = \mathbf{b} , \qquad (3.2)$$

where $\mathbf{L}$ denotes the finite-difference matrix, which is complex-valued and sparse. $\mathbf{E}_z$ describes the complex-valued electric field, that is to be computed and $\mathbf{b}$ contains the boundary conditions. With this, the magnitude of the field at any point of the domain can be determined by solving the linear system of Eq. (3.2).

The power at any point on the target surface $(x(\theta), y(\theta))$ for an incident angle θ is computed through interpolation using the nearest four mesh points and their standard Gaussian weights $\mathbf{W}(\theta)$ with respect to $(x(\theta), y(\theta))$ as

$$s_{\mathbf{mod}}(\theta) = \frac{\mathbf{W}(\theta_k)}{2} \cdot \mathbf{diag}(\mathbf{E_z}) \cdot \mathbf{E_z} . \qquad (3.3)$$
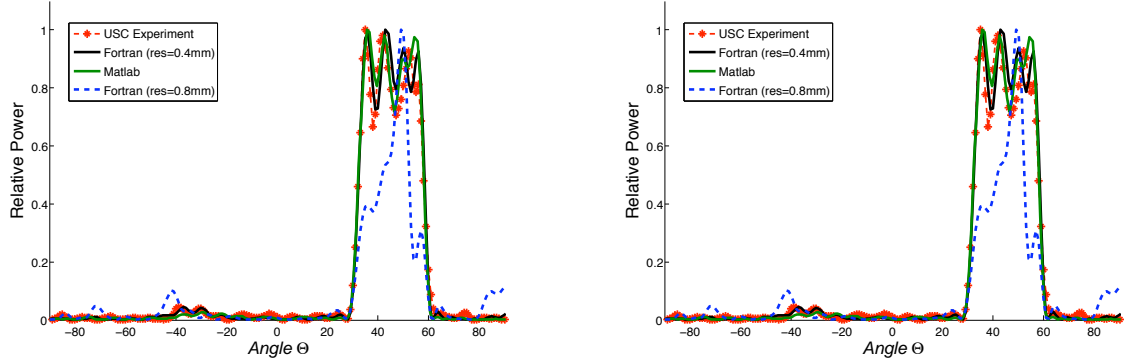
Figure 3-2: Comparison between experimental data (circles) [51] and simulations in a) linear and b) logarithmic scale. The solid lines are simulation results for smallest mesh-size at $\Delta = 0.4mm$, and the dashed lines for $\Delta = 0.8mm$.

In the numerical implementation, we utilized the UMFPACK-library to LU decompose **L** as well as to solve the linear system directly [20]. Furthermore, our implementation uses the Goto-BLAS library for basic vector and matrix operations [27]. By exploiting the sparsity of **L**, we improved the efficiency of the algorithm significantly. In fact, the solution of a realistic forward problem ($\sim 70,000 \times 70,000$ matrix), including 50 dielectric scatterers requires about 0.7 second on a commercially available Intel Xeon 3.4 GHz. Since the size of **L** determines the size of the problem, the computational efficiency of our implementation is independent of the number of scattering cylinders.

To verify this finite-difference technique for the power along the target surface (radius = 60 mm from the domain center), we compared our simulations with experimental measurements from Reference [51] for the same optimal arrangement of 50 dielectric scatterers ($\epsilon_r = 2.05$ and 3.175 ± 0.025 diameter). Figure 3-2(a) illustrates the good agreement between experimental and model data on a linear scale for an objective top-hat function. The log-scale in Figure 3-2(b) emphasizes the relative intensities of the side-lobes to the peak. This comparison also shows that the simulation agrees well with experimental measurements only for a sufficiently small mesh-size of $\Delta = 0.4mm \leq \lambda_0/20$.

3.2   Robust Optimization Problem

By varying the positions of 50 scattering cylinders a top-hat power profile over the target surface, as shown in Fig. 3-1(a), is sought. The desired objective function is denoted by $s_{\mathbf{obj}}$. A cylinder configuration is given by a vector $\mathbf{p} \in \mathbb{R}^{100}$. The actual power profile along the target surface $s_{\mathbf{mod}}$ is computed using Equation (3.3). For any given discretized angle θ_k and configuration $\mathbf{p}$, a cost-functional J measures the deviation of $s_{\mathbf{mod}}$ from $s_{\mathbf{obj}}$ through

$$J(\mathbf{p}) = \sum_{k=1}^{m} |s_{\mathbf{mod}}(\theta_k) - s_{\mathbf{obj}}(\theta_k)|^2 . \qquad (3.4)$$

Therefore, the optimization problem is to minimize the area between $s_{\mathbf{obj}}$ and $s_{\mathbf{mod}}$. This *nominal optimization problem* is given through

$$\min_{\mathbf{p} \in \mathcal{P}} J(\mathbf{p}). \qquad (3.5)$$

The minimization is with respect to the configuration vector $\mathbf{p}$ from a feasible set $\mathcal{P}$. Note that $J(\mathbf{p})$ is not convex in $\mathbf{p}$, and depends on $\mathbf{p}$ only over the linear system $\mathbf{L}(\mathbf{p}) \cdot \mathbf{E}_z(\mathbf{p}) = \mathbf{b}$.

It needs to be emphasized that $\mathcal{P}$ is not a convex set. Instead, $\mathcal{P}$ is a 100 dimensional hypercube containing a large number of non-empty infeasible subsets, which represent non-physical configurations with overlapping cylinders. Defining these infeasible subsets explicitly through introducing constraints in the optimization problem (3.5) is not practical due to the large number of constraints required. We took the alternative approach of avoiding configurations with overlapping cylinders.

To consider possible implementation errors $\Delta\mathbf{p}$, the *robust optimization problem* is defined as

$$\min_{\mathbf{p} \in \mathcal{P}} \max_{\Delta\mathbf{p} \in \mathcal{U}} J(\mathbf{p} + \Delta\mathbf{p}). \qquad (3.6)$$

The uncertainty set $\mathcal{U}$ contains all the implementation errors, against which we want to protect the design. Therefore, the robust optimization problem minimizes the worst

case cost under implementation error. These errors can arise due to misplacement of the scattering cylinders in laboratory experiments or actual manufacturing of the design.

We adopted a two-step strategy. In the first step, a good configuration to the nominal optimization problem in Eq. (3.5) is found. This configuration is used as an initial solution to the second step, since, with all factors being equal, a configuration with a low *nominal cost* $J(\mathbf{p})$ will have a low *worst case cost* $\max_{\Delta\mathbf{p}\in\mathcal{U}} J(\mathbf{p} + \Delta\mathbf{p})$. In the second step, we iteratively update the configuration under evaluation with a more robust configuration through a local shift until terminating conditions are satisfied. This robust optimization algorithm does not assume any problem intrinsic structures. We first discuss the nominal problem before we continue with the robust optimization problem.

3.2.1 Nominal Optimization Problem

To solve the nominal Problem (3.5), we conducted a large number of random searches. Because of the large dimensionality, a coarse-grained random search did not deliver a significant and sufficiently fast improvement in $\min_{\mathbf{p}\in\mathcal{P}} J(\mathbf{p})$. Therefore, we developed two alternative algorithms that efficiently returned a good solution to the nominal optimization problem, as required in Step 1 of the robust optimization method.

Gradient Free Stochastic Algorithm

The first algorithm is adapted from the Simultaneous Perturbation Stochastic Approximation (SPSA) algorithm [55]. It relies only on function evaluations $J(\mathbf{p})$. Under general conditions, SPSA converges to a local minimum more efficiently, in expectation, than a gradient descent approach using finite-difference gradient estimates [55].

In iteration k, the algorithm seeks a better configuration along a direction $\mathbf{d}^k$ emanating from the configuration vector $\mathbf{p}^k$. The direction $\mathbf{d}^k$ is a random vector generated from a symmetric Bernoulli distribution where $P(d_i^k = \pm 1) = \frac{1}{2}$, $\forall i$, and is deemed acceptable only when $\mathbf{p}^k \pm t^k \mathbf{d}^k$ is feasible. Here, d_i^k is the i-th coordinate of

$\mathbf{d}^k$ and t^k is a small positive scalar decreasing with k. Next, $\delta^k = J(\mathbf{p}^k + t^k\mathbf{d}^k) - J(\mathbf{p}^k - t^k\mathbf{d}^k)$ is evaluated. Consequently, $\mathbf{p}^{k+1}$ is set to $\mathbf{p}^k - \alpha^k\delta^k\mathbf{d}^k$, where α^k is another small positive scalar decreasing with k. Note that δ^k approximates the directional gradient $\mathbf{d}^k \cdot \nabla_\mathbf{p}J(\mathbf{p} = \mathbf{p}^k)$, if t^k is small enough.

Modified Gradient Descent Algorithm

We computed the gradient of the cost-functional $\nabla_\mathbf{p}J$ using the adjoint method. In general, since the linear operator $\mathbf{L}$ maps the entire vector space $\mathcal{C}^n \leftrightarrow \mathcal{C}^n$, the components of the cost-functional gradient can be determined from the equations (3.3) and (3.4) through the adjoint equation as

$$
\begin{aligned}
\frac{\partial J}{\partial p_i} &= \left\langle \mathbf{g} \,\middle|\, \frac{\partial E}{\partial p_i} \right\rangle \quad \text{with } \mathbf{g} = \frac{\partial J}{\partial s_{\text{mod}}}\frac{\partial s_{\text{mod}}}{\partial E} \\
&= -\left\langle \mathbf{h} \,\middle|\, \frac{\partial \mathbf{L}}{\partial p_i} E \right\rangle \quad \text{with } \mathbf{L}^* \cdot \mathbf{h} = \mathbf{g}.
\end{aligned}
\tag{3.7}
$$

Note, that $\mathbf{L}^*$ is the adjoint operator to $\mathbf{L}$, which was regularized in the implementation to warrant that J is differentiable. Therefore, in order to compute the gradient, we have to solve the adjoint linear system $\mathbf{L}^* \cdot \mathbf{h} = \mathbf{g}$. This equation has the same structure and uses the same linear operator as the linear system for the function evaluation in Eq. (3.2). Consequently, we exploited the structure of the problem and utilize the LU decomposition of $\mathbf{L}$ for both the function and the gradient evaluation at practically no additional computational cost.

For this optimization problem, standard gradient descent steps quickly led to infeasible configurations and terminated at solutions with high cost. Nevertheless, gradient information is pertinent. To make use of it, we modified the standard algorithm to avoid configurations with overlapping cylinders. These modifications are: (1) if a gradient step leads to an infeasible configuration, the step size is repeatedly halved until a threshold, or (2) otherwise, apply the gradient step only to those cylinders that would not overlap. If the threshold is consistently breached, the algorithm approximates a coordinate descent algorithm which has similar convergence properties
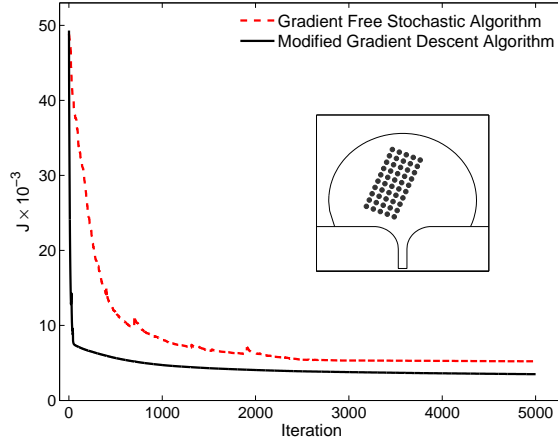
Figure 3-3: Performance comparison between the gradient free stochastic algorithm and the modified gradient descent algorithm on the nominal problem. Results show that modified gradient descent is more efficient and converges to a better solution.

to standard gradient descent [37].

3.2.2 Nominal Optimization Results

The starting configuration for the optimization is obviously significant for the performance. Due to the high-dimensional and non-convex response surface, a global optimum can only be found through large-scale random searches, which is computationally exhaustive and, thus, beyond the scope of this work. Randomly generated initial configurations often lead to overlapping cylinders. These infeasible arrangements can only be overcome by human intervention, which we intended to omit. The performance of a large number of regular PC-like structures with and without random perturbation was simulated to obtain the best starting configuration. The inset of Figure 3-3 illustrates this initial arrangement of the dielectric scattering cylinders, as it appears to be an intuitively good structure as well.

We applied the gradient free stochastic algorithm and the modified gradient descent algorithm to this initial configuration. Figure 3-3 shows that the modified gradient descent algorithm reduces the objective function more efficiently. The gradient-free algorithm took ~ 2500 iterations to converge to an objective value of 0.0052. In contrast, the modified gradient algorithm required ~ 750 iterations to obtain con-

figurations with a cost lower than 0.0052; it eventually converged to a configuration with a cost of 0.0032.

It is not surprising that the modified gradient descent algorithm outperforms the gradient free stochastic algorithm. Note, that at each iteration step, the gradient free algorithm uses two function evaluations and twice the time as compared to the modified gradient descent algorithm. The gradient free algorithm does not decrease the objective value monotonically, because, at any step, c^k and α^k may be too large. Adopting a strategy employing smaller scalars can alleviate the spikes but increase the overall time required to converge. Nevertheless, it is worthwhile to note the viability of using a gradient free optimization approach, since an efficient cost-functional gradient for such high-dimensional problems is not always available.

When the iteration count is high, both algorithms improve the objective value monotonically, albeit very slowly because infeasible configurations are encountered more often. Once the improvement rate went below a certain threshold, we terminated the search and used the final nominal configuration as the initial configuration for the robust optimization method.

3.2.3 Robust Local Search Algorithm

In laboratory experiments, implementation errors $\Delta\mathbf{p}$ are encountered, when physically placing the cylinders. To include most of the errors, we define the uncertainty set $\mathcal{U}$ such that the probability $P(\Delta\mathbf{p} \in \mathcal{U}) = 99\%$. Consequently,

$$\mathcal{U} \;=\; \left\{ \Delta\mathbf{p} \mid \|\Delta\mathbf{p}\|_2 \leq \Gamma \right\}, \tag{3.8}$$

where Δp_i is assumed to be independently and normally distributed with mean 0 and standard deviation $40\mu m$, as observed in experiments [36]. We chose Γ to be $550\mu m$.

Evaluating the worst cost under implementation errors involves solving an inner maximization problem

$$\max_{\Delta\mathbf{p}\in\mathcal{U}} J(\mathbf{p} + \Delta\mathbf{p}) \tag{3.9}$$
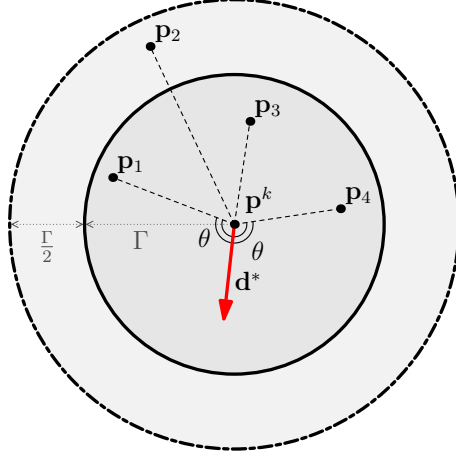
Figure 3-4: A 2-D illustration of the neighborhood $\{\mathbf{p} \mid \|\mathbf{p} - \hat{\mathbf{p}}\|_2 \leq \Gamma\}$. The solid arrow indicates an optimal direction $\mathbf{d}^*$ which makes the largest possible angle with the vectors $\mathbf{p}_i - \hat{\mathbf{p}}$ and points away from all bad neighbors $\mathbf{p}_i$.

which does not have a closed form solution. Thus, we can only find an estimate of the worst case cost, $\tilde{J}_{max}(\mathbf{p})$, through efficient local searches. These searches are conducted within the *neighborhood* $\mathcal{N}$ of a configuration $\hat{\mathbf{p}}$, defined as

$$\mathcal{N} = \{\mathbf{p} \mid \|\mathbf{p} - \hat{\mathbf{p}}\|_2 \leq \Gamma\}. \tag{3.10}$$

This set is illustrated in Figure 2-7.

These searches form the first part of the robust local search algorithm. The obtained worst case costs within $\mathcal{N}$ are used to find the next configuration with a local move, which aims to improve the worst case cost. The local move forms the second part of the robust local search algorithm. These two parts are repeated iteratively until the termination conditions are met. Next, we discuss these two parts in more detail.

Neighborhood Search

The local search within a neighborhood $\mathcal{N}$ is conducted with several modified gradient ascents. To ensure that $\mathcal{N}$ is explored thoroughly, an additional boundary penalty is applied whenever an ascent step is near the boundary.

For this 100-dimensional problem, 101 gradient ascent sequences are carried out. The first sequence starts from $\hat{\mathbf{p}}$ while the remaining 100 sequences start from $\hat{\mathbf{p}} + \frac{\Gamma}{3}\mathbf{e}_i$, if $\frac{\partial J(\mathbf{p}=\hat{\mathbf{p}})}{\partial p_i} \geq 0$ or from $\hat{\mathbf{p}} - \frac{\Gamma}{3}\mathbf{e}_i$, otherwise. p_i is a coordinate of $\mathbf{p}$ and $\mathbf{e}_i$ denotes the ith unit vector. A sequence is terminated when either a local maximum is obtained, a configuration outside the neighborhood is visited, or a time limit is exceeded.

Finally, the results of all function evaluations up to iteration k are stored in a set $\mathcal{H}^k$ and used to evaluate $\tilde{J}_{max}(\mathbf{p}^k)$.

Robust Local Move

In the second part of the robust local search algorithm, we update the configuration $\mathbf{p}^k$ such, that the previously discovered "bad" neighbors are excluded from the new neighborhood $\mathcal{N}^{k+1}$. We define the set of these bad neighbors as

$$\mathcal{M}^k = \{\mathbf{p}|\mathbf{p} \in \mathcal{H}^k, \mathbf{p} \in \mathcal{N}^k, J(\mathbf{p}) \geq \tilde{J}_{max}(\mathbf{p}^k) - \sigma^k\}.$$

The cost factor σ^k governs the size of the set and may be changed within an iteration to ensure a feasible move.

The problem of determining a good direction $\mathbf{d}$, which points away from bad neighbors, can be formulated as

$$
\begin{aligned}
\min_{\mathbf{d},\epsilon} \quad & \epsilon \\
s.t. \quad & \|\mathbf{d}\|_2 \leq 1 \\
& \left(\frac{\mathbf{p}-\mathbf{p}^k}{\|\mathbf{p}-\mathbf{p}^k\|}\right) \cdot \mathbf{d} \leq \epsilon \quad \forall \mathbf{p} \in \mathcal{M}^k \\
& \epsilon \leq 0.
\end{aligned}
\tag{3.11}
$$

Because the first constraint is a conic quadratic constraint and all others are linear, this problem is a second order cone problem (SOCP), which can be solved efficiently using both commercial and noncommercial solvers. The optimal solution of this SOCP delivered a direction $\mathbf{d}^*$ forming the maximum possible angle with all the vectors $\mathbf{p} - \mathbf{p}^k$, $\mathbf{p} \in \mathcal{M}^k$, as shown in Fig. 2-7. This angle is at least 90° due to the constraint $\epsilon \leq 0$. However, if a good direction is not found, we reduce σ^k, reassemble
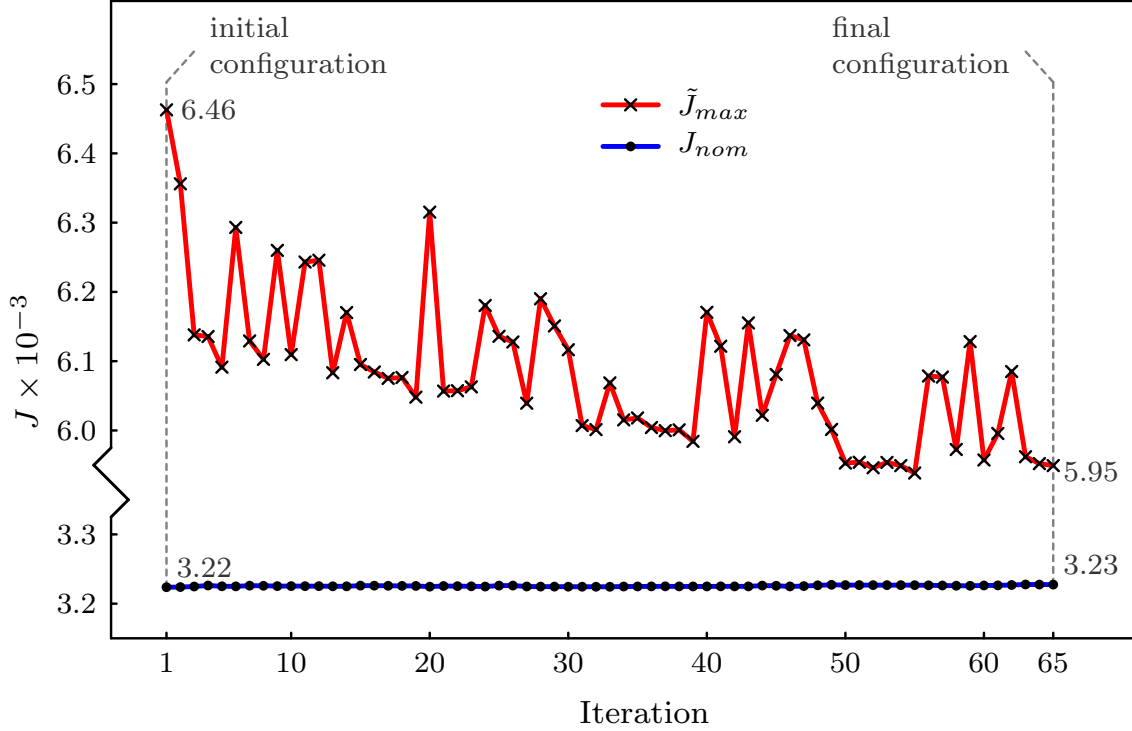
Figure 3-5: Performance of the robust local search algorithm. The worst case cost for the final configuration $\mathbf{p}^{65}$ is improved by 8%, while the nominal cost remained constant.

$\mathcal{M}^k$, and solve the updated SOCP. The terminating condition is attained, when σ^k decreases below a threshold.

3.2.4 Computation Results

As the first step of the robust optimization method, the nominal optimization also decreases the worst case cost significantly. For the PC-like initial configuration (see inset of Fig. 3-3), a worst case cost of $\tilde{J}_{max} = 0.05413$ was estimated, whereas the final nominal configuration delivered $\tilde{J}_{max}(\mathbf{p}^1) = 0.00646$, as shown in Fig. 3-5. While the nominal optimization primarily aims to reduce the nominal cost and increases the robustness indirectly, only the robust local search algorithm directly minimizes the worst case cost and, thus, improves the robustness further.

In the robust local search, the worst case cost at the terminating iteration step 65, $\tilde{J}_{max}(\mathbf{p}^{65})$, was estimated with 110000 configurations in the neighborhood of $\mathbf{p}^{65}$.

As the iteration counts increase, the knowledge about the neighborhood grows and the more robust configurations are discovered. Figure 3-5 shows the improvement after 65 iterations of the robust local search algorithm. Here, the nominal cost of the design remains practically constant, while the estimated worst case cost decreases significantly. Overall, we observe a 90% improvement in robustness of the final design, when compared to the initial PC-like structure.

Since we can only estimate the worst case cost by local searches, there is always a chance for late discoveries of worst implementation errors. Therefore, the decrease of the estimated worst case cost may not be monotonic.

3.3   Sensitivity Analysis

We have probed the neighborhood of $\mathbf{p}^1$ and $\mathbf{p}^{65}$ each with 10000 normally distributed random perturbations. When the standard deviation of the perturbation is comparable to the assumed implementation errors, $\mathbf{p}^{65}$ is up to 2% less sensitive as $\mathbf{p}^1$.

It is evident, that a 100-dimensional random sampling is computationally challenging, e.g., when estimating $\tilde{J}_{max}(\mathbf{p}^1)$, random sampling is far inferior to the multiple gradient ascent method: the best estimate attained by the former with 30000 random samples is 96% of the estimate obtained with only 3000 multiple gradient ascent steps. Furthermore, a perturbation sensitivity analysis does not improve the worst case performance. To the best of our knowledge, there is no practical approach that improves sensitivities for a problem at such high dimensions. In contrast, our approach incorporates the widely used concept of probabilistic robustness through the variable size of the uncertainty set $\mathcal{U}$.

3.4   Conclusions

We have presented a novel robust optimization technique for electromagnetic scattering problems and applied it to the optimization of aperiodic dielectric structures. This generic method only assumes the capability of function evaluation. We have

demonstrated that using a modified gradient descent will increase the efficiency of the robust algorithm significantly. However, if the function gradient is not accessible, a gradient-free stochastic algorithm can be utilized to obtain a robust solution. The application of our robust optimization method to improve the configuration of 50 dielectric cylinders showed that the final design configuration matches the shape of the desired function whose top-hat maximum is at $30° \leq \theta \leq 60°$. Since the problem is high-dimensional and highly non-convex, a global optimum can be estimated only through local searches. While the deviation from an optimal solution (perfect matching) is negligible, the robustness against implementation errors in laboratory experiments or manufacturing increased by 8%. Furthermore, laboratory measurements have verified our model [51].

The generic aspect of the presented method allows it to be employed in various engineering problems in electromagnetics, in particular when function evaluation is provided. Moreover, the demonstrated approach for the dielectric scattering structure scales with frequency and can be applied to nano-photonic design to achieve novel and desired functionalities.

Chapter 4

Nonconvex Robust Optimization for Problems with Constraints

Constraints appear in many real-world problems. In a manufacturing application, the number of items produced must exceed the quantity promised to the customers. In cancer radiation therapy, a treatment plan must deliver the required radiation dosage to a cancerous tumor, while sparing healthy organs. Due to the presence of uncertainties, an otherwise "optimal" solution might violate critical constraints, rendering it to become un-implementable. Therefore, for an optimization method to be applicable to a wide range of real-world problems, it must admit constraints.

The robust local search technique for an unconstrained problem has been introduced in Chapter 2. The proposed technique makes only one generic assumption: the availability of a subroutine providing the cost and the gradient, when given a design. Because only a simple assumption is made, the proposed method is much more general than the robust models found in current literature, which assumes a convex problem defined with linear, convex quadratic, conic-quadratic and semidefinite constraints [1, 4, 6, 8]. Consequently, the robust local search can be used for many practical problems, convex or not. This applicability is demonstrated in Chapter 3, when robust optimization in an actual engineering problem with a nonconvex objective is carried out.

Our goal in this chapter is to generalize the robust local search further to ad-

mit constraints. The objective and the constraints can all be nonconvex. The basic assumption on the availability of the cost and the gradient remains. In addition, we assume the availability of the constraint value and the gradient of the constraint value for every single constraint. This assumption is, again, a generic one. Therefore, the proposed method remains applicable to a wide range of practical problems. Furthermore, we consider how the efficiency of the algorithm can be improved, if some constraints are simple, e.g. linear constraints.

To illustrate the technique more clearly, we start by considering a problem with implementation errors only, before generalizing it to admit both implementation and parameter uncertainties. The chapter is structured as follows.

Structure of the Chapter   In Section 4.1, the robust local search is generalized to handle a constrained problem with implementation errors. We also explore how the efficiency of the algorithm can be improved, if some of the constraints have simple structures, i.e. linear constraints. In Section 4.2, the algorithm is further generalized to admit problems with implementation and parameter uncertainties. Application III in Section 4.3 is designed to develop intuitions. Application IV in Section 4.4 considers a similar problem as Application III, but with linear constraints. The robust local search is shown to be more efficient when the simple constraints are exploited. The final application, reported in Section 4.5, is an actual healthcare problem in Intensity Modulated Radiation Therapy (IMRT) for cancer treatment. This problem has 85 decision variables.

4.1 Constrained Problem under Implementations Errors

4.1.1 Problem Definition

Consider the nominal optimization problem

$$\begin{aligned}
\min_{\mathbf{x}} \quad & f(\mathbf{x}) \\
s.t. \quad & h_j(\mathbf{x}) \leq 0, \quad \forall j,
\end{aligned} \tag{4.1}$$

where both the objective function and the constraints may be nonconvex. To find a good design which is robust against implementation errors in Problem (4.1), we formulate the robust problem

$$\begin{aligned}
\min_{\mathbf{x}} \quad \max_{\Delta\mathbf{x} \in \mathcal{U}} \quad & f(\mathbf{x} + \Delta\mathbf{x}) \\
s.t. \quad \max_{\Delta\mathbf{x} \in \mathcal{U}} \quad & h_j(\mathbf{x} + \Delta\mathbf{x}) \leq 0, \quad \forall j,
\end{aligned} \tag{4.2}$$

where $\Delta\mathbf{x}$ are implementation errors. In this robust problem, we protect the design against errors residing within an ellipsoidal uncertainty set $\mathcal{U}$, given by

$$\mathcal{U} \quad := \quad \{\Delta\mathbf{x} \in \mathbb{R}^n \mid \|\Delta\mathbf{x}\|_2 \leq \Gamma\}. \tag{4.3}$$

Here, a larger scalar Γ indicates that larger perturbations will be taken into considerations. A design is robust if and only if no constraint is violated, for any errors from set $\mathcal{U}$. Of all the robust designs, we seek one with the lowest worst case cost,

$$g(\mathbf{x}) \quad = \quad \max_{\Delta\mathbf{x} \in \mathcal{U}} \quad f(\mathbf{x} + \Delta\mathbf{x}). \tag{4.4}$$

When a design $\hat{\mathbf{x}}$ is implemented with errors from set $\mathcal{U}$, the realized design falls within the neighborhood,

$$\mathcal{N} \quad := \quad \{\mathbf{x} \mid \|\mathbf{x} - \hat{\mathbf{x}}\|_2 \leq \Gamma\}, \tag{4.5}$$
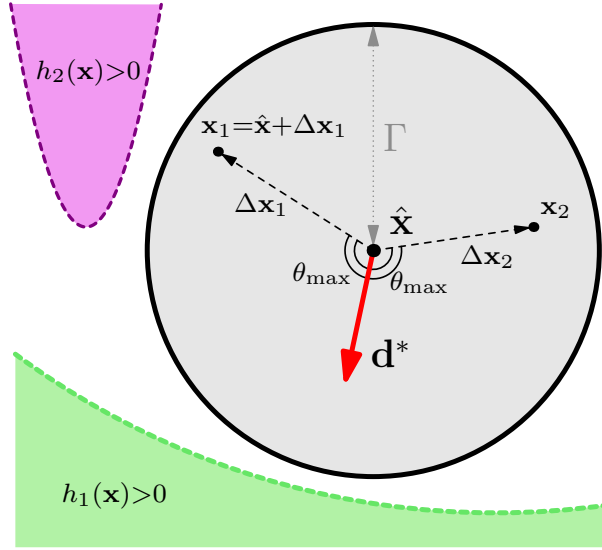
Figure 4-1: A 2-D illustration of the neighborhood $\mathcal{N} = \{\mathbf{x} \mid \|\mathbf{x} - \hat{\mathbf{x}}\|_2 \leq \Gamma\}$ in the design space $\mathbf{x}$. The shaded circle contains all the possible realizations when implementing $\hat{\mathbf{x}}$, when an error $\Delta\mathbf{x} \in \mathcal{U}$ is present. $\mathbf{x}_i$ is a neighboring design ("neighbor") which will be the outcome if $\Delta\mathbf{x}_i$ is the error. The shaded regions $h_j(\mathbf{x}) > 0$ contain designs violating the constraints j. Note, that h_1 is a convex constraint but not h_2. As discussed in Chapter 2, if $\mathbf{x}_i$ are neighbors with the highest nominal cost in the $\mathcal{N}$ ("bad neighbors"), $\mathbf{d}^*$ is an update direction under the robust local search method for the unconstrained problem. $\mathbf{d}^*$ makes the largest possible angle θ^* with these bad neighbors.

as illustrated in Fig. 4-1. $\mathbf{x}$ is a neighbor of $\hat{\mathbf{x}}$ if it lies within the latter's neighborhood. Therefore, $\hat{\mathbf{x}}$ is robust if and only if none of its neighbors violate any constraints. Equivalently, there is any overlap between the neighborhood of $\hat{\mathbf{x}}$ and the shaded regions $h_j(\mathbf{x}) > 0$ in Fig. 4-1.

4.1.2   Robust Local Search for Problems with Constraints

When constraints do not come into play in the vicinity of the neighborhood of $\hat{\mathbf{x}}$, the worst cost can be reduced iteratively, using the robust local search algorithm for the unconstrained problem. Such a step, as indicated in Fig. 4-1, consists of

  (i) <u>Neighborhood Search</u>: finding neighbors $\mathbf{x}_i$ with the highest nominal costs in $\mathcal{N}$, and

  (ii) <u>Robust Local Move</u>: taking a small step along an update direction $\mathbf{d}^*$, which

points away from these bad neighbors, $\mathbf{x}_i$.

For further details of this algorithm, including methods to find these bad neighbors, and the convex optimization approach to find the update direction efficiently, see Section 2.2.

When constraints are present, the additional procedures required for the robust local search algorithm include

(i) Neighborhood Search: Find neighbors $\mathbf{x}_i$ that violates the constraints.

(ii) Check Feasibility Under Perturbations: If infeasible neighbors are found, $\hat{\mathbf{x}}$ is not feasible under perturbations. Else, it is deemed to be feasible.

(iii) Robust Local Move:

    a. If $\hat{\mathbf{x}}$ is not feasible under perturbations, find one that is, or

    b. If $\hat{\mathbf{x}}$ is feasible under perturbations, find one with a lower worst case cost.

With respect to an unconstrained problem, the additional procedures include:

(i) Neighborhood Search   To determine if there are neighbors violating constraint h_j, the constraint maximization problem

$$\max_{\Delta \mathbf{x} \in \mathcal{U}} \quad h_j(\hat{\mathbf{x}} + \Delta \mathbf{x}) \tag{4.6}$$

is solved using multiple gradient ascents from different starting designs. Gradient ascents are used because Problem (4.6) is a nonconvex optimization problem, in general. We shall consider in Section 4.1.3 the case where h_j is a simple constraint, and consequently, Problem (4.6) can be solved using techniques more efficient than multiple gradient ascents.

The implementation of the multiple gradient ascents can follow the generic neighborhood search algorithm, described in Section 2.2, but with the cost function $f(\mathbf{x})$ replaced by the constraint functions $h_j(\mathbf{x})$. If a neighbor has a constraint value exceeding zero, for any constraint, it is recorded in a history set $\mathcal{Y}$.

(ii) Check feasibility under perturbations   If $\hat{\mathbf{x}}$ has neighbors in the history set $\mathcal{Y}$, then it is not feasible under perturbations. Else, the algorithm treats $\hat{\mathbf{x}}$ to be

feasible under perturbations.

(iii)a. Robust local move if $\hat{\mathbf{x}}$ is not feasible under perturbations   Because constraint violations are more important than cost considerations, and we want the algorithm to operate within the feasible region of robust problem, cost is ignored when neighbors violating constraints are encountered.

To ensure that the new neighborhood does not contain neighbors in $\mathcal{Y}$, an update step along a direction $\mathbf{d}^*_{feas}$ is taken. $\mathbf{d}^*_{feas}$ is required to point away from these neighbors. This is illustrated in Fig. 4-2, where $\mathbf{y}_i$ denotes a neighbor violating constraints and $\mathbf{d}^*_{feas}$ makes the largest possible angle with all the vectors $\mathbf{y}_i - \hat{\mathbf{x}}$. Such a $\mathbf{d}^*_{feas}$ can be found by solving the SOCP

$$
\begin{aligned}
\min_{\mathbf{d},\beta} \quad & \beta \\
s.t. \quad & \|\mathbf{d}\|_2 \leq 1, \\
& \mathbf{d}' \left(\frac{\mathbf{y}_i - \hat{\mathbf{x}}}{\|\mathbf{y}_i - \hat{\mathbf{x}}\|_2} \right) \leq \beta, \quad \forall \mathbf{y}_i \in \mathcal{Y}, \\
& \beta \leq -\epsilon.
\end{aligned}
\tag{4.7}
$$

As shown in Fig. 4-2, a sufficiently large step along $\mathbf{d}^*_{feas}$ yields a robust design, take for instance $\hat{\mathbf{x}} + \mathbf{d}^*_{feas}$.

(iii)b. Robust local move if $\hat{\mathbf{x}}$ is feasible under perturbations   When $\hat{\mathbf{x}}$ is feasible under perturbations, the update step is similar to that for an unconstrained problem. However, ignoring designs violating constraints and lying just beyond the neighborhood might lead to a non-robust design. To prevent that from happening, such designs are considered when finding the update direction $\mathbf{d}^*_{cost}$, as illustrated in Fig. 4-3.
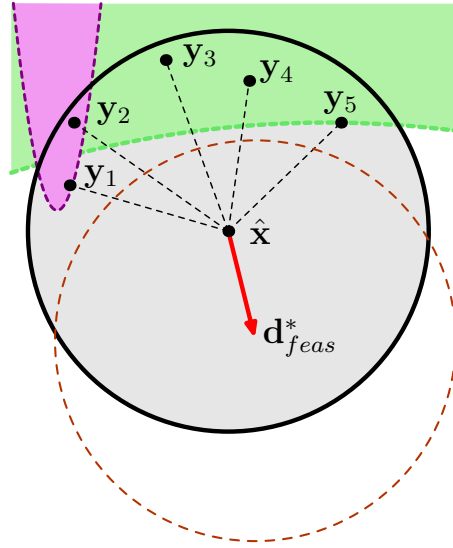
Figure 4-2: A 2-D Illustration of the robust local move, if $\hat{\mathbf{x}}$ is non-robust. The upper shaded regions contain constraint-violating designs, including infeasible neighbors $\mathbf{y}_i$. Vector $\mathbf{d}^*_{feas}$, which points away from all $\mathbf{y}_i$ can be found by solving SOCP (4.7). The circle with the broken circumference denotes the updated neighborhood of $\hat{\mathbf{x}} + \mathbf{d}^*_{feas}$, which is robust.
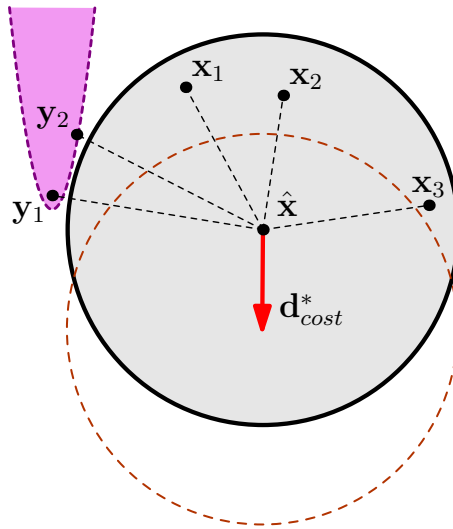
Figure 4-3: A 2-D Illustration of the robust local move when $\hat{\mathbf{x}}$ is robust. $\mathbf{x}_i$ denotes a bad neighbor with high nominal cost, while $\mathbf{y}_i$ denotes an infeasible neighbor lying just outside the neighborhood. By solving SOCP (4.8), $\mathbf{d}^*_{cost}$, a vector which points away from $\mathbf{x}_i$ and $\mathbf{y}_i$, can be found. The neighborhood of $\hat{\mathbf{x}} + \mathbf{d}^*_{cost}$ contains neither the designs with high cost nor the infeasible designs.

The update direction $\mathbf{d}^*_{cost}$ can be found by solving the SOCP

$$
\begin{aligned}
\min_{\mathbf{d},\beta} \quad & \beta \\
s.t. \quad & \|\mathbf{d}\|_2 \leq 1, \\
& \mathbf{d}' \left(\frac{\mathbf{x}_i - \hat{\mathbf{x}}}{\|\mathbf{x}_i - \hat{\mathbf{x}}\|_2} \right) \leq \beta, \quad \forall \mathbf{x}_i \in \mathcal{M}, \\
& \mathbf{d}' \left(\frac{\mathbf{y}_i - \hat{\mathbf{x}}}{\|\mathbf{y}_i - \hat{\mathbf{x}}\|_2} \right) \leq \beta, \quad \forall \mathbf{y}_i \in \mathcal{Y}_+, \\
& \beta \leq -\epsilon,
\end{aligned}
\tag{4.8}
$$

where $\mathcal{M}$ contains neighbors with cost that is among the highest within the neighborhood, and $\mathcal{Y}_+$ is the set of known infeasible designs lying in the slightly enlarged neighborhood $\mathcal{N}_+$,

$$
\mathcal{N}_+ := \left\{ \mathbf{x} \mid \|\mathbf{x} - \hat{\mathbf{x}}\|_2 \leq (1 + \delta)\Gamma \right\},
\tag{4.9}
$$

δ being a small positive scalar.

Since $\hat{\mathbf{x}}$ is robust, there are no infeasible designs in the neighborhood $\mathcal{N}$. Therefore, if there are any infeasible designs in $\mathcal{Y}_+$, they lie at a distance between Γ and $(1 + \delta)\Gamma$. With δ being small, these designs are lying just beyond the neighborhood, as illustrated in Fig. 4-3.

Termination criteria We shall first define the robust local minimum for a problem with constraints:

Definition 3
$\mathbf{x}^*$ *is a robust local minimum for the problem with constraints if*

   (i) *Feasible Under Perturbations*

      $\mathbf{x}^*$ *remains feasible under perturbations,*

$$
h_j(\mathbf{x}^* + \Delta\mathbf{x}) \leq 0, \quad \forall j, \forall \Delta\mathbf{x} \in \mathcal{U},
\tag{4.10}
$$

    and

(ii) _No Descent Direction_

there are no improving direction $\mathbf{d}^*_{cost}$ at $\mathbf{x}^*$.

Given the above definition, we can only terminate in Step (iii)b where $\mathbf{x}^*$ is feasible under perturbations. Furthermore, for there to be no direction $\mathbf{d}^*_{cost}$ at $\mathbf{x}^*$, it must be surrounded by neighbors with high cost, and infeasible designs in $\mathcal{N}_+$.

4.1.3   Enhancements when Constraints are Simple

In the context of the robust local search, a constraint is simple when the corresponding constraint maximization problem (4.6) is convex. When Problem (4.6) is convex, it can be solved with techniques that are more efficient than multiple gradient ascents. Moreover, it is possible to obtain (i) the global optimizer $\Delta\mathbf{x}^*_j$ to the Prob. (4.6), (ii) the maximum constraint value attained in the neighborhood,

$$h_j^{rob}(\hat{\mathbf{x}}) = \max_{\Delta\mathbf{x}\in\mathcal{U}} h_j(\hat{\mathbf{x}} + \Delta\mathbf{x}) = h_j(\hat{\mathbf{x}} + \Delta\mathbf{x}^*_j),$$

and consequently, (iii) confirmation whether any neighbor of $\hat{\mathbf{x}}$ violate constraint j.

Many constraints lead to a convex constraint maximization problem (4.6), including $\mathbf{x} \geq 0$, linear or convex quadratic constraints. Table 4.1 summarizes the procedure required to solve Problem (4.6). Note, that in Problem (4.6), $\hat{\mathbf{x}}$ is a constant and $\Delta\mathbf{x}$ are the only variables.

$\mathbf{h}_i(\mathbf{x})$	Problem (4.6)	Effort required
$\mathbf{a}'\mathbf{x} + b$	$\mathbf{a}'\hat{\mathbf{x}} + \Gamma\|\mathbf{a}\|_2 + b \ \leq \ 0$	Computations
$\mathbf{x}'\mathbf{Q}\mathbf{x} + 2\mathbf{b}'\mathbf{x} + c,$ $\mathbf{Q}$ symmetric	Single trust region problem[1]	Solving a SDP in the worst case
$-\mathbf{h}_i$ is convex	Convex problem	Just 1 gradient ascent is required
$\mathbf{h}_i$ is a polynomial	Polynomial problem	May be solved using Gloptipoly [29] to a high accuracy

Table 4.1: Efforts required to solve Prob. (4.6)

The possible improvements to the robust local search are:

---

[1] $\displaystyle\max_{\Delta\mathbf{x}\in\mathcal{U}} \ \ \Delta\mathbf{x}'\mathbf{Q}\Delta\mathbf{x} + 2(\mathbf{Q}\hat{\mathbf{x}} + \mathbf{b})'\Delta\mathbf{x} + \hat{\mathbf{x}}\mathbf{Q}'\hat{\mathbf{x}} + 2\mathbf{b}'\hat{\mathbf{x}} + c,$

(i) <u>Neighborhood Search</u>: Solve Problem (4.6) with method stated in Table 4.1 and not multiple gradient ascents, which requires more computation effort in general.

(ii) <u>Check Feasibility Under Perturbations</u>: If $h_j^{rob}(\hat{\mathbf{x}}) > 0$, $\hat{\mathbf{x}}$ is not feasible under perturbations.

(iii) <u>Robust Local Move</u>: To not violate h_j in the new neighborhood, the direction should be chosen such that

$$\mathbf{d}'_{feas}\nabla_{\mathbf{x}}h_j^{rob}(\hat{\mathbf{x}}) < \beta\|\nabla_{\mathbf{x}}h_j^{rob}(\hat{\mathbf{x}})\|_2$$

and

$$\mathbf{d}'_{cost}\nabla_{\mathbf{x}}h_j^{rob}(\hat{\mathbf{x}}) < \beta\|\nabla_{\mathbf{x}}h_j^{rob}(\hat{\mathbf{x}})\|_2$$

in SOCP (4.7) and SOCP (4.8), respectively. Note, that $\nabla_{\mathbf{x}}h_j^{rob}(\hat{\mathbf{x}}) = \nabla_{\mathbf{x}}h(\hat{\mathbf{x}} + \Delta\mathbf{x}_j^*)$. This can be evaluated easily.

In particular, if h_j is a linear constraint,

$$h_j^{rob}(\mathbf{x}) \;=\; \mathbf{a}'\mathbf{x} + \Gamma\|\mathbf{a}\|_2 + b \;\leq\; 0$$

is same for all $\mathbf{x}$. Consequently, we can replace the constraint $\max_{\Delta\mathbf{x}\in\mathcal{U}} h_j(\mathbf{x} + \Delta\mathbf{x}) = \max_{\Delta\mathbf{x}\in\mathcal{U}} \mathbf{a}'(\mathbf{x} + \Delta\mathbf{x}) \leq 0$ with its robust counterpart $h_j^{rob}(\mathbf{x})$. $h_j^{rob}(\mathbf{x})$ is a constraint on $\mathbf{x}$ without any uncertainties, as illustrated in Fig. 4-4.

4.1.4 Constrained Robust Local Search Algorithm

Bringing all these procedures together, the constrained robust local search algorithm for Problem (4.2) is:

In Steps 3(i) and 3(ii), t^k is the minimum distance chosen such that the undesirable designs are excluded from the neighborhood of the new iterate $\mathbf{x}^{k+1}$. Finding t^k requires solving a simple geometric problem. For more details, refer to Section 2.2.2.
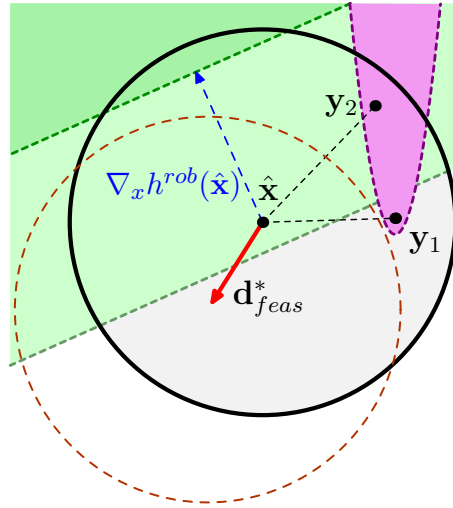
Figure 4-4: A 2-D Illustration of the neighborhood when one of the violated constraint
is a linear function. The shaded region in the upper left hand corner denotes the
infeasible region due a linear constraint. Because $\hat{\mathbf{x}}$ has neighbors violating the linear
constraint, $\hat{\mathbf{x}}$ lies in the infeasible region of its robust counterpart, denoted by the
region with the straight edge but of a lighter shade. $\mathbf{y}_i$ denotes neighbors violating
a nonconvex constraint. The vector $\mathbf{d}^*_{feas}$ denotes a direction which would reduce
the infeasible region within the neighborhood. It points away from the gradient of
the robust counterpart, $\nabla_x h^{rob}(\hat{\mathbf{x}})$ and all the bad neighbors $\mathbf{y}_i$. It can be found by
solving a SOCP. The circle with the dashed circumference denotes the neighborhood
of the design $\hat{\mathbf{x}} + \mathbf{d}^*_{feas}$, where no neighbors violate the two constraints.

Algorithm 3 Constrained Robust Local Search

Step 0. <u>Initialization</u>: Set $k := 1$. Let $\mathbf{x}^1$ be an arbitrary decision vector.

Step 1. <u>Neighborhood Search</u>:

    i. Find neighbors with high cost by applying $n+1$ gradient ascents on the inner maximization problem (2.12) where n is the dimension of $\mathbf{x}$. For more details, refer to Section 2.2.1. Record all neighbors evaluated and their costs in history set $\mathcal{H}^k$, together with $\mathcal{H}^{k-1}$.

    ii. Let $\mathcal{J}$ be the set of constraints with convex constraint maximization Problem (4.6) that are convex. Find optimizer $\Delta\mathbf{x}_j^*$ and highest constraint value $h_j^{rob}(\mathbf{x}^k)$, for all $j \in \mathcal{J}$, using methods as stated in Table. 4.1. Let $\bar{\mathcal{J}} \subseteq \mathcal{J}$ be the set of violated constraints violated under perturbations.

    iii. For every constraint $j \notin \mathcal{J}$, find infeasible neighbors by applying $n+1$ gradient ascents on Problem (4.6), with $\hat{\mathbf{x}} = \mathbf{x}^k$. Record all infeasible neighbors in history set $\mathcal{Y}^k$, together with set $\mathcal{Y}^{k-1}$.

Step 2. <u>Check Feasibility Under Perturbations</u>: $\mathbf{x}^k$ is not feasible under perturbations if either $\mathcal{Y}^k$ or $\bar{\mathcal{J}}$ is not empty.

Step 3. <u>Robust Local Move</u>:

    i. If $\mathbf{x}^k$ is not feasible under perturbations, solve SOCP (4.7) with additional constraints $\mathbf{d}_{feas}' \nabla_{\mathbf{x}} h_j^{rob}(\mathbf{x}^k) < \beta\|\nabla_{\mathbf{x}} h_j^{rob}(\mathbf{x}^k)\|_2$, for all $j \in \bar{\mathcal{J}}$. Find direction d_{feas}^* and set $\mathbf{x}^{k+1} := \mathbf{x}^{k+1} + t^k d_{feas}^*$.

    ii. If $\mathbf{x}^k$ feasible under perturbations, solve SOCP (4.8) to find a direction d_{cost}^*. Set $\mathbf{x}^{k+1} := \mathbf{x}^{k+1} + t^k d_{feas}^*$. If no direction d_{cost}^* exists, reduce σ; if σ is below a threshold, terminate.

4.1.5 Practical Considerations

Implementation In a practical implementation, some possible modifications to this algorithm include:

- Using less than $n+1$ gradient ascents during the neighborhood search to reduce the computational effort.
- Using bounds or other techniques to identify constraints that would not be violated in the neighborhood, and excluding them when looking for infeasible neighbors.

Difficult Feasibility Problem Even without uncertainties, a problem with non-convex constraints can be a challenging one. Therefore, in a difficult problem, the feasible region for the robust problem (4.2) might be small, not connected, or even non-existent. In this case, the algorithm can be trapped within an endless loop, trying to find designs that are feasible under perturbations. If this is encountered, the robust local search has to be started from an alternate design.

4.2 Generalization to Include Parameter Uncertainties

4.2.1 Problem Definition

Consider the nominal problem:

$$\min_{\mathbf{x}} \quad f(\mathbf{x}, \bar{\mathbf{p}})$$
$$s.t. \quad h_j(\mathbf{x}, \bar{\mathbf{p}}) \leq 0, \quad \forall j, \tag{4.11}$$

where $\bar{\mathbf{p}} \in \mathbb{R}^m$ is a coefficient vector of problem parameters. For our purpose, we can restrict $\bar{\mathbf{p}}$ to parameters with perturbations only. For example, if Problem (4.11) is given by

$$\min_{\mathbf{x}} \quad 4x_1^3 + x_2^2 + 2x_1^2 x_2$$
$$s.t. \quad 3x_1^2 + 5x_2^2 \leq 20,$$

$\mathbf{x} = \begin{pmatrix} x_1 \\ x_2 \end{pmatrix}$ and $\bar{\mathbf{p}} = \begin{pmatrix} 4 \\ 1 \\ 2 \\ 3 \\ 5 \\ 20 \end{pmatrix}$. Note, that uncertainties can even be present in the power factor, e.g. 3 in the monomial $4x_1^3$.

In Problem (4.11), there can be perturbations $\Delta\mathbf{p}$ in the assumed parameter $\bar{\mathbf{p}}$, in addition to implementation errors. The true but unknown parameter $\mathbf{p}$ is $\bar{\mathbf{p}} + \Delta\mathbf{p}$. To protect the design against both types of perturbations, we formulate the robust problem

$$\min_{\mathbf{x}} \quad \max_{\Delta\mathbf{z}\in\mathcal{U}} \quad f(\mathbf{x} + \Delta\mathbf{x}, \bar{\mathbf{p}} + \Delta\mathbf{p})$$
$$s.t. \quad \max_{\Delta\mathbf{z}\in\mathcal{U}} \quad h_j(\mathbf{x} + \Delta\mathbf{x}, \bar{\mathbf{p}} + \Delta\mathbf{p}) \leq 0, \quad \forall j, \tag{4.12}$$

where $\Delta\mathbf{z} = \begin{pmatrix} \Delta\mathbf{x} \\ \Delta\mathbf{p} \end{pmatrix}$. $\Delta\mathbf{z}$ lies within the uncertainty set

$$\mathcal{U} \;=\; \left\{\ \Delta\mathbf{z} \in \mathbb{R}^{n+m} \ \mid\ \|\Delta\mathbf{z}\|_2 \;\leq\; \Gamma\ \right\}, \tag{4.13}$$

$\Gamma > 0$ is a scalar describing the size of perturbations we want to protect the design against.

Similar to Problem (4.2), a design is robust only if no constraint is violated under the assumed perturbations. Of all these robust designs, we seek one minimizing the worst case cost

$$g(\mathbf{x}) \;:=\; \max_{\Delta\mathbf{z}\in\mathcal{U}} \; f\left(\mathbf{x} + \Delta\mathbf{x}, \bar{\mathbf{p}} + \Delta\mathbf{p}\right). \tag{4.14}$$

4.2.2 Generalized Constrained Robust Local Search Algorithm

The idea behind generalizing the constrained robust local search algorithm is analogous to the approach described in Section 2.4.2 for the unconstrained problem. Problem (4.12) is equivalent to the following problem with implementation errors only,

$$\min_{\mathbf{z}} \quad \max_{\Delta\mathbf{z}\in\mathcal{U}} \quad f(\mathbf{z} + \Delta\mathbf{z})$$
$$s.t. \quad \max_{\Delta\mathbf{z}\in\mathcal{U}} \quad h_j(\mathbf{z} + \Delta\mathbf{z}) \leq 0, \quad \forall j, \tag{4.15}$$
$$\mathbf{p} = \bar{\mathbf{p}},$$

where $\mathbf{z} = \left(\begin{smallmatrix}\mathbf{x}\\\mathbf{p}\end{smallmatrix}\right)$. Consequently, the necessary modifications to Algorithm 4.1.4 are:

(i) <u>Neighborhood Search</u> : Given $\hat{\mathbf{x}}$, $\hat{\mathbf{z}} = \left(\begin{smallmatrix}\hat{\mathbf{x}}\\\bar{\mathbf{p}}\end{smallmatrix}\right)$ is the decision vector. The neighborhood is

$$\mathcal{N} \;:=\; \{\mathbf{z} \mid \|\mathbf{z} - \hat{\mathbf{z}}\|_2 \le \Gamma\} \;=\; \left\{\left(\begin{smallmatrix}\mathbf{x}\\\mathbf{p}\end{smallmatrix}\right) \;\middle|\; \left\|\begin{smallmatrix}\mathbf{x}-\hat{\mathbf{x}}\\\mathbf{p}-\bar{\mathbf{p}}\end{smallmatrix}\right\|_2 \le \Gamma\right\}. \tag{4.16}$$

(ii) <u>Robust Local Move</u> : Let $\mathbf{d}^* = \left(\begin{smallmatrix}\mathbf{d}_x^*\\\mathbf{d}_p^*\end{smallmatrix}\right)$ be a update direction in the $\mathbf{z}$ space. Because $\mathbf{p}$ is not a decision vector but a given system parameter, the algorithm has to ensure that $\mathbf{p} = \bar{\mathbf{p}}$ is satisfied at every iterate. Thus, $\mathbf{d}_p^* = \mathbf{0}$.

When finding the update direction, the condition $\mathbf{d}_p = \mathbf{0}$ must be included in either of SOCP (4.7) and SOCP (4.8). For example, in the case where $\mathbf{z}$ is not feasible under perturbations, the SOCP is

$$\begin{aligned}
\min_{\mathbf{d}=(\mathbf{d}_x,\mathbf{d}_p),\beta} \quad & \beta \\
s.t. \quad & \|\mathbf{d}\|_2 \le 1, \\
& \mathbf{d}'\,(\mathbf{z}_i - \hat{\mathbf{z}}) \le \beta\|\mathbf{z}_i - \hat{\mathbf{z}}\|_2, \qquad \forall \mathbf{y}_i \in \mathcal{Y}, \\
& \mathbf{d}'\nabla_{\mathbf{z}} h_j^{rob}(\hat{\mathbf{z}}) < \beta\|\nabla_{\mathbf{z}} h_j^{rob}(\hat{\mathbf{z}})\|_2, \quad \forall j \in \bar{\mathcal{J}}, \\
& \mathbf{d}_p = \mathbf{0}, \\
& \beta \le -\epsilon.
\end{aligned}$$

$\mathcal{Y}^k$ is the set of infeasible designs in the neighborhood. This problem reduces to the following:

$$\begin{aligned}
\min_{\mathbf{d}_x,\beta} \quad & \beta \\
s.t. \quad & \|\mathbf{d}_x\|_2 \le 1, \\
& \mathbf{d}_x'\,(\mathbf{x}_i - \hat{\mathbf{x}}) \le \beta\|\mathbf{z}_i - \hat{\mathbf{z}}\|_2, \qquad \forall \mathbf{y}_i \in \mathcal{Y}, \\
& \mathbf{d}_x'\nabla_{\mathbf{x}} h_j^{rob}(\hat{\mathbf{z}}) < \beta\|\nabla_{\mathbf{z}} h_j^{rob}(\hat{\mathbf{z}})\|_2, \quad \forall j \in \bar{\mathcal{J}}, \\
& \beta \le -\epsilon.
\end{aligned} \tag{4.17}$$

A similar approach is carried out for the case where $\mathbf{z}$ is robust. Consequently, both $\mathbf{d}_{feas}^*$ and $\mathbf{d}_{cost}^*$ satisfy $\mathbf{p} = \bar{\mathbf{p}}$ at every iteration, as illustrated in Fig. 4-5.
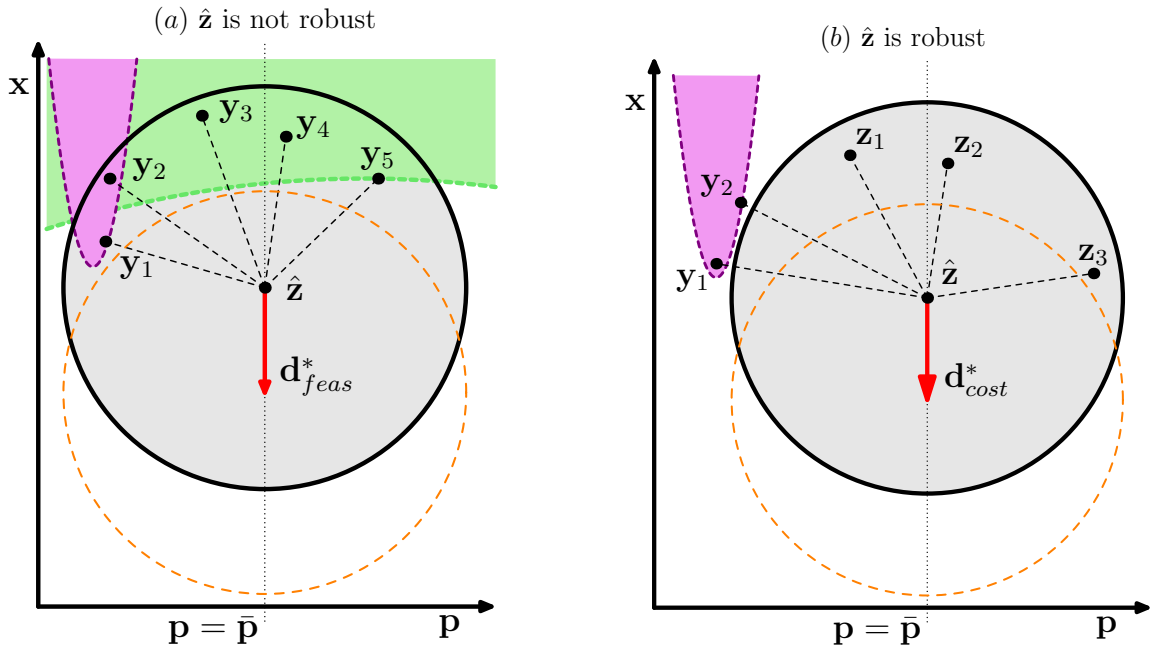
Figure 4-5: A 2-D illustration of the robust local move for problems with both implementation errors and parameter uncertainties, where the neighborhood spans the $\mathbf{z} = (\mathbf{x}, \mathbf{p})$ space. Fig. (a) and (b) are the constrained counterpart of Fig.4-2 and Fig.4-3, respectively. However, the direction found must lie within the hyperplanes $\mathbf{p} = \bar{\mathbf{p}}$.

We have thus arrived at the constrained robust local search algorithm for Problem 4.12 with both implementation errors and parameter uncertainties:

Algorithm 4 Generalized Constrained Robust Local Search

Step 0. <u>Initialization</u>: Set $k := 1$. Let $\mathbf{x}^1$ be an arbitrary decision vector.

Step 1. <u>Neighborhood Search</u>: Same as Step 1 in Algorithm 4.1.4 but over the neighborhood (4.16).

Step 2. <u>Check Feasibility under Perturbations</u>: $\mathbf{z}^k$, and equivalently $\mathbf{x}^k$, is feasible under perturbations if $\mathcal{Y}^k$ and $\bar{\mathcal{J}}^k$ are empty.

Step 3. <u>Robust Local Move</u>:

    i. If $\mathbf{x}^k$ is not feasible under perturbations, find a direction d^*_{feas} by solving SOCP (4.17) with $\hat{\mathbf{z}} = \mathbf{z}^k$. Set $\mathbf{x}^{k+1} := \mathbf{x}^{k+1} + t^k d^*_{feas}$.

    ii. If $\mathbf{x}$ is feasible under perturbations, solve the SOCP

$$
\begin{aligned}
\min_{\mathbf{d}_x,\beta} \quad & \beta \\
s.t. \quad & \|\mathbf{d}_x\|_2 \leq 1, \\
& \mathbf{d}'_x \left(\mathbf{x}_i - \mathbf{x}^k\right) \leq \beta \left\| \begin{pmatrix} \mathbf{x}_i - \mathbf{x}^k \\ \mathbf{p}_i - \bar{\mathbf{p}} \end{pmatrix} \right\|_2, \qquad \forall \mathbf{z}_i \in \mathcal{M}^k, \mathbf{z}_i = \begin{pmatrix} \mathbf{x}_i \\ \mathbf{p}_i \end{pmatrix}, \\
& \mathbf{d}'_x \left(\mathbf{x}_i - \mathbf{x}^k\right) \leq \beta \left\| \begin{pmatrix} \mathbf{x}_i - \mathbf{x}^k \\ \mathbf{p}_i - \bar{\mathbf{p}} \end{pmatrix} \right\|_2, \qquad \forall \mathbf{y}_i \in \mathcal{Y}^k_+, \mathbf{y}_i = \begin{pmatrix} \mathbf{x}_i \\ \mathbf{p}_i \end{pmatrix}, \\
& \mathbf{d}'_x \nabla_{\mathbf{x}} h^{rob}_j(\mathbf{z}^k) < \beta \|\nabla_{\mathbf{z}} h^{rob}_j(\mathbf{z}^k)\|_2, \quad \forall j \in \bar{\mathcal{J}}_+, \\
& \beta \leq -\epsilon,
\end{aligned}
\tag{4.18}
$$

    to find a direction d^*_{cost}. $\mathcal{Y}^k_+$ is the set of infeasible designs in the enlarged neighborhood $\mathcal{N}^k_+$, Eq. 4.9. $\bar{\mathcal{J}}_+$ is the set of constraints which are not violated in the neighborhood of $\hat{\mathbf{x}}$, but are violated in the slightly enlarged neighborhood $\mathcal{N}_+$. Set $\mathbf{x}^{k+1} := \mathbf{x}^{k+1} + t^k d^*_{feas}$. If no direction d^*_{cost} exists, reduce σ; if σ is below a threshold, terminate.

We are now ready to apply the robust local search.

4.3 Application III: Problem with Polynomial Cost Function and Constraints

4.3.1 Problem Description

The first problem in this chapter was obtained by adding two constraints to Application I. The resulting problem is sufficiently simple, so as to develop intuition into the

algorithm. Consider the nominal problem

$$\min_{x,y} \quad f_{poly}(x,y)$$
$$s.t. \quad h_1(x,y) \le 0, \tag{4.19}$$
$$h_2(x,y) \le 0,$$

where

$$
\begin{aligned}
f_{poly}(x,y) &= 2x^6 - 12.2x^5 + 21.2x^4 + 6.2x - 6.4x^3 - 4.7x^2 + y^6 - 11y^5 + 43.3y^4 \\
&\quad -10y - 74.8y^3 + 56.9y^2 - 4.1xy - 0.1y^2x^2 + 0.4y^2x + 0.4x^2y \\
h_1(x,y) &= (x-1.5)^4 + (y-1.5)^4 - 10.125, \\
h_2(x,y) &= -(2.5-x)^3 - (y+1.5)^3 + 15.75.
\end{aligned}
$$

Given implementation errors $\left\| \Delta = \left(\begin{smallmatrix} \Delta x \\ \Delta y \end{smallmatrix} \right) \right\|_2 \le 0.5$, the robust problem is

$$\min_{x,y} \quad \max_{\|\Delta\|_2 \le 0.5} \quad f_{poly}(x+\Delta x, y+\Delta y)$$
$$s.t. \quad \max_{\|\Delta\|_2 \le 0.5} \quad h_1(x+\Delta x, y+\Delta y) \le 0, \tag{4.20}$$
$$\max_{\|\Delta\|_2 \le 0.5} \quad h_2(x+\Delta x, y+\Delta y) \le 0.$$

There are no practical ways to solve such a robust problem, given today's technology [34]. If the relaxation method for polynomial optimization problems [29] is used, Problem (4.20) leads to a large polynomial SDP problem which cannot be solved in practice today [33, 34]. The nominal and the estimated worst cost surface is shown in Fig. 4-6.

4.3.2 Computation Results

The nonconvex cost surface and the feasible region of Problem (4.19) are shown in Figure 4-7(a). Note, that the feasible region is not convex, because h_2 is not a convex
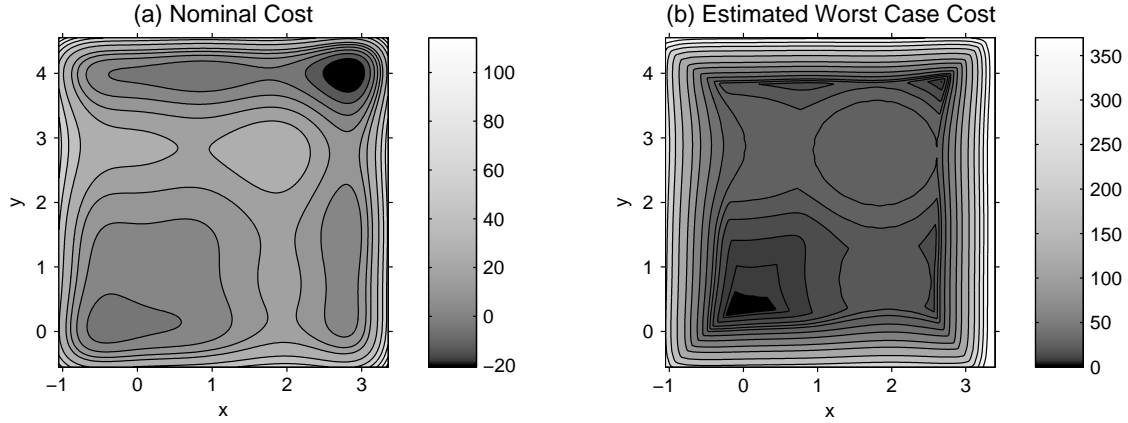
Figure 4-6: Contour plot of nominal cost function $f_{poly}(x, y)$ and the estimated worst case cost function $g_{poly}(x, y)$ in Application I.

constraint. Let $g_{poly}(x, y)$ be the worst case cost function,

$$g_{poly}(x, y) := \max_{\|\Delta\|_2 \leq 0.5} f_{poly}(x + \Delta x, y + \Delta y).$$

Figure 4-7(b) shows the worst case cost estimated using sampling on the cost surface f_{poly}. In the robust problem (4.20), we seek the design minimizing $g_{poly}(x, y)$, among all the designs with a neighborhood lying within the unshaded region. An example of such a design is point C in Fig. 4-7(b).

Applying the constrained robust local search Two separate robust local searches were carried out from initial designs A and B. The algorithm found designs that are feasible under perturbations and with much lower worst case costs in both instances, as shown in Fig. 4-8.

However, it converged to different robust local minima in the two instances, as shown in Fig. 4-9. The presence of multiple robust local minima is not surprising because $g_{poly}(x, y)$ is nonconvex. Figure 4-9 also show that both robust local minima I and II satisfy the terminating conditions stated in Section 4.1.2:

(i) <u>Feasible under Perturbations</u>: Both their neighborhoods do not overlap with the shaded regions.
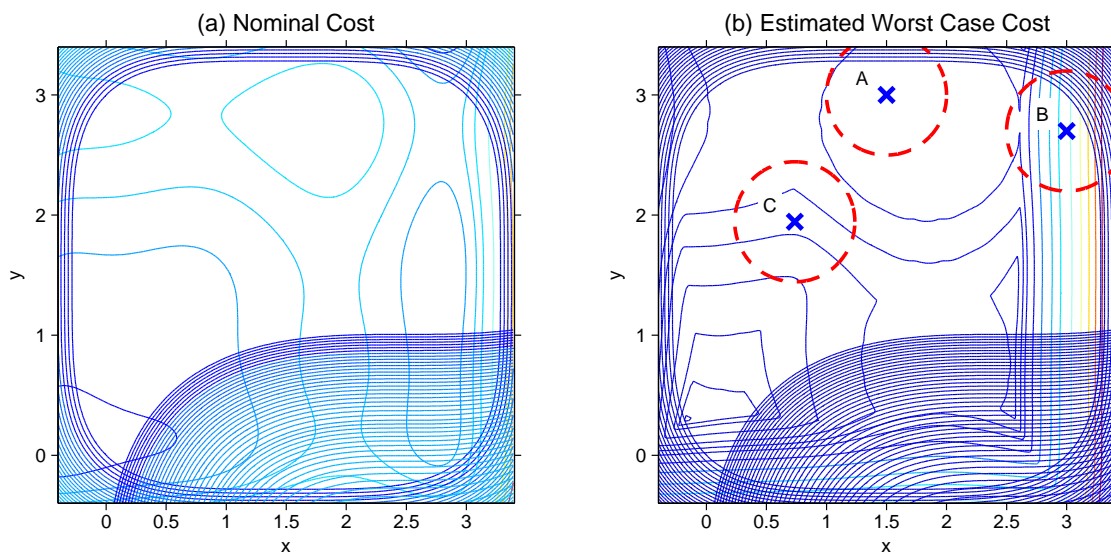
Figure 4-7: Contour plot of (a) the nominal cost function $f_{poly}(x, y)$ and (b) the estimated worst case cost function $g_{poly}(x, y)$ in Application IV. The shaded regions denote designs which violate at least one of the two constraints, h_1 and h_2. While both point A and point B are feasible, they are not feasible under perturbations, because they have infeasible neighbors. Point C, on the other hand, is feasible under perturbations.
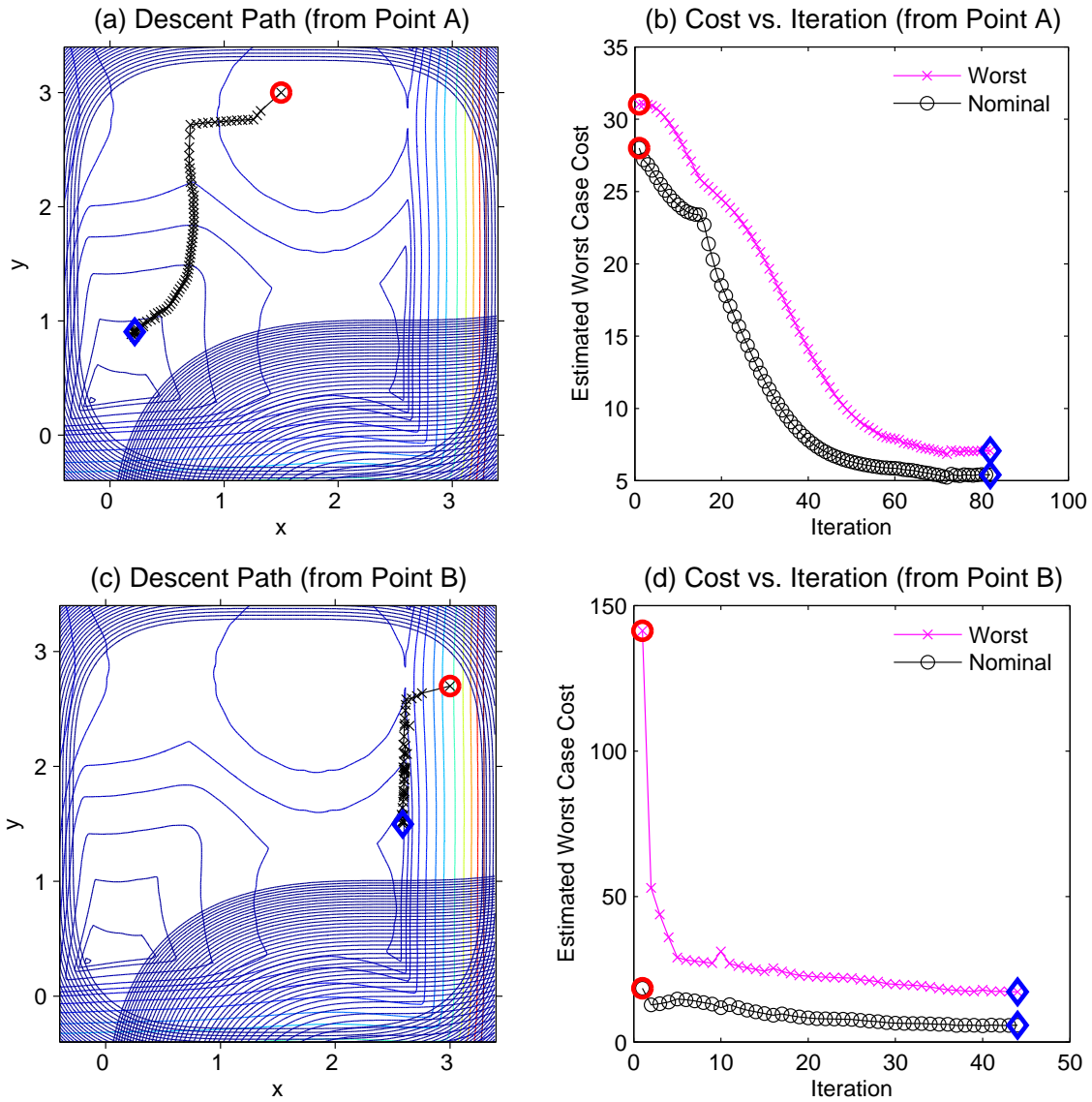
Figure 4-8: Performance of the robust local search algorithm in Application IV from 2 different starting points A and B. The circle marker and the diamond marker denote the starting point and the final solution, respectively. (a) The contour plot showing the estimated surface of the worst case cost, $g_{poly}(x, y)$. The descent path taken to converge at the robust solution is shown. (b) From starting point A, the algorithm reduces both the worst case cost and the nominal cost. (c),(d) From another starting point B, the algorithm converged to a different robust solution, which has a significantly smaller worst case cost and nominal cost.

(ii) <u>No improving direction $\mathbf{d}^*_{cost}$</u>: Both designs are surrounded by bad neighbors and infeasible designs lying just outside their respective neighborhoods. For robust local minimum II, note that the bad neighbors lie on the same contour line even though they are apart.

4.4 Application IV: Polynomial Problem with Simple Constraints

In Section 4.1.3, we argued that the robust local search can be more efficient if simple constraints, such as linear constraints, are replaced by their robust counterparts. The objective of this example is to show this improvement.

4.4.1 Problem Description

The nominal problem is

$$
\begin{aligned}
\min_{x,y} \quad & f_{poly}(x, y) \\
\text{s.t.} \quad & h_1(x, y) \le 0, \\
& h_2(x, y) \le 0,
\end{aligned}
\tag{4.21}
$$

where

$$
\begin{aligned}
f_{poly}(x, y) \;=\; & 2x^6 - 12.2x^5 + 21.2x^4 + 6.2x - 6.4x^3 - 4.7x^2 + y^6 - 11y^5 + 43.3y^4 \\
& -10y - 74.8y^3 + 56.9y^2 - 4.1xy - 0.1y^2x^2 + 0.4y^2x + 0.4x^2y, \\
h_1(x, y) \;=\; & 0.6x - y + 0.17, \\
h_2(x, y) \;=\; & -16x - y - 3.15.
\end{aligned}
$$

Given the uncertainty set $\mathcal{U} = \left\{ \Delta = \left(\begin{smallmatrix} \Delta x \\ \Delta y \end{smallmatrix} \right) \mid \|\Delta\|_2 \le 0.5 \right\}$, the robust problem is

$$
\begin{aligned}
\min_{x,y} \; \max_{\Delta \in \mathcal{U}} \quad & f_{poly}(x + \Delta x, y + \Delta y) \\
\text{s.t.} \; \max_{\Delta \in \mathcal{U}} \quad & h_1(x + \Delta x, y + \Delta y) \le 0 \\
\max_{\Delta \in \mathcal{U}} \quad & h_2(x + \Delta x, y + \Delta y) \le 0.
\end{aligned}
\tag{4.22}
$$
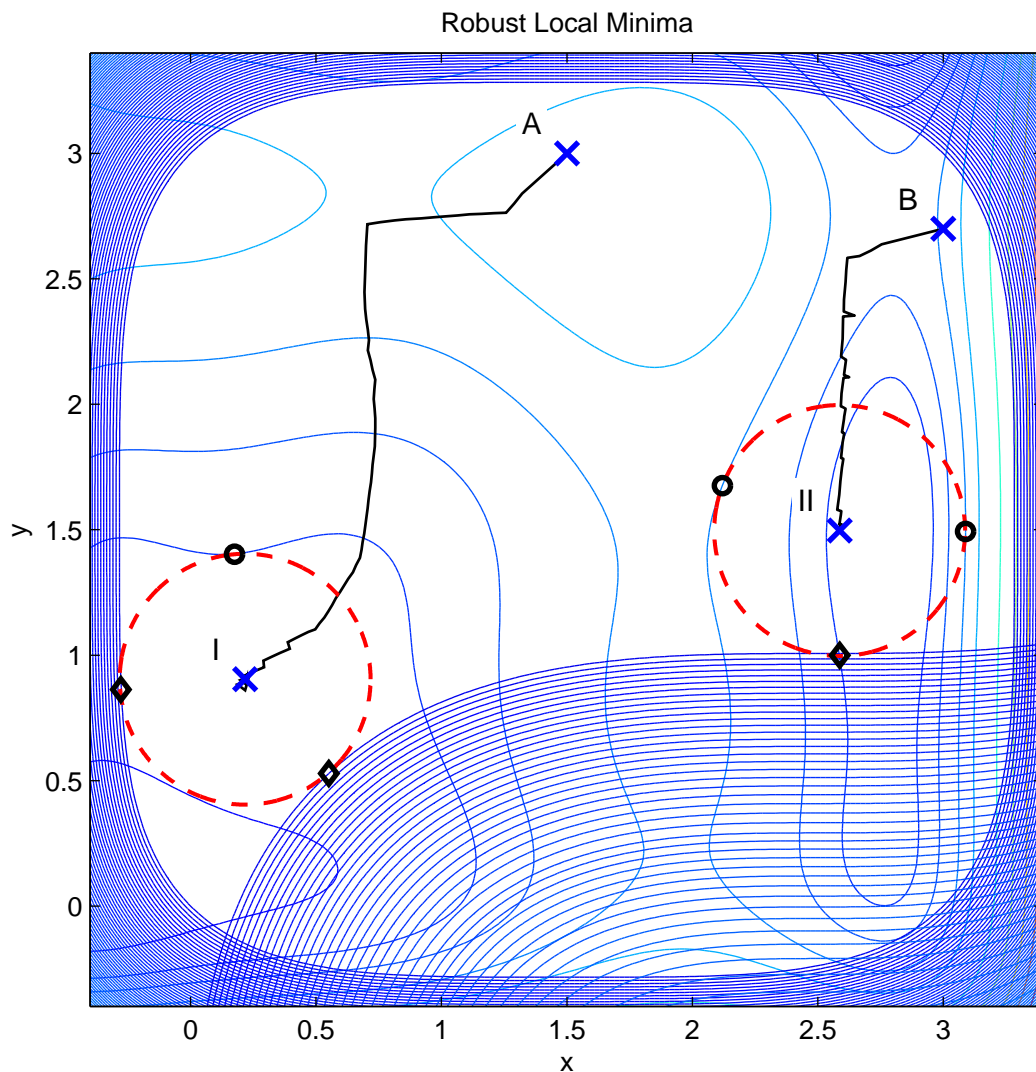
Figure 4-9: Robust local minima found using robust local search algorithm from different initial designs A and B in Application IV. Each of the two broken circles denote the neighborhood of a minimum, which shows that the terminating criteria of the local search have been satisfied. For each minimum, (i) there is no overlap between its neighborhood and the shaded infeasible regions, so it is feasible under perturbations, and (ii) there is no improving directions because it is surrounded by neighbors of high cost (bold circle) and infeasible designs (bold diamond) just beyond the neighborhood. Both the bad neighbors of minimum II share the same cost because they lie on the same contour line.

Because h_j are linear, they have robust counterparts

$$h_1^{rob}(x, y) = 0.6x - y + 0.17 + 0.5831 \leq 0,$$

$$h_2^{rob}(x, y) = -16x - y - 3.15 + 8.0156 \leq 0,$$

as described in Table 4.1. To derive h_j^{rob}, take h_1^{rob} for example:

$$\max_{\Delta \in \mathcal{U}} 0.6(x + \Delta x) - (y + \Delta y) + 0.17 = 0.6x - y + 0.17 + 0.5 \left\| \left(\begin{smallmatrix} 0.6 \\ -1 \end{smallmatrix} \right) \right\|_2$$

$$= 0.6x - y + 0.17 + 0.5831.$$

Therefore, Problem (4.22) is equivalent to the problem

$$\begin{aligned}
\min_{x,y} \max_{\Delta \in \mathcal{U}} \quad & f_{poly}(x + \Delta x, y + \Delta y) \\
s.t. \quad & h_1^{rob}(x, y) \leq 0 \\
& h_2^{rob}(x, y) \leq 0.
\end{aligned} \tag{4.23}$$

We applied the robust local search on both Problem (4.22) and Problem (4.23), using the same initial design. The difference in performance is then compared. The nominal and the estimated worst cost surface is shown in Fig. 4-6.

4.4.2   Computation Results

The algorithm reduced the worst case cost significantly and converged to the same robust local minimum in both cases. This is shown in Fig. 4-10(a),(b). Fig. 4-10(b) also shows that the reduction in worst case cost is faster when solving Problem (4.23).

The most significant difference was the time required to terminate. While the algorithm took 3600 seconds to terminate for Problem (4.22), it terminated in only 96 seconds when applied to Problem (4.23), which involves robust counterparts.

Fig. 4-10(c) shows that the robust local minimum satisfies the terminating conditions stated in Section 4.1.2:

(i) Design is feasible under perturbations: The robust local minimum lies on line
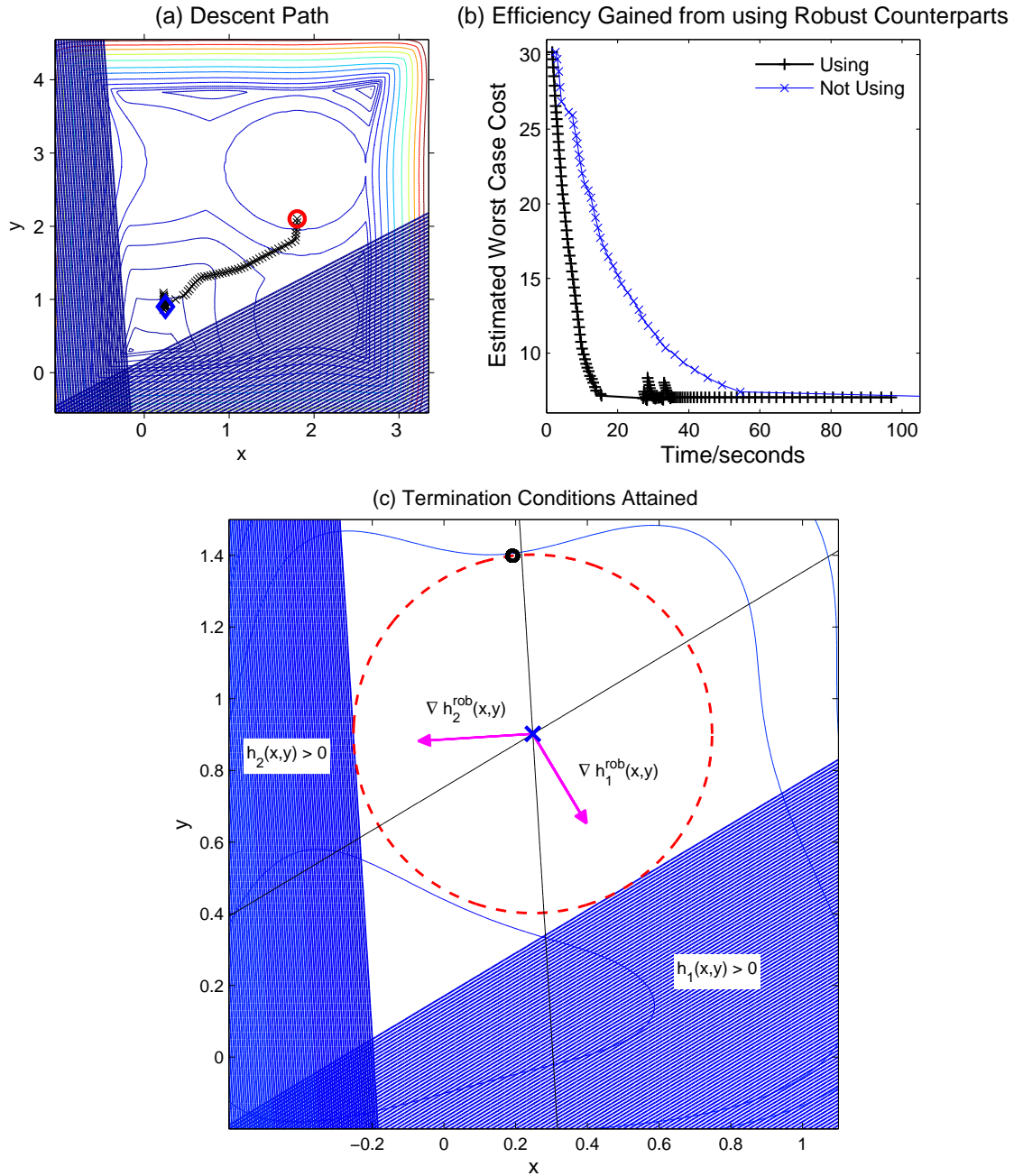
Figure 4-10: Performance of the robust local search algorithm applied to Problem (4.22)-(4.23). (a) In both instances, the algorithm takes a similar descent path and converge at the same robust local minimum. (b) The robust local search is more efficient when applied on the problem formulated with robust counterparts. (c) Termination criteria attained by the robust local minimum (x^*, y^*), which is indicated by the cross marker. The solid line parallel to the shaded infeasible regions $h_j(x, y) > 0$ denote the line $h_j^{rob}(x, y) = 0$, for $j = 1, 2$. (x^*, y^*) is robust because it does not violate the constraints $h_j^{rob}(x, y) \leq 0$. From (x^*, y^*), there are also no vectors pointing away from the bad neighbor (bold circle) and the directions $\nabla h_j^{rob}(x, y)$.

intersection $h_j^{rob}(x, y) = 0$, $j = 1, 2$. Since the constraints are not violated, the design is feasible under perturbations. The robustness is also confirmed by the lack of overlapping between its neighborhood and the shaded regions.

(ii) <u>No improving direction $\mathbf{d}_{cost}^*$</u>: There are no directions (vectors) pointing away from the bad neighbor, and making angle larger than $90°$ with the gradients, $\nabla h_j^{rob}(x, y)$.

4.5   Application V: A Problem in Intensity Modulated Radiation Therapy (IMRT) for Cancer Treatment

Radiation therapy is a key component in cancer treatment today. In this form of treatment, ionizing radiation is directed onto cancer cells with the objective of destroying them. Unfortunately, healthy and non-cancerous cells are exposed to the destructive radiation as well since cancerous tumors are embedded within the patient's body. Even though most healthy cells can repair themselves, an important objective behind the planning process is to minimize the total radiation received by the patient ("objective"), while ensuring that the tumor is subjected to a sufficient level of radiation ("constraints").

Most radiation oncologists adopt the technique of Intensity Modulated Radiation Therapy (IMRT) [10]. In IMRT, the dose distribution is controlled by two set of decisions. First, instead of a single beam, multiple beams of radiation are directed onto the tumor, from different angles. This is illustrated in Fig. 4-11 and accomplished using a rotatable oncology system such as the one shown in Fig. 4-12. Furthermore, the intensity of each individual beam can be modulated using multi-leaf collimators such as the one shown in Fig. 4-13. The beam passes through the gap made by multiple layers of collimators. By sliding the collimators, the shape of the gap and, consequently, the radiation dosage distribution can be controlled.

Fig. 4-14 shows the schematic of a IMRT treatment. In the example illustrated,
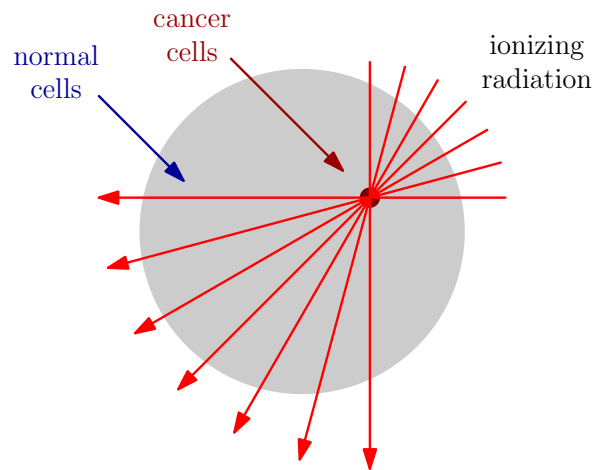
Figure 4-11: Multiple ionizing radiation beams are directed at cancerous cells with the objective of destroying them.

Figure 4-12: A typical oncology system used in IMRT. The radiation beam can be directed onto a patient from different angles, because the equipment can be rotated about an axis. Credits to: Rismed Oncology Systems, http://www.rismed.com/ systems/tps/IMG_2685.JPG, April 15, 2007.

Figure 4-13: A beam's eye-view of the multi-leaf collimators used for beam modulation in IMRT. The radiation beam passes through the gap made by multiple layers of collimators. By sliding the collimators, the shape of the gap is changed. Consequently, the distribution of the radiation dosage introduced to the body can be controlled. Credits to: Varian Medical Systems, http:// www.varian.com, April 15, 2007.

radiation is directed from three angles. Moreover, there are three beamlets in each beam and their intensities are controllable as well. By choosing the beam angles and the beamlet intensities ("decision variables"), it is desirable to make the treated volume conform as closely as possible to the target volume, thereby minimizing radiation dosage on organ-at-risk (OAR) and normal tissues. In a case of prostate cancer, for instance, the target volume would include the prostate glands, while the OAR would include the rectum, the spine and the kidneys. Without careful planning, the treatment can easily damage these organs-at-risk and reduce a patient's quality of life subsequently, even if the cancer has been addressed.

Optimization Problem We obtained our optimization model through a joint research project with the Massachusetts General Hospital. In the model, all the affected body tissue are divided into discrete volume elements called a voxel v [21]. The voxels belong to three sets. They are, namely,

- $\mathcal{T}$: the set of tumor voxels, $|\mathcal{T}| = 145$.
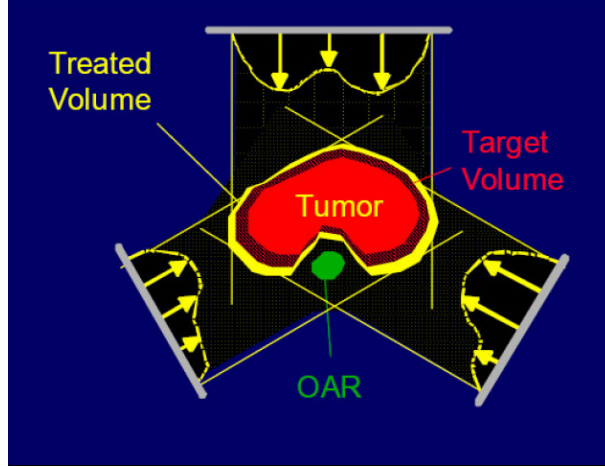
Figure 4-14: Schematic of IMRT. Radiation is delivered on the tumor from three different angles. From each angle, a single beam is made up of 3 beamlets, denoted by the arrows. Credits to: Thomas Bortfeld, Massachusetts General Hospital.

- $\mathcal{O}$: the set of organ-at-risk voxels, $|\mathcal{O}| = 42$.
- $\mathcal{N}$: the set of normal tissue voxels, $|\mathcal{N}| = 1005$.

Let the set of all voxels be $\mathcal{V}$. Therefore, $\mathcal{V} = \mathcal{T} \cup \mathcal{O} \cup \mathcal{N}$ and $|\mathcal{V}| = 1192$; there are a total of 1192 voxels.

In our application example, there are five beams, each from a different angle. In each beam, there are sixteen beamlets. Let $\theta \in \mathbb{R}^5$ be the vector of beam angles and $\mathcal{I}$ be the set of beams. In addition, let $\mathcal{B}_i$ be set of beamlets b belonging to beam i, $i \in \mathcal{I}$. Finally, let x_i^b be the intensity of beamlet b, $b \in \mathcal{B}_i$, and $\mathbf{x} \in \mathbb{R}^{16 \times 5}$ be the vector of beamlet intensities,

$$
\mathbf{x} = \begin{pmatrix} \mathbf{x}_1^1 \\ \vdots \\ \mathbf{x}_1^{16} \\ \mathbf{x}_2^1 \\ \vdots \\ \mathbf{x}_5^{16} \end{pmatrix}. \tag{4.24}
$$

Let $D_v^b(\theta_i)$ be the radiation dosage in voxel v introduced by beamlet b from beam i when the beamlet has an intensity of 1, i.e. $x_i^b = 1$. Thus, $\sum_i \sum_b D_v^b(\theta_i) x_i^b$ denotes the total dosage in voxel v under a treatment plan $(\theta, \mathbf{x})$. Therefore, the objective is to minimize a weighted sum of the radiation dosage in all voxels, while ensuring

that (i) a minimum dosage l_v is delivered to each tumor voxel $v \in \mathcal{T}$, and (ii) the dosage in each voxel v does not exceed an upper limit u_v. Consequently, the nominal optimization problem is

$$
\begin{aligned}
\min_{\mathbf{x}, \theta} \quad & \sum_{v \in \mathcal{V}} \sum_{i \in \mathcal{I}} \sum_{b \in \mathcal{B}_i} c_v D_v^b(\theta_i) x_i^b \\
s.t. \quad & \sum_{i \in \mathcal{I}} \sum_{b \in \mathcal{B}_i} D_v^b(\theta_i) x_i^b \geq l_v, \quad \forall v \in \mathcal{T}, \\
& \sum_{i \in \mathcal{I}} \sum_{b \in \mathcal{B}_i} D_v^b(\theta_i) x_i^b \leq u_v, \quad \forall v \in \mathcal{V}, \\
& x_i^b \geq 0, \quad\quad\quad\quad\quad\quad \forall b \in \mathcal{B}_i, \forall i \in \mathcal{I},
\end{aligned}
\tag{4.25}
$$

where term c_v is the penalty of a unit dose in voxel v. A much higher penalty is set for a voxel in the OAR versus a voxel in the normal tissue.

Note, that if θ is given, Problem (4.25) reduces to an LP and the optimal intensities $\mathbf{x}^*(\theta)$ can be found efficiently. However, the problem is nonconvex in θ because varying a single θ_i changes $D_v^b(\theta_i)$ for all voxel v and for all $b \in \mathcal{B}_i$.

Let ϕ be the angle of a single beam. To get $D_v^b(\phi)$, the values at $\phi = 0°, 2°, \ldots, 358°$ were derived using CERR, a numerical solver for radiotherapy research [21]. Subsequently for a given $\hat{\theta}$, $D_v^b(\hat{\theta})$ is obtained using a linear interpolation using these derived values:

$$
D_v^b(\hat{\theta}) \;\; = \;\; \frac{\phi - \hat{\theta} + 2°}{2°} \cdot D_v^b(\phi) + \frac{\hat{\theta} - \phi}{2°} \cdot D_v^b(\phi + 2°)
\tag{4.26}
$$

where $\phi = 2\lfloor \frac{\hat{\theta}}{2} \rfloor$. It is not practical to use the numerical solver to compute $D_v^b(\hat{\theta})$ directly during optimization because the derivation takes too much time.

Model of Uncertainty   When a design $(\theta, \mathbf{x})$ is implemented, the realized design is of the form $(\theta + \Delta\theta, \mathbf{x} \otimes (\mathbf{1} \pm \delta))$, where $\otimes$ refers to an element-wise multiplication. The sources of errors include equipment limitation, the difference in the patient's posture when measuring and irradiating, and minute body movements. The perturbations

are estimated to be normally and independently distributed:

$$
\begin{aligned}
\delta_i^b &\sim \mathcal{N}(0, 0.01), \\
\Delta\theta_i &\sim \mathcal{N}\left(0, \tfrac{1}{3}^\circ\right).
\end{aligned}
\tag{4.27}
$$

Under the robust optimization approach, we define the uncertainty set

$$
\mathcal{U} = \left\{ \begin{pmatrix} \frac{\delta}{0.03} \\ \Delta\theta \end{pmatrix} \ \Big| \ \left\| \begin{matrix} \frac{\delta}{0.03} \\ \Delta\theta \end{matrix} \right\|_2 \leq \Gamma \right\}.
\tag{4.28}
$$

The factor 0.03 is introduced to compensate for the difference in error magnitudes. Numerous robust designs will be obtained using different values of Γ. These designs will then be compared using 10,000 samples drawn from the distribution in Eq. (4.27).

Given the uncertainty set Eqn.(4.28), the corresponding robust problem is

$$
\begin{aligned}
\min_{\mathbf{x},\theta} \quad & \max_{(\delta,\Delta\theta)\in\mathcal{U}} \sum_{v\in\mathcal{V}}\sum_{i\in\mathcal{I}}\sum_{b\in\mathcal{B}_i} c_v D_v^b(\theta_i + \Delta\theta_i)x_i^b(1+\delta_i^b) \\
s.t. \quad & \min_{(\delta,\Delta\theta)\in\mathcal{U}} \sum_{i\in\mathcal{I}}\sum_{b\in\mathcal{B}_i} D_v^b(\theta_i + \Delta\theta_i)x_i^b(1+\delta_i^b) \geq l_v, \quad \forall v \in \mathcal{T} \\
& \max_{(\delta,\Delta\theta)\in\mathcal{U}} \sum_{i\in\mathcal{I}}\sum_{b\in\mathcal{B}_i} D_v^b(\theta_i + \Delta\theta_i)x_i^b(1+\delta_i^b) \leq u_v, \quad \forall v \in \mathcal{V}, \\
& x_i^b \geq 0, \qquad\qquad\qquad\qquad\qquad\qquad\qquad \forall b \in \mathcal{B}_i, \forall i \in \mathcal{I}.
\end{aligned}
\tag{4.29}
$$

Approximating the Robust Problem It is not practical to apply the robust local search on Problem 4.29 directly. Instead, we approximate the problem with a formulation that can be evaluated more efficiently, as follows.

Because $D_v^b(\theta_i)$ is obtained through a linear interpolation,

$$
D_v^b(\theta_i \pm \Delta\theta) \approx D_v^b(\theta_i) \pm \frac{D_v^b(\phi + 2^\circ) - D_v^b(\phi)}{2^\circ}\Delta\theta,
\tag{4.30}
$$

where $\phi = 2\lfloor\frac{\theta_i}{2}\rfloor$ and $D_v^b(\phi)$, $D_v^b(\phi + 2^\circ)$ are values derived from the numerical solver. Note, that if $\theta_i \pm \Delta\theta \in [\phi, \phi + 2^\circ]$, for all $\Delta\theta$, Eqn. (4.30) is exact.

Let $\frac{\partial}{\partial \theta} D_v^b(\theta_i) = \frac{D_v^b(\phi + 2°) - D_v^b(\phi)}{2°}$. Then,

$$
\begin{aligned}
& D_v^b(\theta_i + \Delta\theta_i) \cdot x_i^b \cdot (1 + \delta_i^b) \\
\approx\; & \left(D_v^b(\theta_i) + \frac{\partial}{\partial\theta} D_v^b(\theta_i) \cdot \Delta\theta_i \right) \cdot x_i^b \cdot (1 + \delta_i^b) \\
=\; & D_v^b(\theta_i) \cdot x_i^b + D_v^b(\theta_i) \cdot x_i^b \cdot \delta_i^b + \frac{\partial}{\partial\theta} D_v^b(\theta_i) \cdot x_i^b \cdot \Delta\theta_i + \frac{\partial}{\partial\theta} D_v^b(\theta_i) \cdot x_i^b \cdot \Delta\theta_i \cdot \delta_i^b \\
\approx\; & D_v^b(\theta_i) \cdot x_i^b + D_v^b(\theta_i) \cdot x_i^b \cdot \delta_i^b + \frac{\partial}{\partial\theta} D_v^b(\theta_i) \cdot x_i^b \cdot \Delta\theta_i. \quad\quad (4.31)
\end{aligned}
$$

In the final approximation step, the second order terms are dropped.

By using Eqn.(4.31) repeatedly,

$$
\begin{aligned}
& \max_{(\delta,\Delta\theta)\in\mathcal{U}} \sum_{v\in\mathcal{V}}\sum_{i\in\mathcal{I}}\sum_{b\in\mathcal{B}_i} c_v \cdot D_v^b(\theta_i + \Delta\theta_i) \cdot x_i^b \cdot (1 + \delta_i^b) \\
\approx\; & \max_{(\delta,\Delta\theta)\in\mathcal{U}} \sum_{v\in\mathcal{V}}\sum_{i\in\mathcal{I}}\sum_{b\in\mathcal{B}_i} \left(c_v \cdot D_v^b(\theta_i) \cdot x_i^b + c_v \cdot D_v^b(\theta_i) \cdot x_i^b \cdot \delta_i^b + c_v \cdot \frac{\partial}{\partial\theta} D_v^b(\theta_i) \cdot x_i^b \cdot \Delta\theta_i \right) \\
=\; & \sum_{v\in\mathcal{V}}\sum_{i\in\mathcal{I}}\sum_{b\in\mathcal{B}_i} c_v \cdot D_v^b(\theta_i) \cdot x_i^b + \\
& \max_{(\delta,\Delta\theta)\in\mathcal{U}} \left\{ \sum_{i\in\mathcal{I}}\sum_{b\in\mathcal{B}_i} \left(\sum_{v\in\mathcal{V}} c_v D_v^b(\theta_i) \right) x_i^b \delta_i^b + \sum_{i\in\mathcal{I}} \left(\sum_{b\in\mathcal{B}_i} \left(\sum_{v\in\mathcal{V}} c_v \frac{\partial}{\partial\theta} D_v^b(\theta_i) \right) x_i^b \right) \Delta\theta_i \right\} \\
=\; & \sum_{v\in\mathcal{V}}\sum_{i\in\mathcal{I}}\sum_{b\in\mathcal{B}_i} c_v \cdot D_v^b(\theta_i) \cdot x_i^b + \Gamma \left\| \begin{matrix} 0.03\cdot\sum_{v\in\mathcal{V}} c_v \cdot D_v^1(\theta_1)\cdot x_1^1 \\ \vdots \\ 0.03\cdot\sum_{v\in\mathcal{V}} c_v \cdot D_v^{16}(\theta_1)\cdot x_1^{16} \\ 0.03\cdot\sum_{v\in\mathcal{V}} c_v \cdot D_v^1(\theta_2)\cdot x_2^1 \\ \vdots \\ 0.03\cdot\sum_{v\in\mathcal{V}} c_v \cdot D_v^{16}(\theta_5)\cdot x_5^{16} \\ \sum_{b\in\mathcal{B}_1}\sum_{v\in\mathcal{V}} c_v \cdot \frac{\partial}{\partial\theta} D_v^b(\theta_1)\cdot x_1^b \\ \vdots \\ \sum_{b\in\mathcal{B}_5}\sum_{v\in\mathcal{V}} c_v \cdot \frac{\partial}{\partial\theta} D_v^b(\theta_5)\cdot x_5^b \end{matrix} \right\|_2. \quad\quad (4.32)
\end{aligned}
$$

Because all the terms in the constraints are similar to those in the objective function, the constraints can be approximated using the same approach. To simplify the notation, the 2-norm term in Eqn.(4.32) shall be represented by

$$
\left\| \begin{matrix} \left\{ 0.03\cdot\sum_{v\in\mathcal{V}} c_v \cdot D_v^b(\theta_i)\cdot x_i^b \right\}_{b,i} \\ \left\{ \sum_{b\in\mathcal{B}_1}\sum_{v\in\mathcal{V}} c_v \cdot \frac{\partial}{\partial\theta} D_v^b(\theta_i)\cdot x_i^b \right\}_i \end{matrix} \right\|_2.
$$

Using this procedure, we obtain the nonconvex robust problem

$$
\min_{\mathbf{x},\theta} \quad \sum_{v\in\mathcal{V}}\sum_{i\in\mathcal{I}}\sum_{b\in\mathcal{B}_i} c_v \cdot D_v^b(\theta_i) \cdot x_i^b + \Gamma \left\| \begin{matrix} \left\{0.03\cdot\sum_{v\in\mathcal{V}} c_v \cdot D_v^b(\theta_i)\cdot x_i^b\right\}_{b,i} \\ \left\{\sum_{b\in\mathcal{B}_i}\sum_{v\in\mathcal{V}} c_v \cdot \frac{\partial}{\partial\theta} D_v^b(\theta_i)\cdot x_i^b\right\}_i \end{matrix} \right\|_2
$$

$$
s.t. \quad \sum_{i\in\mathcal{I}}\sum_{b\in\mathcal{B}_i} D_v^b(\theta_i) \cdot x_i^b - \Gamma \left\| \begin{matrix} \left\{0.03\cdot\sum_{v\in\mathcal{V}} D_v^b(\theta_i)\cdot x_i^b\right\}_{b,i} \\ \left\{\sum_{b\in\mathcal{B}_i}\sum_{v\in\mathcal{V}} \frac{\partial}{\partial\theta} D_v^b(\theta_i)\cdot x_i^b\right\}_i \end{matrix} \right\|_2 \geq l_v, \qquad \forall v \in \mathcal{T}
$$

$$
\sum_{i\in\mathcal{I}}\sum_{b\in\mathcal{B}_i} D_v^b(\theta_i) \cdot x_i^b + \Gamma \left\| \begin{matrix} \left\{0.03\cdot\sum_{v\in\mathcal{V}} D_v^b(\theta_i)\cdot x_i^b\right\}_{b,i} \\ \left\{\sum_{b\in\mathcal{B}_i}\sum_{v\in\mathcal{V}} \frac{\partial}{\partial\theta} D_v^b(\theta_i)\cdot x_i^b\right\}_i \end{matrix} \right\|_2 \leq u_v, \qquad \forall v \in \mathcal{V},
$$

$$
x_i^b \geq 0, \qquad\qquad\qquad\qquad\qquad \forall b \in \mathcal{B}_i, \forall i \in \mathcal{I},
$$

$$(4.33)$$

which closely approximates the original robust problem (4.29). Note, that when θ and $\mathbf{x}$ are known, the objective cost and all the constraint values can be computed efficiently.

4.5.1 Computation Results

A large number of robust designs $(\theta^k, \mathbf{x}^k)$, $k = 1, 2, \ldots$ were found using the following algorithm:

Algorithm 5 Algorithm Applied to IMRT Problem

Step 0. Initialization: Let $(\theta^0, \mathbf{x}^0)$ be the initial design, and Γ^0 be the initial value. Set $k := 1$.

Step 1. Set $\Gamma^k := \Gamma^{k-1} + \Delta\Gamma$ where $\Delta\Gamma$ is a small scalar and can be negative.

Step 2. Find a robust local minimum by apply Algorithm 4.1.4 with
    i. initial design $(\theta^{k-1}, \mathbf{x}^{k-1})$, and
    ii. uncertainty set (4.28) with $\Gamma = \Gamma^k$.

Step 3. Set $(\theta^k, \mathbf{x}^k)$ to the robust local minimum found.

Step 4. Set $k := k + 1$. Go to Step 1; if $k > k_{max}$, terminate.

Two initial designs $(\theta^0, \mathbf{x}^0)$ were used. They are

(i) "Nominal Best": a local minimum of the nominal problem, and

(ii) "Strict Interior": a design lying in the strict interior of the feasible set of the nominal problem. It is found by finding a local minimum to the following

problem:

$$\min_{\mathbf{x},\theta} \quad \sum_{v\in\mathcal{V}}\sum_{i\in\mathcal{I}}\sum_{b\in\mathcal{B}_i} c_v D_v^b(\theta_i)x_i^b$$

$$s.t. \quad \sum_{i\in\mathcal{I}}\sum_{b\in\mathcal{B}_i} D_v^b(\theta_i)x_i^b \geq l_v + buffer, \quad \forall v \in \mathcal{T}$$

$$\sum_{i\in\mathcal{I}}\sum_{b\in\mathcal{B}_i} D_v^b(\theta_i)x_i^b \leq u_v - buffer, \quad \forall v \in \mathcal{V},$$

$$x_i^b \geq 0, \quad\quad\quad\quad\quad \forall b \in \mathcal{B}_i, \forall i \in \mathcal{I}.$$

From the "Nominal Best", Algorithm 4.5.1 is applied with an increasing Γ^k: $\Gamma^0 = 0$ and $\Delta\Gamma = 0.001$, for all k. k_{max} was set to be 250. It is estimated that beyond this value, the probability would be so close to 1 that increasing Γ further would simply increase the cost without reducing the probability any further. Because the "Nominal Best" is an optimal solution to an LP, it lies on the extreme point of the feasible set. Consequently, even small perturbations can cause constraint violations. In every iteration of Algorithm 4.5.1, Γ^k is increased slowly. With each new iteration, the terminating design will remains feasible under a larger perturbation.

The "Strict Interior" design, on the other hand, will not violate the constraints under larger perturbations because of the *buffer* introduced. However, this increased robustness comes with a higher nominal cost. By evaluating Problem 4.33, the "Strict Interior" was found to satisfy the constraints for $\Gamma \leq 0.05$. Thus, we apply Algorithm 4.5.1 using this initial design twice as follows:

(i) $\Gamma^0 = 0.05$ and $\Delta\Gamma = 0.001$, for all k. k_{max} was set o 150, and

(ii) $\Gamma^0 = 0.051$ and $\Delta\Gamma = -0.001$, for all k. k_{max} was set to 50.

Finally, the designs $(\theta^k, \mathbf{x}^k)$ were assessed for their performance under implementation errors, using $10,000$ random scenarios drawn from the assumed normal distributions, Eqn. (4.27).

Pareto Frontiers As discussed, the increase in the robustness of a design often results in a higher cost. Therefore, when comparing robust designs, we look at (i) the mean cost, and (ii) the probability of violation. If the mean cost is replaced by the

114

worst simulated cost, the result is similar and, thus, omitted. Furthermore, from empirical evidences, random sampling is not a good gauge of the worst case cost. To get a good worst cost estimate, multiple gradient ascents are necessary, but that is not practical in this application due to the large number of designs involved.

With multiple performance measures, the best designs lie on the pareto frontier. The two pareto frontiers, attained by the designs found separately using "Nominal Best" and "Strict Interior', are shown in Fig. 4-15.

When the probability of violation is high, the designs found from the "Nominal Best" have lower costs. However, if the constraints have to be satisfied with a high probability, designs found from the "Strict Interior" perform better. Furthermore, the strategy of increasing Γ slowly in Algorithm 4.5.1 adjust the tradeoffs between robustness and cost, thus enabling the algorithm to map out the pareto frontier in a single sweep, as indicated in Fig. 4-15.

Different Modes in a Robust Local Search The robust local search has two distinct modes. When iterates are not robust, the search first seeks a robust design, with no consideration for the worst case cost. (See Step 3(i) in Algorithm 4.2.2) After a robust design has been found, the search then improves the worst case cost until a robust local minimum has been found. (See Step 3(ii) in Algorithm 4.2.2) These two modes are illustrated in Fig. 4-16 for a typical robust local search carried out in Application VI.

4.5.2 Comparison with Convex Robust Optimization Techniques

While the robust problem (4.33) is not convex, convex robust optimization techniques can be used in this special case, by exploiting the convexity of the resulting subproblem when θ is fixed. Note, that when θ is fixed in Problem (4.33), the resulting subproblem is a SOCP problem. Therefore, given a θ, a robust $\mathbf{x}^*(\theta)$ can be found. Because all the constraints are addressed, $(\theta, \mathbf{x}^*(\theta))$ is a robust design. Thus, the problem reduces to finding a local minimum θ. This can be achieved by using a

115
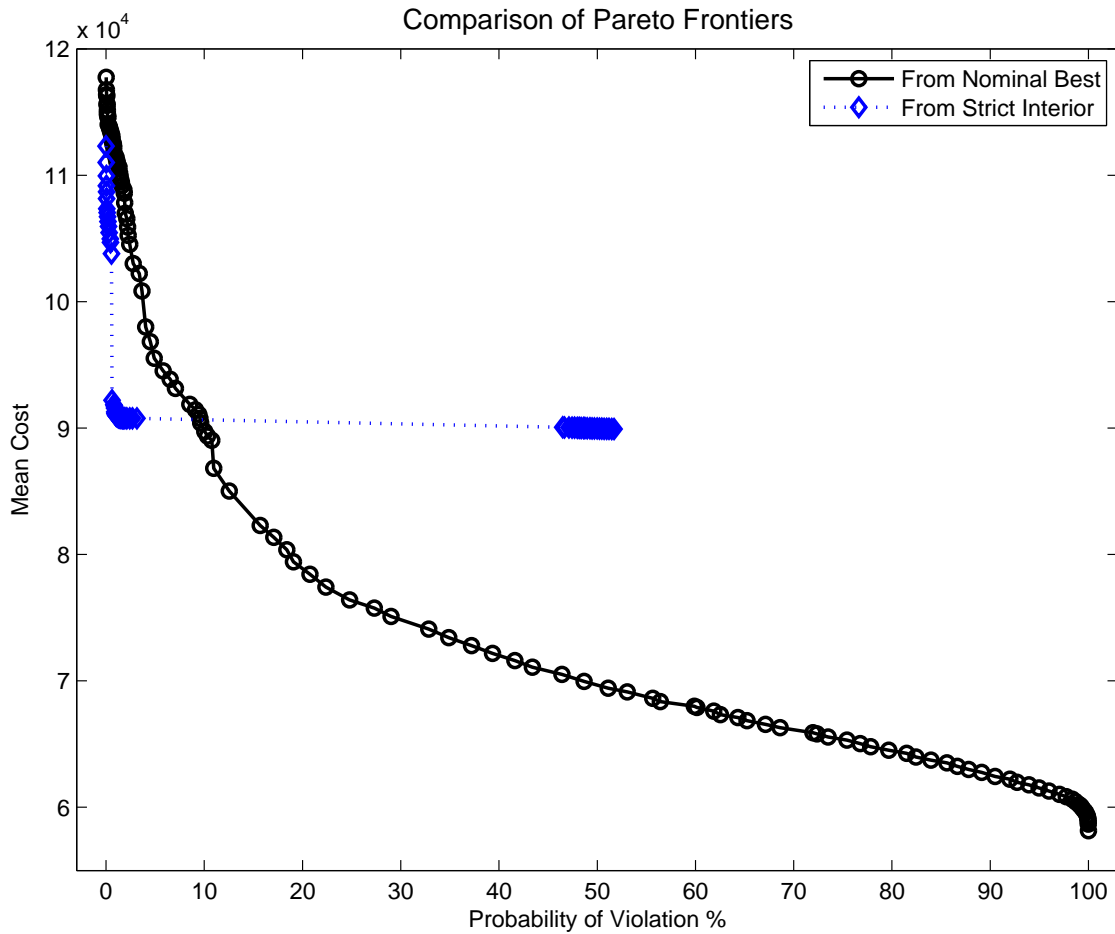
Figure 4-15: Pareto frontiers attained by Algorithm 4.5.1, for different initial designs: "Nominal Best" and "Strict Interior'. The mean cost and the probability of violation were assessed using 10,000 random scenarios drawn from the assumed distribution, Eqn. (4.27). A design that is robust to larger perturbations, as indicated by a larger Γ, has a lower probability of violation but a higher cost. The designs found from "Nominal Best" have lower costs when the required probability of violation is high. When the required probability is low, however, the designs found from "Strict Interior" perform better.
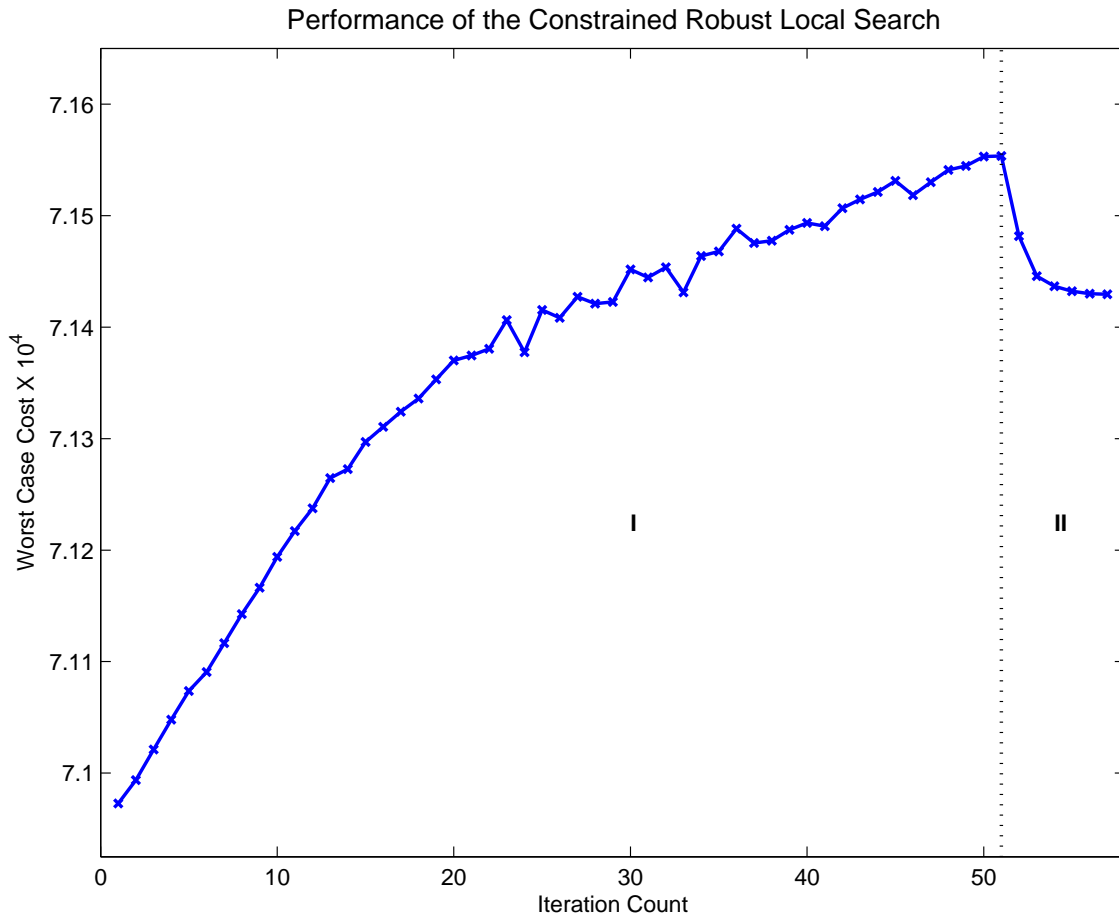
Figure 4-16: A typical robust local search carried out in Step 2 of Algorithm 4.5.1 for Application VI. The search starts from a non-robust design and terminates at a robust local minimum. In phase I, the algorithm looks for a robust design without considerations of the worst case cost. (See Step 3(i) in Algorithm 4.2.2) Due to the tradeoff between cost and feasibility, the worst case cost increases during this phase. At the end of phase I, a robust design is found. Subsequently, the algorithm looks for robust designs with lower worst case cost, in phase II (See Step 3(ii) in Algorithm 4.2.2), resulting in a gradient descent-like improvement in the worst case cost.

steepest descent algorithm with finite-difference estimate of the gradients.

Let $J_{rob}(\theta^k)$ be the cost of Problem (4.33) when $\theta := \theta^k$. The above approach is summarized in the following algorithm:

Algorithm 6 Algorithm Using Convex Techniques in the IMRT Problem

---

Step 0. Initialization: Set $k := 1$. Let θ^1 be the initial design.
Step 1. Get $\mathbf{x}^k(\theta^k)$ by:
    (a) Solve Problem (4.33) with $\theta := \theta^k$.
    (b) Set $\mathbf{x}^k$ to the optimal solution of the subproblem.
Step 2. Estimate gradient $\frac{\partial}{\partial \theta} J_{rob}(\theta^k)$ using finite-differences:
    (a) Solve Problem (4.33) with $\theta = \theta^k \pm \epsilon \cdot \mathbf{e}_i$, for all $i \in \mathcal{I}$, where ϵ is a small
        positive scalar and $\mathbf{e}_i$ is an unit vector in the i-th coordinate.
    (b) For all $i \in \mathcal{I}$,
$$\frac{\partial J_{rob}}{\partial \theta_i} = \frac{J(\theta^k + \epsilon \mathbf{e}_i) - J(\theta^k - \epsilon \mathbf{e}_i)}{2 \cdot \epsilon}.$$
Step 3. Check terminating condition:
    (a) If $\left\| \frac{\partial J_{rob}}{\partial \theta} \right\|_2$ is small enough, terminate. Else, take the steepest descent
        step
$$\theta^{k+1} := \theta^k - t^k \frac{\partial J_{rob}}{\partial \theta},$$
    where t^k is a small and diminishing step size.
    (b) Set $k := k + 1$, go to Step 1.

Unfortunately, Algorithm 4.5.2 cannot be implemented because the subproblem, though convex, cannot be solved efficiently. With 1192 SOCP constraints, it takes more than a few hours for CPLEX 9.1 to solve the problem. Given that 11 subproblems are solved in every iteration and more than a hundred iterations are carried in each run of Algorithm 4.5.2, we need a simpler subproblem.

The compromise lies in defining a different uncertainty set. Instead of an ellipsoidal uncertainty set 4.28, which better describes the independently distributed perturbations, we use the polyhedral uncertainty set

$$\mathcal{U} = \left\{ \left(\begin{smallmatrix} \delta \\ 0.03 \\ \Delta\theta \end{smallmatrix} \right) \mid \left\| \begin{smallmatrix} \delta \\ 0.03 \\ \Delta\theta \end{smallmatrix} \right\|_p \leq \Gamma \right\}, \tag{4.34}$$

with norm $p = 1$ or $p = \infty$. The resulting subproblem becomes

$$
\begin{aligned}
\min_{\mathbf{x}} \quad & \sum_{v \in \mathcal{V}} \sum_{i \in \mathcal{I}} \sum_{b \in \mathcal{B}_i} c_v \cdot D_v^b(\theta_i) \cdot x_i^b + \Gamma \left\| \begin{array}{c} \left\{ 0.03 \cdot \sum_{v \in \mathcal{V}} c_v \cdot D_v^b(\theta_i) \cdot x_i^b \right\}_{b,i} \\ \left\{ \sum_{b \in \mathcal{B}_1} \sum_{v \in \mathcal{V}} c_v \cdot \frac{\partial}{\partial \theta} D_v^b(\theta_i) \cdot x_i^b \right\}_i \end{array} \right\|_q \\
s.t. \quad & \sum_{i \in \mathcal{I}} \sum_{b \in \mathcal{B}_i} D_v^b(\theta_i) \cdot x_i^b - \Gamma \left\| \begin{array}{c} \left\{ 0.03 \cdot \sum_{v \in \mathcal{V}} D_v^b(\theta_i) \cdot x_i^b \right\}_{b,i} \\ \left\{ \sum_{b \in \mathcal{B}_1} \sum_{v \in \mathcal{V}} \frac{\partial}{\partial \theta} D_v^b(\theta_i) \cdot x_i^b \right\}_i \end{array} \right\|_q \geq l_v, \qquad \forall v \in \mathcal{T} \\
& \sum_{i \in \mathcal{I}} \sum_{b \in \mathcal{B}_i} D_v^b(\theta_i) \cdot x_i^b + \Gamma \left\| \begin{array}{c} \left\{ 0.03 \cdot \sum_{v \in \mathcal{V}} D_v^b(\theta_i) \cdot x_i^b \right\}_{b,i} \\ \left\{ \sum_{b \in \mathcal{B}_1} \sum_{v \in \mathcal{V}} \frac{\partial}{\partial \theta} D_v^b(\theta_i) \cdot x_i^b \right\}_i \end{array} \right\|_q \leq u_v, \qquad \forall v \in \mathcal{V}, \\
& x_i^b \geq 0, \qquad\qquad\qquad\qquad\qquad\qquad\qquad\qquad\qquad \forall b \in \mathcal{B}_i, \forall i \in \mathcal{I}
\end{aligned}
$$
(4.35)

where $\frac{1}{p} + \frac{1}{q} = 1$. For $p = 1$ and $p = \infty$, Problem (4.35) is an LP, which takes less than 5 seconds to solve. Note, that θ is a constant in this formulation. Now, by replacing the subproblem of Problem (4.33) with Problem (4.35) every time, Algorithm 4.5.2 can be applied to find a robust local minimum. For a given Γ, Algorithm 4.5.2 takes around one to two hours to terminate.

Computation Results We found a large number of robust designs using Algorithm 4.5.2 with different Γ, and with both "Nominal Best" and "Strict Interior" as the initial designs. This is done for both $p = 1$ ("P1") and $p = \infty$ ("Pinf"). Finally, we compare the pareto frontiers of all the designs found under the robust local search ("RLS"), "P1" and "Pinf". The results are shown in Fig. 4-17. When the required probability of violation is high, the convex techniques find better robust designs. However, the designs found by the robust local search is better when the required probability is low.

Compared to the robust local search, the convex approaches have inherent advantages in that optimal robust designs $\mathbf{x}^*(\theta)$ is guaranteed with every θ. This is an explanation why the convex approaches find better designs for a larger probability of violation.

The robust local search is designed for a far more general problem, and consequently, it did not assume nor exploit convexities in the subproblems. Nevertheless, its performance is comparable to the convex approaches, especially when the required probability of violation is low. To make a conclusive comparison, however,
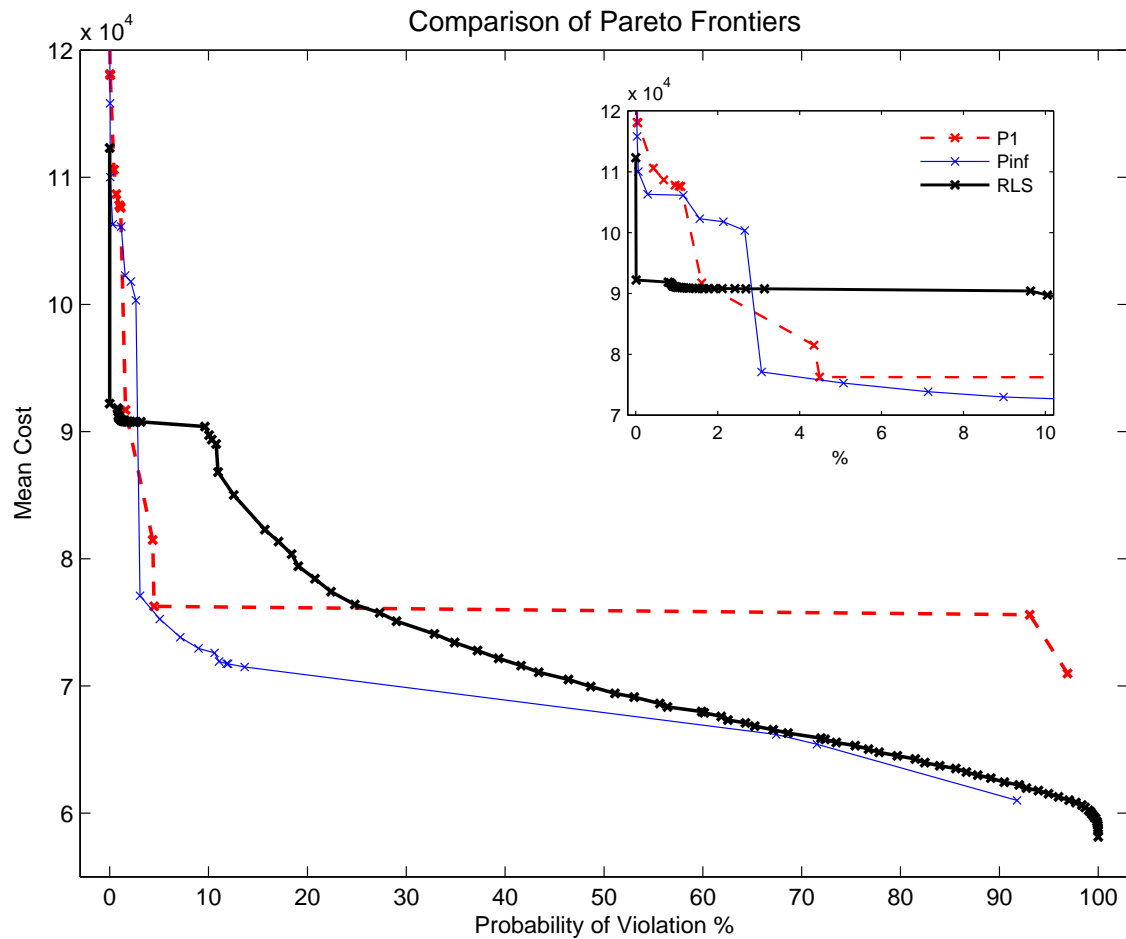
Figure 4-17: Pareto frontiers attained by the robust local search ("RLS") and convex robust optimization technique separately with a 1-norm ("P1") and ∞-norm ("Pinf") uncertainty sets (4.34). While the convex techniques find better robust designs when the required probability of violation is high, the robust local search finds better design when the required probability is low.

would require using the three methods with a large number of initial designs. That, unfortunately, is not practical.

4.6   Conclusions

We have generalized the robust local search technique to handle problems with constraints. Additional constraints do not change the basic structure of the algorithm, which consists of a neighborhood search and a robust local move in every iteration. If one new constraint is added to a problem with n-dimensional uncertainties, $n+1$ additional gradient ascents are required in the neighborhood search step. The robust local move is also modified to avoid infeasible neighbors. We apply the algorithm to Application III, an example with an nonconvex objective and nonconvex constraints. The method finds two robust local minima from different starting points. In both instances, the worst cost is reduced by more than 70%.

When a constraint results in a convex constraint maximization problem (4.6), e.g. when h_j is linear or quadratic constraint, we show that the gradient ascents can be replaced with more efficient procedures. For example, if the constraint is linear, the gradient ascents can be replaced by a single function evaluation. This gain in efficiency is demonstrated in Application IV, a problem with linear constraints. In this example, the standard robust local search takes 3600 seconds to converge at the robust local minimum. The same minimum, however, was obtained in 96 seconds, when the gradient ascents were replaced by the function evaluation.

In the constrained version of the robust local search, the additional assumption is as generic as that on the cost function: the availability of a subroutine which provides the constraint value as well as the gradient. Consequently, the technique is applicable to many real-world applications, including nonconvex and simulation-based problem. The generality of the technique is demonstrated in Application V, an actual healthcare problem in Intensity Modulated Radiation Therapy (IMRT) for cancer treatment. Application V has 85 decision variables, and more than a thousand constraints. The original treatment plan, found using optimization without

considerations for uncertainties, always violates the constraints when uncertainties are introduced. Such constraint violations equate to either an insufficient radiation in the cancer cells, or an unacceptably high radiation dosage in the normal cells. Using the robust local search, we find a large number of robust designs using uncertainty sets of different sizes. By considering the pareto frontier of these designs, a treatment planner can find the ideal trade-off between the amount of radiation introduced and the probability of violating the dosage requirements.

Chapter 5

Conclusions

Numerous contributions to the field of robust optimization are made in this thesis. First, we have developed a new robust optimization technique, which is applicable to nonconvex and simulation-based problems. The method makes only a generic assumption - the availability of cost, constraint values and gradients. Thus, it is applicable to most real-world problems. Compared to existing robust optimization techniques, this proposed method is also unique in that it operates directly on the surface of objective function. This is a new approach in robust optimization.

In addition, when developing the robust local search, we have introduced the concept of descent direction for the robust problem as well as the concept of robust local minimum. We derived the relationship between descent directions and the worst uncertainties at a decision. Furthermore, we obtained the conditions under which such descent directions disappeared; equivalently, these are the conditions for a robust local minimum. Descent directions and local minima are important and well studied concepts in optimization theory, and form the building blocks of powerful optimization techniques, such as steepest descent and subgradient methods. The concepts introduced in this thesis share the same potential, but for the robust problem, or as Dantzig puts it, for the real problem.

We demonstrated the generality of the robust local search by extending it to admit additional considerations including parameter uncertainties and nonconvex constraints. In each instance, the basic structure of the algorithm, namely a neighbor-

hood search and a robust local move in every iteration, does not change. This is a testimony to the generic nature of the method, and an indication of its potential to be a component of future robust optimization techniques.

Finally, the practicality of the approach is verified in two actual nonconvex applications: nanophotonic design and Intensity Modulated Radiation Therapy (IMRT) for cancer treatment. In both cases, the numerical models are verified by actual experiments; the method significantly improved the robustness of the design, showcasing the relevance of robust optimization to real-world problems. The first application has 100 decision variables; out technique enables robust optimization in nanophotonic design. The IMRT application has 85 variables and more than a thousand nonconvex constraints; our robust technique enables a trade-off analysis between radiation introduced and probability of violating dosage requirements in radiotherapy.

The intuition developed in this thesis is straightforward and powerful. Robust optimization can be divided into two separate tasks: (i) assessing the worst outcomes of a decision (Neighborhood Search), and (ii) adjusting the decision to counter those undesired outcomes (Robust Local Move). This generic strategy, when applied repeatedly, often lead to better robust designs.

5.1   Areas for Future Research

Besides applying the robust local search technique to myriad real-world applications, possible related research include:

- **Multi-period Robust Local Search**

  In multi-period decision problems, decisions are made not at once, but in stages. Some uncertainties are also revealed in between the stages. Multi-period problems is an active research area in stochastic optimization; there are some recent work in robust optimization on this topic as well. Can the robust local search be generalized to a multi-period problem?

- **Application in Convex Problems**

124

While the robust local search is developed with nonconvex problems in mind, it can also be applied to convex problems. Often, even though a convex problem can be solved readily, solving the robust counterpart of the same problem can be challenging. An example of this is a convex quadratic problem, whose robust counterpart is a SDP. How does the robust local search compare with the robust counterpart approach in this case? In the continuum of convex problems, at which point is the robust local search more efficient than existing convex techniques?

- **Nonconvex Applications with Convex Subproblems**

  Consider a convex problem with an additional nonconvex constraint. Can the robust counterpart approach be generalized to admit this constraint? How does the robust local search compare with the robust counterpart approach in this case? On the other hand, consider a nonconvex problem with a convex subproblem. Can the subproblem be exploited to improve the efficiency of the robust local search?

- **Relationship Between Stochastic and Robust Optimization**

  Robust optimization is stochastic optimization with a value-at-risk objective, when the risk level is zero. Consequently, a common criticism made against robust optimization is its over-conservativeness. However, such conservativeness can be adjusted by changing the size of the uncertainty set. For example, when given a probability distribution of the uncertainties, we can define a uncertainty set to include only a subset of the random outcomes. Subsequently, robust optimization techniques, which may be more efficient than available stochastic optimization techniques, can be applied. The question is: what is the quality of such a robust solution in the stochastic context? What is the best way to define the uncertainty set?

  Optimization under uncertainty is an important but difficult field. The best approach may require ideas from both stochastic and robust optimization. A

unifying theory bringing together these two complementary fields should be the holy grail of researchers in this area.

Appendix A

Robust Local Search (Matlab Implementation)

A.1   Introduction

This appendix is a guide to the robust local search algorithm, implemented in Matlab codes. A constrained robust local search algorithm for a nonconvex problem with general constraints, developed for Application III, is developed and archived. For a copy of the archive, please contact the author at the email address: kwong-meng@alum.mit.edu. When applied to a new problem, the necessary changes required is discussed at the end of the appendix.

A.2   Files Included

The files in the archive can be divided into:

- matlab .m script and function files,

- matlab .mat data-files, and

- auxiliary files generated during the robust local search.

These files are identified in Table A.1-A.3.

Filename	Remarks
reset_constrained.m	To initialize the parameters
RLS_constrained.m	Main robust local search routine
NeighborhoodSearch.m	Neighborhood search on current iterate
NeighborhoodSearchCost.m	Neighborhood search on objective function
NeighborhoodSearchConstraint1.m	Neighborhood search on constraint 1
NeighborhoodSearchConstraint2.m	Neighborhood search on constraint 2
GA_obj.m	Gradient ascent on cost function
GA_h1.m	Gradient ascent on constraint 1
GA_h2.m	Gradient ascent on constraint 2
solver_constrained.m	To get cost, gradients and constraint values
FindDescentDirection.m	Solve SOCP given bad neighbor set

Table A.1: Matlab .m files in archive

Filename	Remarks
parameters_RLS_SE.mat	Parameter file for robust local search
history_RLS_SE.mat	History set $\mathcal{H}^k$
RLS_SE.mat	Result from robust local search
GA.mat	Neighborhood search result from the latest iteration

Table A.2: Matlab .mat data-files in archive

Filename	Remarks
RLS_constrained.txt	Status reports of the robust local search
temp_dist_distory.mat	distance between records in history & and current iterate
neighbor.mat	set of bad neighbor in current iteration

Table A.3: Auxiliary files in archive

A.3 Pseudocode of the Robust Local Search Algorithm

Algorithm 7 Constrained Robust Local Search Algorithm

1: load *parameters_RLS_SE.mat*   ▷ load parameters
2: load *RLS_SE.mat*   ▷ load starting point
3: **for** #iteration = 1 to required number **do**
4:     NEIGHBORHOODSEARCH($\mathbf{x}_k$)   ▷ neighborhood search of current iterate
5:     ROBUSTLOCALMOVE   ▷ make robust local move
6:     update $\mathcal{H}_k$ and *RLS_SE.mat*
7: **end for**

Algorithm 8 Neighborhood Search

1: **procedure** NEIGHBORHOODSEARCH
2:     NEIGHBORHOODSEARCHCOST   ▷ search on objective function
3:     NEIGHBORHOODSEARCHCONSTRAINT1   ▷ search on constraint 1
4:     NEIGHBORHOODSEARCHCONSTRAINT2   ▷ search on constraint 2
5: **end procedure**

Algorithm 9 Neighborhood Search on the cost

1: **procedure** NEIGHBORHOODSEARCHCOST
2:     GRADIENTASCENT($\mathbf{x}^k$,$\mathbf{x}^k$,Cost)   ▷ gradient ascent on the cost from $\mathbf{x}^k$
3:     **for** $i = 1$ to problem dimension **do**
4:        GRADIENTASCENT($\mathbf{x}^k + sgn(\frac{\partial f(\mathbf{x}^k)}{\partial x_i}) \cdot offset \cdot \mathbf{e}_i$,$\mathbf{x}^k$,Cost)
5:     **end for**
6: **end procedure**

A.4 Required changes for a new problem

To adapt the codes to a new problem, the file solver_constrained.m has to be changed, to call a different Oracle. In the archive, the Oracle is another matlab code. In general, however, the solver_constrained.m can call an external numerical solver as follows:

- solver_constrained.m writes $\mathbf{x}$ in a text file

Algorithm 10 Neighborhood Search on constraint 1

1: **procedure** NEIGHBORHOODSEARCHCONSTRAINT
2:     GRADIENTASCENT($\mathbf{x}^k$,$\mathbf{x}^k$,Constraint 1)   ▷ gradient ascent on constraint 1 from $\mathbf{x}^k$
3:     **for** $i = 1$ to problem dimension **do**
4:         GRADIENTASCENT($\mathbf{x}^k + sgn(\frac{\partial h_1(\mathbf{x}^k)}{\partial x_i}) \cdot offset \cdot \mathbf{e}_i$,$\mathbf{x}^k$,Constraint 1)
5:     **end for**
6: **end procedure**

Algorithm 11 Gradient Ascent Procedure

1: **procedure** GRADIENTASCENT(StartingPoint,Neighborhood,Function)
2:     Take gradient steps until distance from $\mathbf{x}^k > 0.8\Gamma$
3:     Take gradient steps with barrier penalty until distance from $\mathbf{x}^k > \Gamma$ or time limit exceeded
4:     Take gradient steps until distance from $\mathbf{x}^k > outer\_radius\_factor \cdot \Gamma$
5: **end procedure**

Algorithm 12 Robust Local Move

1: **procedure** ROBUSTLOCALMOVE
2:     check worst cost & feasibility under perturbations ▷ from neighborhood search and history set
3:     **while** descent direction not found **do**
4:         DEFINEBADNEIGHBORSET   ▷ define set of bad neighbors
5:         FINDDESCENTDIRECTION   ▷ find descent direction
6:     **end while**
7:     take descent direction
8: **end procedure**

Algorithm 13 Procedure to define bad neighbor set

1: **procedure** DEFINEBADNEIGHBORSET
2:     **if** feasible under perturbations **then**
3:         find neighbors with high cost   ▷ from neighborhood search and history set
4:         find nearest bad neighbor   ▷ estimate min. distance to move
5:         define expanded neighborhood   ▷ find bad decisions outside neighborhood
6:         find neighbors with high cost in expanded neighborhood
7:         find infeasible neighbors in expanded neighborhood
8:     **else**
9:         find infeasible neighbors   ▷ from neighborhood search and history set
10:        find nearest infeasible neighbor   ▷ estimate min. distance to move
11:        define expanded neighborhood ▷ find infeasible decisions outside neighborhood
12:        find infeasible neighbors in expanded neighborhood
13:     **end if**
14: **end procedure**

Algorithm 14 Procedure to find descent direction

1: **procedure** FINDDESCENTDIRECTION
2:     **if** feasible under perturbations **then**
3:         **if** too many neighbors **then**
4:             decrease σ ▷ strengthen requirement for bad neighbor
5:         **else if** too few neighbors **then**
6:             increase σ ▷ weaken requirement for bad neighbor
7:         **else**
8:             find descent direction   ▷ by solving SOCP
9:             **if** no direction found **then**
10:                 Decrease σ ▷ strengthen requirement for bad neighbor
11:                 **if** σ small enough **then**
12:                     TEMINATE   ▷ Robust feasible, no descent direction when σ small
13:                 **end if**
14:             **else**
15:                 find distance to move
16:             **end if**
17:         **end if**
18:     **else**
19:         find descent direction   ▷ by solving SOCP
20:         **if** no direction found **then**
21:             TEMINATE   ▷ Not robust feasible, no descent direction, trapped
22:         **else**
23:             find distance to move
24:         **end if**
25:     **end if**
26: **end procedure**

- solver_constrained.m initiates call to Oracle (e.g. PDE and other numerical solver) to evaluate **x**

- Oracle updates a status file when evaluation is complete

- solver_constrained.m reads and returns the results to the robust local search algorithm

When there are more constraints, changes in NeighborhoodSearch.m has to be made to include the additional multiple gradient ascents. Additional files such as NeighborhoodSearchConstraint1.m and GA_h1.m are required. Conversely, when there are less constraints, redundant files such as NeighborhoodSearchConstraint1.m and GA_h1.m has to be removed.

For a new problem, the parameters of the robust local search may need to be changed as well. These parameters are defined in *reset_constrained.m* and include:

- $\mathbf{x}^1$

- *radius*, Γ, radius of uncertainty set

- *initial_step_size*, initial stepsize during gradient ascent (GA)

- *min_step_size*, initial minimum stepsize during GA

- *dim*, dimension of problem

- *sigma*, σ^1

- *MaxNeighbor*, maximum number of neighbors allowed before decreasing sigma

- *MinNeighbor*, minimum number of neighbors allowed before increasing sigma

- *small_sigma_threshold*, termination requirement

Bibliography

[1] A. Ben-Tal and A. Nemirovski. Robust convex optimization. *Mathematics of Operations Research*, 23:769–805, 1998.

[2] A. Ben-Tal and A. Nemirovski. Robust solutions of linear programming problems contaminated with uncertain data. *Mathematical Programming*, 88(3):411–424, 2000.

[3] A. Ben-Tal and A. Nemirovski. *Lectures on Modern Convex Optimization: Analysis, Algorithms, and Engineering Applications*, volume 2 of *MPS/SIAM Series on Optimization*. SIAM, Philadelphia, 2001.

[4] A. Ben-Tal and A. Nemirovski. Robust optimization — methodology and applications. *Mathematical Programming*, 92(3):453–480, 2003.

[5] J. P. Berenger. Three-dimensional perfectly matched layer for the absorption of electromagnetic waves. *Journal of Computational Physics*, 127:363, 1996.

[6] D. Bertsimas and M. Sim. Robust discrete optimization and network flows. *Mathematical Programming*, 98(1–3):49–71, 2003.

[7] D. Bertsimas and M. Sim. The price of robustness. *Operations Research*, 52(1):35–53, 2004.

[8] D. Bertsimas and M. Sim. Tractable approximations to robust conic optimization problems. *Mathematical Programming*, 107(1):5–36, 2006.

[9] J. R. Birge and F. Louveaux. *Introduction to stochastic programming.* Springer-Verlag, New York, 1997.

[10] T. Bortfeld. REVIEW: IMRT: a review and preview. *Physics in Medicine and Biology*, 51:363–+, July 2006.

[11] A. Charnes and W. W. Cooper. Chance-constrained programming. *Management Science*, 6(1):73–79, October 1959.

[12] W. Chen, J. K. Allen, K. L. Tsui, and F. Mistree. Procedure for robust design: Minimizing variations caused by noise factors and control factors. *Journal of Mechanical Design, Transactions Of the ASME*, 118:478–485, 1996.

[13] P. G. Ciarlet. *Finite Element Method for Elliptic Problems.* Society for Industrial and Applied Mathematics, Philadelphia, PA, USA, 2002.

[14] R. D. Cook, D. S. Malkus, M. E. Plesha, and R. J. Witt. *Concepts and Applications of Finite Element Analysis.* John Wiley & Sons, 2007.

[15] J. M. Danskin. The theory of max-min, with applications. *SIAM Journal on Applied Mathematics*, 14(4):641–664, 1966.

[16] J. M. Danskin. *The theory of max-min and its application to weapons allocation problems.* Econometrics and Operations Research. Springer-Verlag, New York, 1967.

[17] G. B. Dantzig. Linear programming under uncertainty. *Management Science*, 1(3/4):197–206, apr 1955.

[18] G. B. Dantzig. Linear programming. *Operations Research*, 50(1):42–47, 2002.

[19] G. B. Dantzig. Linear Programming Under Uncertainty. *Management Science*, 50(12 supplement):1764–1769, 2004.

[20] T. A. Davis. A column pre-ordering strategy for the unsymmetric-pattern multifrontal method. *ACM Transactions on Mathematical Software*, 30(2):165–195, 2004.

[21] J. O. Deasy, A. I. Blanco, and V. H. Clark. Cerr: A computational environment for radiotherapy research. *Medical Physics*, 30(5):979–985, 2003.

[22] M. Dyer and L. Stougie. Computational complexity of stochastic programming problems. *Mathematical Programming*, 106(3):423–432, 2006.

[23] J. M. Geremia, J. Williams, and H. Mabuchi. Inverse-problem approach to designing photonic crystals for cavity QED experiments. *Physical Review E*, 66(6):066606–+, December 2002.

[24] L. E. Ghaoui and H. Lebret. Robust solutions to least-squares problems with uncertain data. *SIAM Journal on Matrix Analysis and Applications*, 18(4):1035–1064, 1997.

[25] L. E. Ghaoui, F. Oustry, and H. Lebret. Robust solutions to uncertain semidefinite programs. *SIAM Journal on Optimization*, 9(1):33–52, 1998.

[26] I. L. Gheorma, S. Haas, and A. F. J. Levi. Aperiodic nanophotonic design. *Journal of Applied Physics*, 95:1420–1426, 2004.

[27] K. Goto and R. Geijn. On reducing tlb misses in matrix multiplication. technical report tr-2002-55. Technical report, The University of Texas at Austin, Department of Computer Sciences, 2002.

[28] A. Hakansson, J. Sanchez-Dehesa, and L. Sanchis. Inverse Design of Photonic Crystal Devices. *ArXiv Condensed Matter e-prints*, March 2005.

[29] D. Henrion and J. B. Lasserre. Gloptipoly: Global optimization over polynomials with matlab and sedumi. *ACM Transactions on Mathematical Software*, 29(2):165–194, 2003.

[30] R. Horst and P. M. Pardalos. *Handbook of Global Optimization*. Kluwer Academic Publishers, The Netherlands, 1995.

[31] R. Jin, W. Chen, and T. W. Simpson. Comparative studies of metamodelling techniques under multiple modelling criteria. *Structural and Multidisciplinary Optimization*, 23(1):1–13, December 2001.

[32] D. M. Kingsland, J. Gong, J. L. Volakis, and J. F. Lee. Performance of an anisotropic artificial absorber for truncating finite-element meshes. *IEEE Transactions on Antennas Propagation*, 44:975, 2006.

[33] M. Kojima. Sums of squares relaxations of polynomial semidefinite programs, Research Report B-397, Tokyo Institute of Technology, 2003.

[34] J. B. Lasserre. Robust global optimization with polynomials. *Mathematical Programming*, 107(1-2):275–293, 2006.

[35] K. H. Lee, I. S. Eom, G. J. Park, and W. I. Lee. Robust design for unconstrained optimization problems using the Taguchi method. *American Institute of Aeronautics and Astronautics Journal*, 34:1059–1063, May 1996.

[36] A. F. J. Levi. Private communications, 2006.

[37] Z. Q. Luo and P. Tseng. On the convergence of the coordinate descent method for convex differentiable minimization. *Journal of Optimization Theory and Applications*, 72(1):7–35, 1992.

[38] I. J. Lustig. In his own voice - interview with George B. Dantzig. *[Online] http://www2.informs.org/History/dantzig/index.htm, http://www.e-optimization.com/directory/trailblazers/dantzig*, 2000.

[39] H. Markowitz. Portfolio selection. *The Journal of Finance*, 7(1):77–91, March 1952.

[40] J. M. Mulvey and A. Ruszczynski. A new scenario decomposition method for large-scale stochastic optimization. *Operations Research*, 43(3):477–490, May 1995.

[41] J. M. Mulvey, R. J. Vanderbei, and S. J. Zenios. Robust optimization of large-scale systems. *Operations Research*, 43:264–281, 1995.

[42] A. Nemirovski. On tractable approximations of randomly perturbed convex constraints. *Proceedings. 42nd IEEE Conference on Decision and Control*, 3:2419–2422, December 2003.

[43] J. Nocedal and S. J. Wright. *Numerical Optimization.* Springer-Verlag, 1999.

[44] G. J. Park, T. H. Lee, K. H. Lee, and K. H. Hwang. Robust design — an overview. *American Institute of Aeronautics and Astronautics Journal*, 44:181–191, 2006.

[45] A. Prekopa and A. Ruszczynski, editors. *Special Issue on Stochastic Programming.* Taylor & Francis Group, London, etc., 2002. Optimization Methods and Software (OMS), Volume 17, Number 3.

[46] B. Ramakrishnan and S. S. Rao. A robust optimization approach using taguchi's loss function for solving nonlinear optimization problems. *Advances in Design Automation*, 32(1):241–248, 1991.

[47] R. T. Rockafellar and R. J. B. Wets. Scenarios and policy aggregation in optimization under uncertainty. *Math. Oper. Res.*, 16(1):119–147, 1991.

[48] A. Ruszczynski and A. Shapiro. Optimization of risk measures. Risk and Insurance 0407002, EconWPA, July 2004. available at http://ideas.repec.org/p/wpa/wuwpri/0407002.html.

[49] A. Saltelli, S. Tarantola, F. Campolongo, and M. Ratto. *Sensitivity Analysis in Practice: A Guide to Assessing Scientific Models.* Halsted Press, New York, NY, USA, 2004.

[50] L. Sanchis, A. HaKansson, D. Lopez-Zanon, J. Bravo-Abad, and J. Snchez-Dehesa. Integrated optical devices design by genetic algorithm. *Applied Physics Letters*, 84:4460–+, May 2004.

[51] P. Seliger, M. Mahvash, C. Wang, and A. F. J. Levi. Optimization of aperiodic dielectric structures. *Journal of Applied Physics*, 100:4310–+, August 2006.

[52] N. Z. Shor. *Nondifferentiable Optimization and Polynomial Problems.* Econometrics and Operations Research. Kluwer Academic Publishers, 1998.

[53] T. W. Simpson, J. D. Poplinski, P. N. Koch, and J. K. Allen. Metamodels for computer-based engineering design: Survey and recommendations. *Engineering with Computers*, 17(2):129–150, 2001.

[54] A. L. Soyster. Convex programming with set-inclusive constraints and applications to inexact linear programming. *Operations Research*, 21(5):1154–1157, September 1973.

[55] J. C. Spall. Multivariate stochastic approximation using a simultaneous perturbation gradient approximation. *IEEE Transactions on Automatic Control*, 37:332–341, 1992.

[56] S. Sundaresan, K. Ishii, and D. R. Houser. A robust optimization procedure with variations on design variables and constraints. *Engineering Optimization*, 24(2):101, 1995.

[57] G. Taguchi. Performance analysis design. *International Journal of Production Research*, 16:521–530, 1978.

[58] B. Temelkuran, S. D. Hart, G. Benoit, J. D. Joannopoulos, and Y. Fink. Wavelength-scalable hollow optical fibres with large photonic bandgaps for CO_2 laser transmission. *Nature*, 420:650–653, December 2002.

[59] S. Uryasev and R. T. Rockafellar. Conditional value-at-risk: optimization approach. In *Stochastic optimization: algorithms and applications (Gainesville, FL, 2000)*, volume 54 of *Appl. Optim.*, pages 411–435. Kluwer Acad. Publ., Dordrecht, 2001.